NZGW

26th International Applied Geochemistry Symposium

Application of
Indicator Mineral Methods
to Mineral Exploration

Convenors: M.B. McClenaghan, A. Plouffe & D. Layton-Matthews

November 17, 2013

Short Course 07

Application of Indicator Mineral Methods to Mineral Exploration
Convenors: M.B. McClenaghan A. Plouffe & D. Layton-Matthews
November 17, 2013

26th International Applied Geochemistry Symposium
Rotorua, New Zealand

WORKSHOP OVERVIEW

This one-day workshop builds on the success of the indicator mineral workshops held at the 24th and 25th International Applied Geochemistry Symposia (IAGS). This one-day workshop will review principles, methods, and developments in indicator mineral methods in mineral exploration around the world and consists of presentations by some of the most experienced practitioners in the field. Indicator mineral methods applied to exploration for gold, porphyry Cu, VMS, and W-Mo will be presented, as well as the application of Fe oxide mineral chemistry to exploration for a broad range of deposit types. Topics to be covered include heavy mineral sample processing methods, quality assurance, and mineral chemistry methods.

Beth McClenaghan, Alain Plouffe & Dan Layton-Matthews
September, 2013

Overview of indicator mineral recovery methods for sediments and bedrock: 2013 update

M. Beth McClenaghan

Geological Survey of Canada, 601 Booth Street, Ottawa, Ontario, Canada K1A 0E8
(e-mail: bmcclena@nrcan.gc.ca)

These short course notes are a summary of a more detailed paper (McClenaghan 2011) describing common sample processing methods (Fig. 1) used to reduce sample volume, concentrate heavy minerals, and recover indicator minerals in support of mineral exploration. It is an updated version of previously published workshop notes presented in 2009 and 2011 (McClenaghan 2009, 2011).

The application of indicator mineral methods to mineral exploration has expanded and developed significantly over the past two decades and these methods are now used around the world to explore for a broad spectrum of deposit types including kimberlite (diamonds) (e.g. McClenaghan & Kjarsgaard 2007), lode gold (e.g. McClenaghan & Cabri 2011; Moles & Chapman 2011), magmatic Ni-Cu-PGE (e.g. Averill, 2001, 2011; McClenaghan *et al.* 2011), metamorphosed VMS (e.g. Heiman *et al.* 2005), porphyry Cu (e.g. Kelley *et al.* 2011; Averill 2011), Mississippi Valley-type Pb-Zn (e.g. Paulen *et al.* 2011), U, Sn, W, IOCG (e.g. McMartin *et al.* 2011), and rare metals (e.g. Averill 2001).

Indicator minerals, including ore, accessory and alteration minerals, are usually sparsely distributed in their host rocks. In sediments derived from rocks, these indicator minerals may be even sparser, thus sediment samples must be concentrated in order to recover and examine the indicators. Most indicator minerals have a moderate to high specific gravity; therefore most processing techniques use some type of density separation, often in combination with sizing and/or magnetic separations, to concentrate the minerals. The presence of specific indicator minerals in unconsolidated sediments provides evidence of a bedrock source and, in some cases, the chemical composition of the minerals may reflect the ore grade of the bedrock source. As few as one sand-sized grain of a specific indicator mineral in a 10 kg sample may be significant. To recover such potentially small quantities (equivalent to ppb) of indicator minerals, samples are processed to reduce the volume of material that must be examined. The processing techniques employed must retain the indicator mineral(s) without contaminating the sample and must have a reasonable cost.

Indicator minerals can be recovered from a variety of sample media, including stream, alluvial, glacial, beach, or eolian sediments, and residual soils. They can also be recovered from weathered and fresh bedrock, as well as mineralized float. The combinations of processing techniques used for recovering indicator minerals by exploration companies and government agencies are quite variable (e.g. Gregory & White 1989; Peuraniemi 1990; Davison 1993; Towie & Seet 1995; Chernet *et al.* 1999; McClenaghan *et al.* 1999; Gent *et al.* 2011; Plouffe *et al.* in press). The processing methods used will depend on the commodities being sought as well as the cost per sample. Most oxide and silicate indicator minerals are easily recovered from
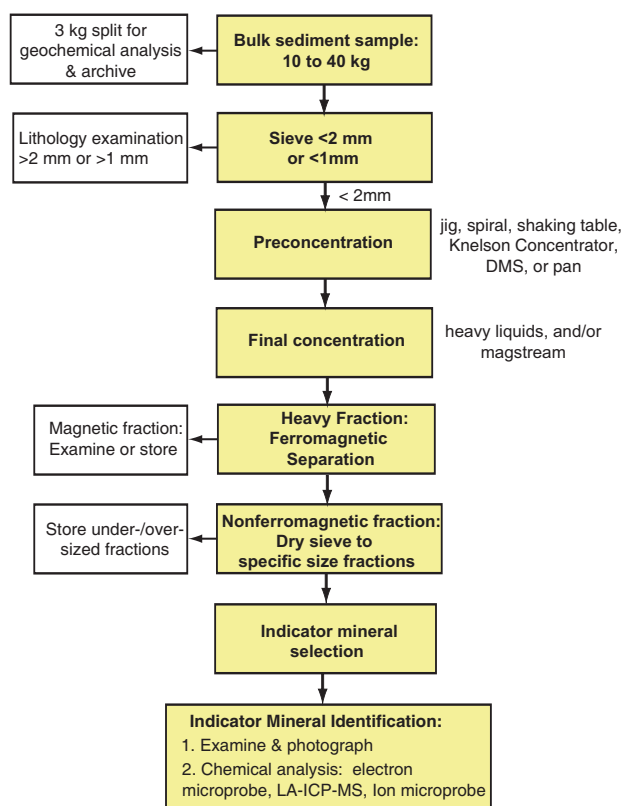
Fig. 1. Generalized flow sheet showing steps in sample processing used to reduce sample weight, concentrate heavy minerals, and recover indicator minerals.

the medium to coarse sand-sized (0.25–2.0 mm) fraction. Therefore, concentration techniques that recover the sand-sized heavy minerals can be used. In contrast, a significant proportion of gold, platinum group minerals (PGM), sulphide minerals, and rare metal minerals (Laukkanen *et al.* 2011) are silt-sized (<0.063 mm), thus concentration of these indicators requires a preconcentration technique that includes recovery of the silt- as well as the sand-sized fractions.

SAMPLE WEIGHT

The sample weight of material required for indicator mineral studies will vary depending on the type of surficial sediment collected, the grain size characteristics of the sample material, the commodity being sought, and shipping costs (Table 1). For example, in glaciated terrain clay-rich till samples may have to be 20 to 30 kg (or more) to recover a sufficient weight of sand-sized heavy minerals (Table 2, #5) (e.g. Spirito *et al.* 2011). In contrast, coarse-grained silty sand till typical of shield terrain

Table 1. Examples of variation in sample weight and processing procedures with sample and target type at Overburden Drilling Management Ltd.'s heavy mineral processing laboratory (Averill & Huneault 2006).

Target	Typical Sample Weight	Required Separations				
		Table	Micropan	Heavy Liquid (specific gravity)	Ferromagnetic separation?	Paramagnetic separation?
A. Sediment Samples						
Gold	10	Single	Yes	3.3	Yes	No
Kimberlite	10–30	Double	No	3.2	Yes	Yes
Massive sulphides (Ni-Cu-PGE, BHT, VMS, IOCG, MVT, skarn)	10	Single	Yes (PGM only)	3.2	Yes	Yes
Porphyry Cu	0.5	No	No	2.8, 3.2	Yes	Two
Uranium	10	Single	Yes	3.3	Yes	No
Heavy mineral sands (grade evaluation)	20	Triple	No	3.3	Yes	Optional
Tampering (investigation)	Variable	Optional	Yes	3.3	Yes	Optional
B. Rock Samples						
Gold, PGE, base metals	1	Optional	Yes	3.3	Yes	Optional
Kimberlite	1-10	Optional	No	3.2	Yes	Yes
Tampering (investigation)	1	No	Yes	3.3	Yes	Optional

requires smaller (10 to 15 kg) samples because it contains more sand-sized material in the matrix (Table 2, #1 to 4) (Spirito *et al.* 2011). Alluvial sand and gravel samples collected for recovery of porphyry Cu indicator minerals (PCIM) can be as small as ~0.5 kg because porphyry Cu alteration systems are large and rich in indicator minerals (Averill 2007). Bedrock and float samples usually vary from 1 to 10 kg.

BEDROCK PREPARATION

Bedrock or float (mineralized boulders) samples often need to be disaggregated or crushed prior to processing to reduce rock fragment/mineral grain size to <2 mm. Electric pulse disaggregation (EPD) using an electric current from a high-voltage power source in a water bath is an efficient means of liberating mineral grains from a rock (Cabri *et al.* 2008). The major advantage of this method is that individual mineral grains can be recovered in their original shape and form regardless of grain size. Conventional rock crushers may also be used, however, they 1) are more difficult to clean between samples and thus pose a higher risk of cross contamination, 2) often cause rock fragments to break across grain boundaries, and 3) mark/damage grains as they are liberated. Barren quartz can be disaggre-

gated or crushed as a blank between routine rock samples to reduce and monitor contamination.

PRECONCENTRATION

If sample shipping costs are an issue, samples may be partly processed in the field to reduce the weight of material shipped to the processing laboratory. Samples may be sieved to remove the coarse (>1 or >2 mm) fraction, which may reduce weights from a few % to 30% (e.g. Table 2, columns B-C). Preconcentrating samples using a pan, jig, sluice box or centrifugal concentrator also may be carried out in the field to further reduce the weight of material to be shipped. Preconcentrates may be examined in the field, significantly reducing the time to obtain results for follow up. However, preconcentrating in the field can itself be expensive and time consuming and the available methods may not provide optimal recovery of the indicator minerals of interest. Field setup of concentrating equipment may be more rudimentary than at the processing laboratory, thus extra care is required to avoid cross contamination or material loss during the pre-concentration procedures.

Whether sieved off in the field or in the laboratory, the coarse >2 mm fraction may be examined to provide additional infor-

Table 2. Weight of each fraction generated by a combination of tabling and heavy liquid separation to reduce till sample weight, concentrate heavy minerals, and recover indicator minerals: A) initial sample weight; B) sieving off <2 mm; C & D) tabling; E) heavy liquid separation; F) magnetic separation; G) final heavy mineral concentrate weight. Till samples are from (1) the South Pit of the Thompson Ni Mine, Thompson, Manitoba; (2) Broken Hammer Cu-PGE deposit, Sudbury, Ontario; (3) Pamour Mine, Timmins, Ontario; (4) Triple B kimberlite, Lake Timiskaming field, Ontario; and (5) Buffalo Head Hills, northern Alberta.

Location	Texture	A: total sample weight (kg)	B: weight >2 mm clasts (kg)	C: weight of sample put across shaking table (kg)	D: weight shaking table concentrate produced (g)	E: weight of heavy liquid light fraction (g)	F: weight magnetic fraction (g)	G: weight of non-magnetic heavy mineral concentrate (g) 0.25–2.0 mm
1. Thompson Ni Belt	silty sand till	15.0	3.0	12.0	1015.9	104.5	36.4	47.9
2. Sudbury	sandy till	15.0	5.6	9.4	1125.1	402.6	13.0	18.9
3. Timmins Gold camp	silty sand till	11.8	2.3	9.5	353.1	319.8	5.2	28.1
4. Triple B kimberlite	silty sand till	9.8	1.2	8.6	438.7	377.0	22.0	35.8
5. Northern Alberta	clayey till	67.4	2.4	65.0	1,307.0	1,235.2	5.6	11.5

mation about sample provenance and transport distance. The <2 (or <1 mm) fraction is preconcentrated most commonly using sieving and/or density methods (e.g. jig, shaking table, spiral concentrator, dense media separator, pan, centrifugal concentrator) to reduce the weight of material to be examined without losing indicator minerals. Some of the more common preconcentration equipment and techniques are described below.

Pans

Panning is the oldest method used to recover indicator minerals, primarily for gold and PGM. Sediment is placed in a pan and shaken sideways in circular motion while being held just under water. Heavy minerals sink to the pan bottom and light minerals rise and spill out over the top (Zeschke 1961; Silva 1986; English *et al.* 1987; Ballantyne & Harris 1997). Pans have varying shapes (flat bottomed or conical) and sizes, and can be made out of plastic, metal or wood. The advantages of this technique include that it can be a field or laboratory-based operation, is inexpensive in terms of equipment costs, and if used in the field it reduces sample shipping weight and thus cost. If field based, indicator minerals can be examined immediately and results can be used to guide on going exploration while still in the field. Panning is often used in combination with other preconcentration and/or heavy liquid methods to recover silt-sized precious metal grains (e.g. Grant *et al.* 1991; Leake *et al.* 1991, 1998; Ballantyne & Harris 1997; Wierchowiec 2002). The disadvantages of this method are that is slow, is highly dependent on the experience and skill of operator and therefore requires consistent personnel to perform the panning. It is considered to be a rough concentrating method when used in the field and is followed up with further laboratory-based concentration techniques (e.g. Zantop & Nespereira 1979; Stendal & Theobald 1994).

Shaking tables

Preconcentration using a shaking (e.g. Wilfley) table is another one of the oldest methods for concentrating and separating heavy minerals on the basis of density. It recovers silt- to coarse sand-sized heavy minerals for a broad spectrum of commodities including diamonds, precious and base metals, and uranium (Averill & Huneault 2006). A brief description of the method is summarized below from Sivamohan & Forssberg (1985), Silva (1986), and Stewart (1986). The table consists of a deck with up to 1 cm high riffles covering over half the surface. A motor mounted on one end drives a small arm that shakes the table along its length. A slurry of <2.0 mm sample material is put across the shaking table to prepare a preconcentrate. If kimberlite indicators are targeted, the sample is tabled twice to ensure higher recovery of the key lower density minerals (Cr-diopside and forsteritic olivine) and the coarsest grains. The advantages of this method are the ability to recover both silt- and sand-sized indicator minerals for a broad spectrum of commodities at a moderate cost. It is a well established method for the recovery of precious metal mineral grains as well as kimberlite indicator minerals (e.g. English *et al.* 1987; McClenaghan *et al.* 1998, 2004). The disadvantages of this method include the loss of some coarse heavy minerals as well as the finer <0.10 mm grains (Gent *et al.* 2011), the lengthy time required to process each sample; and its dependency on the skill of the operator.

Dense Media Separators

A micro-scale dense media separator (DMS), which is used in commercial labs, employs a gravity-based method to preconcentrate kimberlite indicator minerals. An overview of the method described by Baumgartner (2006) is presented below. Heavy mineral concentration is carried out using a gravity-fed high-pressure cyclone. The <1 mm fraction of the sample is mixed with fine-grained ferrosilicon (FeSi) to produce a slurry of a controlled density. The slurry is fed into the cyclone where the grains travel radially and helically, forcing the heavier particles toward the wall of the cyclone and the lighter particles toward the centre (Gent *et al.* 2011). The lighter and heavier particles exit the cyclone through different holes, with the light fraction discarded and the heavy fraction collected on a 0.25 or 0.3 mm screen. The heavy mineral concentrate on the screen is then dried and screened to remove residual FeSi. A Tromp curve is used to define the efficiency and precision of the DMS separation. The DMS is calibrated to recover the common kimberlite indicator minerals that have a specific gravity (SG) >3.1: pyrope garnet, chrome-spinel, Mg-ilmenite, Cr-diopside, forsteritic olivine, and diamond. It is tested using synthetic density tracers before processing samples. The density settings and cut points are checked once per day. The advantages of the micro DMS system are that it is fast, less susceptible to sample contamination than other heavy mineral concentrating techniques, and is not operator dependent. The method, however, is more expensive than other methods described here and it does not recover the silt-sized precious and base metal indicator minerals.

Centrifugal concentrators

Centrifugal concentrators were originally designed for concentrating gold and platinum from placer and bedrock samples. However, in recent years they have also been used to recover kimberlite indicator minerals from sediment samples (e.g. Chernet *et al.* 1999; Lehtonen *et al.* 2005). They can handle particle sizes from >10 μm to a maximum of 6 mm. The general processing procedure is summarized below for one type of centrifugal concentrator, the Knelson Concentrator, from the manufacturer's website (www.knelsongravitysolutions.com). In summary, water is introduced into a concentrate cone through a series of holes in rings on the side of the cone. The sample slurry is then introduced into the concentrate cone from a tube at the top. When the slurry reaches the bottom of the cone, it is forced outward and up the cone wall by the centrifugal force generated by the spinning cone. The slurry fills each ring on the inside of the cone wall to capacity, creating a concentrating bed. High specific gravity particles are captured in the rings and retained in the concentrating cone. At the end of the concentrate cycle, concentrates are flushed from the cone into the sample collector. The advantages of centrifugal concentrators are that they are fast, inexpensive, and can be mobilized to the field and used to reduce the weight of material that must be shipped to the laboratory. However, recovery of kimberlite indicator minerals from silt-poor material such as esker sand or stream sediments is difficult due to the absence of fine-grained material to keep the slurry in suspension (Chernet *et al.* 1999). Alternatively, too much fine-grained material can impede the settling of fine-grained heavy minerals. Centrifugal concentrators are optimal for the recovery of gold and PGM.

Spiral concentrators

Heavy minerals can be recovered using a rotary spiral concentrator, which consists of a flat circular stainless steel bowl with rubber ribs that spiral inward; a detailed description of its use is reported by Silva (1986). A spiral concentrator is mounted on a frame so it can be tilted and has a water wash bar extending laterally from one side of the bowl to the center. As the bowl spins, water is sprayed from the bar and heavy mineral grains move up and inward along the spirals to the central opening where they are collected in a container behind the bowl. The water washes light minerals down to the bottom of the bowl. The heaviest minerals are recovered first. The advantages of the spiral concentrator are that it can be field-based and thus used to reduce sample weight to be shipped, it is inexpensive to acquire and operate, it requires little time if the material is sandy, and it recovers indicator minerals across a broad size range, from silt- to sand-sized grains. The method, however, is dependent on the experience and skill of the operator, the lower density threshold is variable, there is some loss of heavy minerals, and the method is slow if the sample is clay-rich. It is used mainly for gold recovery (e.g. Maurice & Mercier 1986; Silva 1986; Sarala *et al.* 2009) but in the past 10 years it also has been used for the recovery of kimberlite indicator minerals (e.g. Sarala & Peuraniemi 2007).

Jigs

Jigging is one of the oldest gravity concentration methods; this method separates heavy minerals based on differential settling velocities of mineral grains in water (Stendal & Theobald 1994). Jigging is performed by hand or by mechanically jerking a partially filled screen of material up and down underwater for several minutes. While submersed in water, mineral grains separate through suspension and gravity effects into layers of varying specific gravity. Heavier grains concentrate on the surface of the screen, with the heaviest generally concentrated towards the centre of the screen forming an 'eye'. Very heavy minerals, such as ilmenite and magnetite, will be found at the very centre of the screen and lighter heavy mineral, such as garnet and pyroxene, will concentrate at the periphery of the eye. Diamonds tend to concentrate towards the centre, despite their moderate specific gravity (SG 3.51). A spoon is used to remove the heavy minerals in the eye for more detailed examination. For optimal recovery, the jig tailings should be re-jigged 2 to 3 times until no eye forms. The method is typically used for recovery of gold (e.g. Silva 1986) and kimberlite indicator minerals (Muggeridge 1995). The advantages of using a jig are that it can be field-based and thus used to reduce the weight of the samples to be shipped, is inexpensive to operate, is relatively fast, and works best for fine to coarse sand-sized grains. However, it is best used in a fixed, laboratory-based setting with an experienced operator.

FINAL CONCENTRATION

Heavy liquid separation

A preconcentrate is usually further refined using heavy liquids of a precise density (Gent *et al.* 2011) to further reduce the size of the concentrate prior to heavy mineral selection (Table 2-column E). Heavy liquid separation provides a sharp separation between heavy (sink) and light minerals (float) at an exact known density. However, it is slow and expensive, and there-

fore is not economical for large volumes of sample material; hence, it is advantageous to use the preconcentration procedures described above to reduce sample volume before this step (Stendal & Theobald 1994). It is common to remove the finer fraction (<0.063 mm) of a sample by sieving before using heavy liquid separation, as this material can be difficult to separate due to its small size (M. Lehtonen, pers. comm. 2013).

The most common heavy liquids used include methylene iodide (MI) with a SG of 3.3 and tetrabromoethane (TBE) or the low-toxicity heavy liquid lithium heteropolytungstates (LST), both with SG of 2.9. The density of the heavy liquid required will depend on the indicator minerals being sought. Some laboratories use a combination of both heavy liquids, separating first using the lower density heavy liquid at about SG 2.9 to reduce the volume of material to be further separated at SG 3.2 or 3.3 (e.g. Le Couteur & McLeod 2006; de Souza 2006; Mircea 2006). The recovery of kimberlite and magmatic Ni-Cu-PGE indicator minerals requires heavy liquid separation at SG 3.2 using dilute methylene iodide to include the lowest density indicators, Cr-diopside and forsteritic olivine. Recovery of porphyry Cu indicator minerals requires separation at SG 2.8 to 3.2 to recover the mid-density indicators tourmaline (dravite), alunite, jarosite, and turquoise (Averill 2007). Some indicator minerals, such as apatite and fluorite, are of intermediate density but are recovered mainly from the mid-density rather than the heavy fraction.

Magnetic separation

Magnetic separation may be used to further refine heavy mineral concentrates and reduce concentrate volume for picking of mineral species with specific magnetic susceptibilities (Towie & Seet 1995). The most common magnetic separation involves splitting the ferromagnetic from the non-ferromagnetic fraction. Ferromagnetic minerals can comprise a considerable proportion of the concentrate (e.g. Table 2, column F) and therefore removing the ferromagnetic minerals decreases concentrate size prior to indicator mineral selection and removes any steel contaminants derived, in most instances, from sampling tools or drilling equipment. The ferromagnetic fraction may then be (1) set aside, (2) examined to determine the abundance and mineral chemistry of magnetite (e.g. Beaudoin *et al.* 2011), pyrrhotite (McClenaghan *et al.* 2012), or magnetic Mg-ilmenite, as is the case for some kimberlites (e.g. McClenaghan *et al.* 1998), or (3) analyzed geochemically (e.g. Theobald *et al.* 1967). A hand magnet or plunger magnet is most commonly used to carry out this separation.

A specific size fraction of the non-ferromagnetic heavy mineral fraction may be further separated electromagnetically into fractions with different paramagnetic characteristics to help reduce the volume of material to be examined for indicator minerals (Averill & Huneault 2006). Minerals such as diamond are nonparamagnetic; pyrope garnet, eclogitic garnet, Cr-diopside and forsteritic olivine are nonparamagnetic to weakly paramagnetic; and Cr-spinel and Mg-ilmenite are moderately to strongly paramagnetic (see Table 1 in McClenaghan & Kjarsgaard 2007). If the non- or paramagnetic portion of the concentrate contains a significant amount of almandine garnet it may be processed through a magstream separator to separate the orange almandine from similar looking eclogitic or pyrope garnet grains. In this case, magstream separation divides the concentrate into (1) a fraction containing most of

the silicates (e.g. pyrope and eclogitic garnet) and no almandine, and (2) a fraction containing ilmenite, chromite, and other moderately magnetic minerals such as almandine (Baumgartner 2006).

INDICATOR MINERAL SELECTION AND EXAMINATION

The non-ferromagnetic fraction is commonly sieved into two or three (e.g. 0.25–0.5 mm, 0.5–1.0 mm, 1.0–2.0 mm) size fractions for picking of indicator minerals; however the final size range will depend on the commodity sought. For example, kimberlite indicator minerals are most abundant in the 0.25 to0.5 mm fraction (McClenaghan & Kjarsgaard 2007) and thus, to maximize recovery and minimize counting time and cost, the 0.25 to 0.5 mm fraction is most commonly picked.

Indicator minerals are selected from non-ferromagnetic heavy mineral concentrates during a visual scan, in most cases, from the finer size (e.g. 0.25–0.5 mm, or 0.3–0.5 mm, 0.25–0.86 mm) fractions using a binocular microscope. The grains are counted and a selection of grains is removed from the sample for analysis using an electron microprobe (EMP) to confirm their identification. Methods for examining a sample for counting/picking vary from rolling conveyor belts to dishes/paper marked with lines or grids. If a concentrate is unusually large, then a split is examined and the indicator mineral counts are normalized to the total weight of the concentrate. If a split is picked, the weight of the split and the total weight should both be recorded. Not all grains counted in a sample will be removed for EMP analyses. If this is the case, the total number of grains counted and the number of grains removed should both be recorded.

Indicator minerals are visually identified in concentrates on the basis of colour, crystal habit, and surface textures, which may include features such as kelyphite rims and orange peel textures on kimberlitic garnet (e.g. Garvie 2003; McClenaghan & Kjarsgaard 2007). Scheelite and zircon in a concentrate may be counted under shortwave ultraviolet light. Gold and PGM grains may be panned from concentrates that were prepared such that the silt-sized fraction has been retained (e.g. tabling). The grains may be counted and classified with the aid of optical or scanning electron microscopy. Commonly, gold grains are classified according to their shape/degree of wear (e.g. DiLabio 1990; Averill 2001), which are characteristics that can provide information about relative transport distances (McClenaghan & Cabri 2011).

INDICATOR MINERAL CHEMISTRY

Mineral chemical analysis by EMP, scanning electron microprobe (SEM), laser ablation-ICP-MS, or secondary ion mass spectrometry (SIMS) may be carried out to determine major, minor and trace element contents of specific indicator minerals because mineral chemistry is used to confirm identity, establish mineral paragenesis, and in some cases deposit grade (e.g., Ramsden *et al.* 1999; Belousova *et al.* 2002; Scott 2003; Heimann *et al.* 2005). For example, kimberlite indicator minerals are characterized by a specific range of compositions that reflect their mantle source and diamond grade (e.g. Fipke *et al.* 1995; Schulze 1997; Grütter *et al.* 2004; Wyatt *et al.* 2004). Gold, PGM and sulphide grains may be analyzed to determine their trace element chemistry or isotopic compositions (e.g. Grant *et*

al. 1991; Leake *et al.* 1998; Chapman *et al.* 2009). Prior to indicator mineral grains being selected from a heavy mineral concentrate, newer techniques such as mineral liberation analysis (MLA), computer-controlled scanning electron microscopy (CCSEM), or quantitative evaluation of materials by scanning electron microscopy (QEMSCAN) may provide quantitative mineralogical analysis and identification of indicator minerals in a portion of the heavy mineral concentrate that has been prepared as a polished epoxy grain mount, in the 0.25 to 2.0 mm fraction of the rarely examined <0.25 mm fraction. These methods can be used to identify indicator minerals of interest and prioritize grains for further detailed and more costly EMP analysis, thus reducing EMP analytical costs. The cost per sample for these new techniques is, in general, more expensive than conventional methods.

QUALITY CONTROL

Project geologists may use a combination of blank samples (which contain no indicator minerals), spiked samples (which are known to contain a quantity of specific indicator mineral species or density blocks/beads (e.g. Gent *et al.* 2011)), and field duplicates, as well as repicking of 10% of the heavy mineral concentrates to monitor a laboratory's potential for sample contamination and quality of mineral grain selection. In addition, heavy mineral processing and identification laboratories can be asked to report their own quality control monitoring procedures and test results. Quality assurance and control measures implemented at the Geological Survey of Canada for indicator mineral surveys are described in Spirito *et al.* (2011) and Plouffe *et al.* (in press).

SUMMARY

These workshop notes describe some of the procedures available for processing surficial media and rocks to recover indicator minerals for mineral exploration. The processing method used will depend on: sample media, commodities being sought, budget, bedrock and surficial geology of the survey area, as well as processing methods used for previous batches. When reporting indicator mineral results in company assessment files, government reports, or scientific papers, it is helpful to report the laboratory name, processing methods used, and sample weights. A complete list of metadata that should be reported so that the indicator mineral data can be fully understand, interpreted, and archived is reported in Plouffe *et al.* (in press). Monitoring of quality control is essential at each stage in the processing, picking, and analytical procedures described here and should be monitored both by the processing laboratories and clients. Geologists are encouraged to visit processing and picking laboratories so they have a clear understanding of the procedures being used and can discuss customizations needed for specific sample batches.

REFERENCES

AVERILL, S.A. 2001. The application of heavy indicator minerals in mineral exploration with emphasis on base metal indicators in glaciated metamorphic and plutonic terrains. *In*: MCCLENAGHAN, M.B., BOBROWSKY, P.T., HALL, G.E.M & COOK, S. (eds) *Drift Exploration in Glaciated Terrain*. Geological Society of London, Special Volume **1985**, 69–82.

AVERILL, S.A. 2007. Recent advances in base metal indicator mineralogy: An update from Overburden Drilling Management Limited. *EXPLORE, Newsletter of the Association of Applied Geochemists*, **134**, 2–6.

AVERILL, S.A. 2011. Viable indicator minerals in surficial sediments for two major base metal deposit types: Ni-Cu-PGE and porphyry Cu. *Geochemistry: Exploration, Environment, Analysis*, **11**, 279–292.

AVERILL, S.A. & HUNEAULT. R. 2006. Overburden Drilling Management Ltd: Exploring heavy minerals. *EXPLORE, Newsletter of the Association of Applied Geochemists*, **133**, 1–5.

BALLANTYNE, S.B & HARRIS, D.C. 1997. Alluvial platinum-group minerals and gold in Alberta: Results from the "Orientation Studies Project" and their significance to exploration. *In:* MACQUEEN, R.W. (ed), *Exploring for Minerals in Alberta*. Geological Survey of Canada Geoscience Contributions, Canada-Alberta Agreement on Mineral Development (1992–1995), Geological Survey of Canada, Bulletin **500**, 279–329.

BAUMGARTNER, M. 2006. Industry leading laboratory services for diamond explorers. *EXPLORE, Newsletter of the Association of Applied Geochemists*, **133**, 5–10.

BEAUDOIN, G., DUPUIS, C., MCCLENAGHAN, B., BLAIN, J., & MCMARTIN, I. 2011. Application of iron-oxide discriminant diagrams in mineral exploration. *In:* MCCLENAGHAN, M.B., PEURANIEMI, V. & LEHTONEN, M.L. (Convenors), *Indicator Mineral Methods in Mineral Exploration, Workshop 3*. 25th International Applied Geochemistry Symposium, August 21, 2011, 35–40.

BELOUSOVA, E.A., GRIFFIN, W.L., O'REILLY, S. & FISHER, N.I. 2002. Apatite as an indicator mineral for mineral exploration: Trace element compositions and their relationship to host rock type. *Journal of Geochemical Exploration*, **76**, 45–69.

CABRI, L.J., RUDASHEVSKY, N.S., RUDASHEVSKY, V.N. & OBERTHÜR, T. 2008. Electric-Pulse Disaggregation (EPD), Hydroseparation (HS) and their use in combination for mineral processing and advanced characterization of ores. *In: Proceedings*. Canadian Mineral Processors 40th Annual Meeting, Paper **14**, 211–235.

CHAPMAN, R.J., LEAKE, R.C., BOND, D.P.G., STEDRA, V. & FAIRGRIEVE, B. 2009. Chemical and mineralogical signatures of gold formed in oxidizing chloride hydrothermal systems and their significance within populations of placer gold grains collected during reconnaissance. *Economic Geology*, **104**, 563–585.

CHERNET, T. MARMO, J. & NISSINEN, A. 1999. Technical note. Significantly improved recovery of slightly heavy minerals from Quaternary samples using GTK modified 3" Knelson preconcentrator. *Minerals Engineering*, **12**, 1521–1526.

DAVISON, J.G. 1993. Diamond exploration samples: laboratory processing. *In:* SHEAHAN P. & CHATER, A. (Chairmen) *Diamond: Exploration, Sampling and Evaluation*. Prospectors and Developers Association of Canada, Short Course Proceedings, Toronto, March 27, 1993, 315–341.

DE SOUZA, H. 2006. Indicator mineral processing at SGS Minerals Services. *EXPLORE, Newsletter of the Association of Applied Geochemists*, **133**, 13–15

DILABIO, R.N.W. 1990. Classification and interpretation of the shapes and surface textures of gold grains from till on the Canadian Shield. *In: Current Research, Part C*. Geological Survey of Canada, Paper **90-1C**, 323–329.

ENGLISH, B.L., DESBOROUGH, G.A. & RAYMOND, W.H. 1987. *A mechanical panning technique for separation of fine-grained gold and other heavy minerals*. United States Geological Survey, Open File Report **97-0364**.

FIPKE, C.E., GURNEY, J.J. & MOORE, R.O. 1995. *Diamond exploration techniques emphasizing indicator mineral geochemistry and Canadian examples*. Geological Survey of Canada, Bulletin **423**.

GARVIE, O.G. 2003. Surface textures found on kimberlite indicator minerals. *In: Indicator Mineral Methods in Mineral Exploration*. Prospectors and Developers Association of Canada, Short Course **2**, March 8, p. 23.

GRANT, A.H., LAVIN. O.P. & NICHOL, I. 1991. The morphology and chemistry of transported gold grains as an exploration tool. *Journal of Geochemical Exploration*, **40**, 73–94.

GREGORY, G.P. & WHITE, D.R. 1989. Collection and treatment of diamond exploration samples. *In:* ROSS, J. (ed) *Kimberlites and Related Rocks Volume 2 Their Crust/Mantle Setting, Diamonds and Diamond Exploration*. Geological Society of Australia, Special Publication **14**, Blackwell Scientific Publications, Oxford, 1123–1134.

GRÜTTER, H.S., GURNEY, J.J., MENZIES, A.H. & WINTER, F. 2004. An updated classification scheme for mantle-derived garnet, for use by diamond explorers. *Lithos*, **77**, 841–857.

GRÜTTER, H.S., THIS VOLUME

HEIMANN, A., SPRY, P. & TEALE, G.S. 2005. Zincian spinel associated with metamorphosed Proterozoic base-metal sulfide occurrences, Colorado: A re-evaluation of gahnite composition as a guide in exploration. *Canadian Mineralogist*, **43**, 601–622.

KELLEY, K.D., EPPINGER, R.G., LANG, J., SMITH, S.M. & FEY, D.L. 2011. Porphyry copper indicator minerals (PCIMs) in glacial till samples as an exploration tool: example from the giant Pebble porphyry Cu-Au-Mo deposit. *Geochemistry: Exploration, Environment, Analysis*, **11**, 321–334.

LAUKKANEN, J., LEHTONEN, M. & SARALA, P. 2011. Exploring RE and REE mineralization using indicator minerals. *In: Workshop 3: Indicator Mineral Methods in Mineral Exploration*. 26th International Applied Geochemistry Symposium, Association of Applied Geochemists, 13–18.

LEAKE, R.C., BLAND, D.J., STYLES, M.T. & CAMERON, D.G. 1991. Internal structure of Au-Pd-Pt grains from south Devon, England, in relation to low temperature transport and deposition. *Transactions of the Institute of Mining and Metallurgy*, Section B, Applied Earth Sciences, **100**, B159–B178.

LEAKE, R.C., CHAPMAN, R.J., BLAND, D.J., STONE, P., CAMERON, D.G. & STYLES, M.T. 1998. The origin of alluvial gold in the Leadhills areas of Scotland: evidence from interpretation of internal characteristics. *Journal of Geochemical Exploration*, **63**, 7–36.

LEHTONEN, M.L., MARMO, J.S., NISSINEN, A.J., JOHANSON, B.S. & PAKKANEN, L.K. 2005. Glacial dispersal studies using indicator minerals and till geochemistry around two eastern Finland kimberlites. *Journal of Geochemical Exploration*, **87**, 19–43.

LE COUTEUR, P.C. & MCLEOD, J.A. 2006. Heavy mineral processing at Vancouver Indicator Processors Inc./Teck Cominco Global Discovery Lab. *EXPLORE, Newsletter of the Association of Applied Geochemists*, **133**, 15–18.

MAURICE, Y.T. & MERCIER, M.M. 1986. A new approach to sampling heavy minerals for regional geochemical exploration. *In: Current Research Part A*. Geological Survey of Canada, Paper **86-1A**, 301–305.

MCCLENAGHAN, M.B. 2009. Processing methods for recovery of indicator minerals from sediment and bedrock. *In: Workshop B Indicator Mineral Methods in Mineral Exploration*. 26th International Applied Geochemistry Symposium, Association of Applied Geochemists, 13–20.

MCCLENAGHAN, M.B. 2011. Overview of common processing methods for recovery of indicator minerals from sediment and bedrock in mineral exploration. *Geochemistry: Exploration, Environment, Analysis*, **11**, 265–278.

MCCLENAGHAN, M.B & CABRI, L.J. 2011. Review of gold and platinum group element indicator minerals methods for surficial sediment sampling. *Geochemistry: Exploration, Environment, Analysis*, **11**, 251–263.

MCCLENAGHAN, M.B. & KJARSGAARD, B.A. 2007. Indicator mineral and surficial geochemical exploration methods for kimberlite in glaciated terrain, examples from Canada. *In:* GOODFELLOW, W.D. (ed.) *Mineral Resources of Canada: A Synthesis of Major Deposit Types, District Metallogeny, the Evolution of Geological Provinces and Exploration Methods*. Geological Association of Canada, Special Publication No. **5**, 983–1006.

MCCLENAGHAN, M.B., PAULEN R.C., AYER, J.A., TROWELL, N.F. & BAUKE, S. 1998. R*egional till and humus geochemistry of the Timmins-Kamiskotia (NTS 42A/11, 12, 13, 14) area, northeastern Ontario*. Geological Survey of Canada, Open File **3675**.

MCCLENAGHAN, M.B., KJARSGAARD B.A., KJARSGAARD I.M., & PAULEN, R.C. 1999. *Mineralogy and geochemistry of the Peddie kimberlite and associated glacial sediments, Lake Timiskaming, Ontario*. Geological Survey of Canada, Open File **3775**.

MCCLENAGHAN, M.B., KJARSGAARD, I.M. & KJARSGAARD, B.A. 2004. *Kimberlite indicator mineral chemistry and till geochemistry around the Seed and Triple B kimberlites, Lake Timiskaming, Ontario*. Geological Survey of Canada, Open File **4822**.

MCCLENAGHAN, M.B., AVERILL, S.A., KJARSGAARD, I.M., LAYTON-MATTHEWS, D. & MATILE, G. 2011. Indicator mineral signatures of magmatic Ni-Cu deposits, Thompson Nickel Belt, central Canada. *In: Workshop 3: Indicator Mineral Methods in Mineral Exploration*. 26th International Applied Geochemistry Symposium, Association of Applied Geochemists, 67–72.

MCCLENAGHAN, M.B., BUDULAN, G., AVERILL, S.A., LAYTON-MATTHEWS, D. & PARKHILL, M.A. 2012. *Indicator mineral abundance data for bedrock and till samples from the Halfmile Lake Zn-Pb-Cu volcanogenic massive sulphide deposit*, Bathurst Mining Camp, New Brunswick. Geological Survey of Canada, Open File **7076.**

MCMARTIN, I., CORRIVEAU, L. & BEAUDOIN, G. 2011. An orientation study of the heavy mineral signature of the NICO Co-Au-Bi deposit, Great Bear magmatic zone, NWT, Canada. *Geochemistry: Exploration, Environment, Analysis*, **11**, 293–307.

MIRCEA, C. 2006. Kimberlite indicator mineral services offered by SRC Geoanalytical Laboratories. *EXPLORE, Newsletter of the Association of Applied Geochemists*, **133**, 10–13.

MUGGERIDGE, M.T. 1995. Pathfinder sampling techniques for locating primary source of diamond: recovery of indicator minerals, diamonds and geochemical signatures. *Journal Geochemical Exploration*, **53**, 183–204.

PAULEN, R.C., PARADIS, S., PLOUFFE, A. & SMITH, I.R. 2011. Pb and S isotopic composition of indicator minerals in glacial sediments from northwest Alberta, Canada: implications for Zn-Pb base metal exploration. *Geochemistry: Exploration, Environment, Analysis*, **11**, 309–320.

PLOUFFE, A., MCCLENAGHAN, M.B., PAULEN, R.C., MCMARTIN, I., CAMPBELL, J.E. & SPIRITO, W.A. In press. Processing of glacial sediments for the

recovery of indicator minerals: protocols used at the Geological Survey of Canada. *Geochemistry: Exploration, Environment, Analysis*.

PEURANIEMI, V. 1990. Chapter 10. Heavy minerals in glacial sediment. *In:* KUJANSUU, R. & SAARNISTO, M. (eds), *Glacial Indicator Tracing*. A.A. Balkema, Rotterdam, 165–185.

RAMSDEN, A.R., GRIFFIN, W.L. & FRENCH, D.H. 1999. Application of resistate indicator mineralogy to metalliferous exploration: tourmaline. *In: Research Review*. CSIRO Exploration and Mining, 49–52.

SARALA, P. & PEURANIEMI, V. 2007. Exploration using till geochemistry and heavy minerals in the ribbed moraine area of southern Finnish Lapland. *Geochemistry: Exploration, Environment, Analysis*, **7**, 195–205.

SARALA, P., PULKKINEN, E., JUHANI OJALA, V. & PELTONIEMI-TAIVALKOSKI, A. 2009. Gold exploration using till at Petäjälehto, northern Finland. *Geochemistry: Exploration, Environment, Analysis*, **9**, 247–255.

SCHULZE, D.J. 1997. The significance of eclogite and Cr-poor megacryst garnets in diamond exploration. *Exploration and Mining Geology*, **6**, 349–366.

SCOTT, K. 2003. Rutile geochemistry as a guide to mineralization at the Northparkes porphyry copper deposit, New South Wales, Australia. *In: Programme and Abstract*. International Geochemical Exploration Symposium 2003- North Atlantic Minerals Symposium 2003, 44.

SILVA, M. 1986. *Placer gold recovery methods*. California Department of Conservation, Division of Mines and Geology, Special Publication **87**.

SIVAMOHAN, R. & FORSSBERG, E. 1985. Principles of tabling. *International Journal of Mineral Processing*, **15**, 281–295.

SPIRITO, W., MCCLENAGHAN, M.B., PLOUFFE, A., MCMARTIN, I., CAMPBELL, J.E., PAULEN, R.C., GARRETT, R.G. & HALL, G.E.M. 2011. *Till sampling and analytical protocols for GEM projects: from field to archive*. Geological Survey of Canada, Open File **6850**.

STENDAL, H. & THEOBALD, P.K. 1994. Heavy-mineral concentrates in geochemical exploration. *In:* HALE, M. & PLANT, J.A. (eds), *Drainage Geochemistry*. Handbook of Exploration Geochemistry, **6**, 185–225.

STEWART, R. 1986. Routine heavy mineral analysis using a concentrating table. *Journal of Sedimentary Research*, **56**, 555–556.

THEOBALD, P.K., OVERSTREET, W.C. & THOMPSON, C.E. 1967. *Minor elements in alluvial magnetite from the Inner Piedmont Belt, North and South Carolina*. United States Geological Survey, Professional Paper **554-A**.

TOWIE, N.J. & SEET, L.H. 1995. Diamond laboratory techniques. *Journal of Geochemical Exploration*, **53**, 205–212.

WIERCHOWIEC, J. 2002. Morphology and chemistry of placer gold grains – indicators of the origin of the placers: an example from the East Sudetic Foreland, Poland. *Acta Geologica Polonica*, **52**, 563–576.

WYATT, B.A., BAUMGARTNER, M., ANCKAR, E. & GRÜTTER, H. 2004. Compositional classification of kimberlitic and non-kimberlitic ilmenite. *Lithos*, **77**, 819-840.

ZANTOP, H. & NESPEREIRA, J. 1979. Heavy-mineral panning techniques in the exploration for tin and tungsten in NW Spain. *In:* WATTERSON, J.R. & THEOBALD, P.K. (eds) *Geochemical Exploration 1978*. Association of Exploration Geochemists, 329–336.

ZESCHKE, G. 1961. Prospecting for ore deposits by panning heavy minerals from river sands. *Economic Geology*, **56**, 1250–1257.

Mineral chemistry: modern techniques and applications to exploration

D. Layton-Matthews[1]*, C. Hamilton[2] & M.B. McClenaghan[3]

[1]Department of Geological Sciences, Queen's University, Kingston, Ontario, Canada K7L 3N6
[2]Systems for Research, #45, 155 Tycos Drive, Toronto, Ontario, Canada M6B 1W6
[3]Geological Survey of Canada, 601 Booth Street, Ottawa, Ontario, Canada K1A 0E8
**Corresponding author e-mail: dlayton@geol.queensu.ca*

It is likely that undiscovered ore reserves are currently buried under recently deposited sedimentary cover. As such, our capacity to see through the complexities of this cover and to perceive the nature of the underlying bedrock ore environment has become a fundamental aspect of modern mineral exploration and ore deposit science. To date, the recognition of buried mineral deposits has been aided by our ability to (1) predict indicator minerals in bedrock sources, (2) identify and separate indicator minerals from sedimentary cover, and (3) measure the unique chemical and isotopic composition of these indicator minerals.

A substantial amount of research has been devoted to chemical and physical dispersal of minerals and elements at the Earth's surface in the development of bedrock weathering and erosional footprints. The aerial and spatial extent of these footprint models has been partially limited by our incomplete understanding of the processes involved in mineral and chemical dispersal, but moreover, by the technological challenges of identifying and measuring subtle mineral and chemical changes in these footprint sediments. Within mineral deposit footprints, the examination of the physical dispersion of relatively large (>63 micron) and heavy (>2.85 g/cm^3) mineral concentrates (HMC) from bedrock sources during glaciation has met with great successes in the exploration for kimberlite (Thorleifson 1993; Ward *et al.* 1996; McClenaghan & Kjarsgaard 2001; McClenaghan 2002; McClenaghan *et al.* 2002), base metals (Sarala & Peuraniemi 2007; Kelley *et al.* 2010; Averill 2011; Eppinger *et al.* 2011; McClenaghan *et al.* 2011; McClenaghan *et al.* 2012a,c; McClenaghan & Peter 2013), and gold (Averill & Zimmerman 1984; Sauerbrei *et al.* 1987; Craw *et al.* 1999; Averill 2013) deposits. By using HMC and the mineral chemistry of these indicator minerals, which have been separated from sediments using complex and expensive techniques (e.g. sieved, tabling, heavy liquids, magnetic separation, and hand-picking), the recognition of the spatial extent of the mineral deposit footprint has increased from 100s of metres to 1000s of metres.

In this paper, we present an overview of the current methods and the applications of mineral chemistry using indicator minerals recovered from sedimentary cover. We also discuss new methods and instrumental developments, highlight current research on mineral chemistry, indicator minerals, and mineral exploration, and consider future research directions.

MINERAL IDENTIFICATION AND MINERAL CHEMISTRY

Indicator minerals, by definition, are minerals that have a physical or chemical characteristics that allow them to be readily recovered from stream, alluvial, glacial, or aeolian sediments or
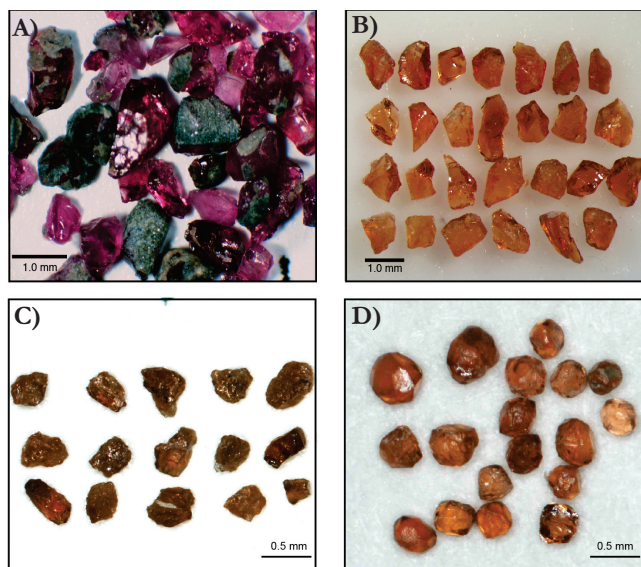
Fig. 1. Examples of colour and habit variation in indicator minerals using optical techniques (modified after McClenaghan & Kjarsgaard 2007; Hicken 2012). **A)** Purple -pyrope, some retaining kelyphite (dark). **B)** Orange eclogitic pyrope-almandine garnets. **C)** Staurolite in sample 09-MPB-006, 0.25–0.5 mm. **D)** Spessartine with deltoidal icositetrahedron habit in sample 09-MPB-031, 0.25–0.5 mm

soils samples (McClenaghan *et al.* 2000; McClenaghan & Kjarsgaard 2001). Traditionally, the identification and separation of indicator minerals rely on the characteristics largely related to the minerals' chemistry, i.e., visual distinctiveness and moderate to high density.

Optical techniques

Indicator minerals are traditionally selected from samples after the samples have undergone heavy mineral separation (see McClenaghan *et al.* 2000b; McMartin & McClenaghan 2001; McClenaghan 2005). Indicator minerals are "picked" from concentrates during an optical examination under a stereoscopic microscope, a process that may require up to 3 hours per sample. A few tens to several thousand grains may be separated into vials based on colour (Fig. 1A,B) and mineral habit (Fig. 1C,D). The success of a laboratory to produce high-quality mineral concentrates and subsequent mineral picking using experienced technicians is the first critical step in any indicator mineral chemical study.

Electron-based techniques

Once indicator minerals have been recovered, they are commonly epoxy-mounted, polished, and carbon-coated for exam-
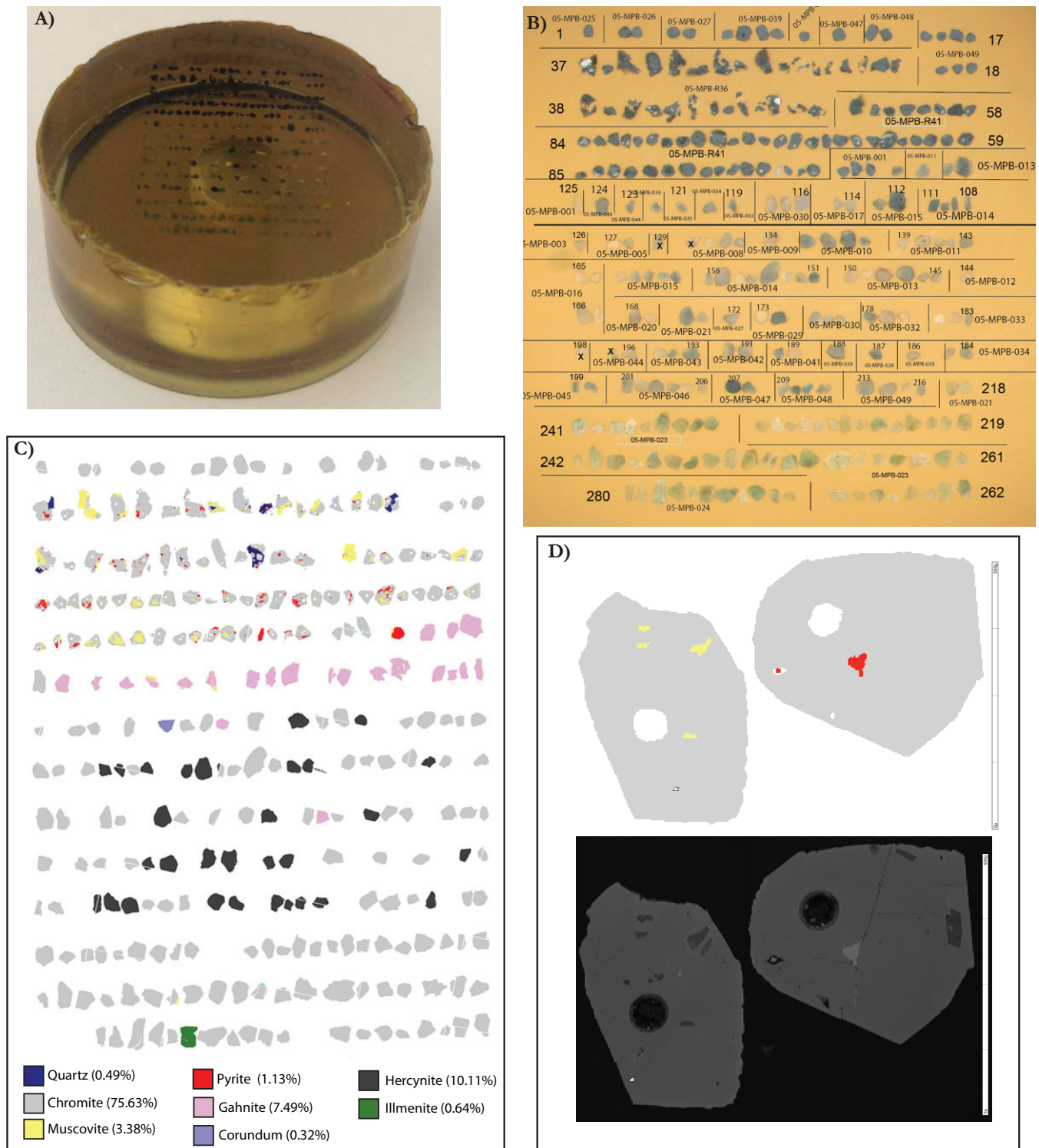
Fig. 2. Example of indicator mineral chemistry workflow from epoxy mount to laser ablation. **A)** Epoxy-mounted mineral grains after mineral separation. **B)** Optical stereo binocular photomicrograph. **C)** False colour processed Mineral Liberation Analysis (MLA) image. **D)** MLA image of chromite (upper) and corresponding BSE image (lower). Note the circular 50 micron laser ablations spots in each grain.

ination using micro-analytical techniques (Fig. 2A). Most mineral chemical investigation methods examine these indicator mineral mounts using an electron-based instrument. Traditionally, a scanning electron microscope (SEM) is used to examine the spatial distribution of backscatter secondary electrons (BSE), which is a reflection of differences in the average atomic number of an area of a grain. This is done in combi-

nation with energy dispersive spectrometry (EDS) in order to identify relative element concentrations within mineral phases and mineralogy.

The goals of using an SEM are to (1) confirm of mineralogy that has determined through mineral picking, (2) document mineral associations, (3) document mineral textures and morphology (shape, rounding, size, etc.), and (4) identify opti-
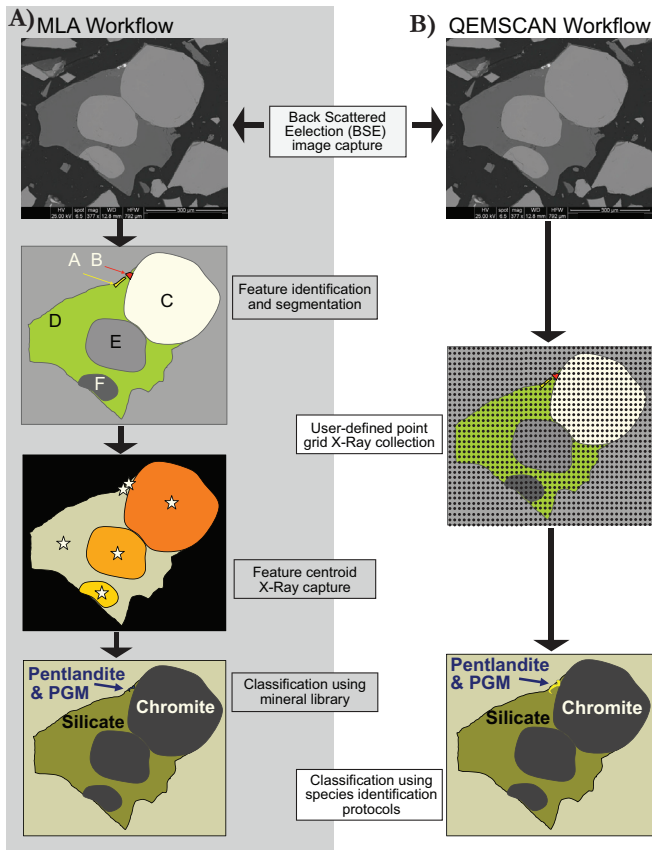
Fig. 3. Comparison of sample work-flow for automated mineralogy for **(A)** mineral liberation analysis and **(B)** QEMSCAN®.

mal mineral grains for further, more costly, mineral chemical characterization. The full characterization of a single epoxy mount with 200 to 500 grains can take 6 to 12 hours on a traditional SEM. Recent advances in automated scanning electron microscopy coupled with energy-dispersive X-ray spectroscopy (EDS) are transforming the analysis of mineral grain mounts. Time-consuming and qualitative mineral descriptions are now been replaced with fast, quantitative, and repeatable SEM analysis. These automated SEM methods provide confirmation of mineralogy, quantification of mineral textures and morphology, and reduces grain mount analysis time to 1 to 2 hours.

The most popular automated SEM supplier is FEI™; the company currently offers a tungsten-based or a field emission gun-based hardware that can be coupled with either Quantitative Evaluation of Minerals by SCANning electron microscopy (QEMSCAN®) or Mineral Liberation Analysis (MLA™) software. Mineral Liberation Analysis was initially developed for the mining industry by the University of Queensland, Australia (JKTech) (Burrows & Gu 2006; Gu *et al.* 2012); QEMSCAN® was developed for the mining industry by CSIRO, Australia (Butcher *et al.* 2000; Gottlieb *et al.* 2000; Pirrie *et al.* 2004; Pirrie & Rollinson 2009). However, both software packages are currently licensed and sold through FEI™ and their regional supply companies (e.g. Systems for Research, Canada).

MLA automated mineralogy is based on high-resolution BSE images, image analyses, and elemental chemistry from EDS. Collections of BSE images are combined to create a mosaic image of an epoxy grain mount (Fig. 3). Each BSE

image is used to remove epoxy from the image, and centroid image analysis segments grains and minerals into individual particles. The MLA software then collects a full X-Ray spectrum (EDS) at the centre of each particle (Fig. 3). In post-collection processing, the full X-Ray spectrum is compared with a user-defined mineral EDS library and the BSE image to create a coherent data set, which includes a false-colour mineral map, modal mineralogy, grain size, mineral associations (occurrence and interlocking), particle properties (roundness, area, shape), and mineral liberation.

QEMSCAN® automated mineralogy is fundamentally different than MLA, in that is based on fast mineral identification using point analysis on a finely spaced grid. Similar to MLA, QEMSCAN® collects BSE images to create a mosaic image of an epoxy grain mount; however, during automated measurement, the system collects EDS spectra along a pre-defined grid (similar to modal counting using a petrographic microscope). QEMSCAN® uses the EDS spectra in combination with the BSE image data to determine areas of epoxy and areas of mineral, minimizing the collection of background data. On mineral phases, a low-count EDS spectrum is collected that allows for ultra-fast discrimination of most minerals. QEMSCAN® also differs from MLA in the way that mineralogy is determined. In MLA, minerals are identified through comparison of unknown EDS with a user-defined EDS database of known minerals. QEMSCAN® uses a built-in library of 72 elemental reference spectra are used to build a composite elemental spectra that is then used in conjunction with user-defined Species Identification Protocols (SIP) to identify discrete minerals. In addition to output data similar to MLA, QEMSCAN® produces elemental maps in addition to mineral maps.

MLA- or QEMSCAN®-generated BSE and false-colour images of a mineral concentrate have many advantages over traditional optical microscopy (Hartner *et al.* 2011; Gu *et al.* 2012; Sylvester 2012): 1) measurement of compositional data, 2) measurement of thousands of points per sample mount, 3) repeatable and quantitative measurements, 4) fully automated work-folk, 5) faster processing time, 6) less training required, 7) modal mineralogy calculated assay data, 8) micron-scale resolution, and 9) better determination of analysis points for texturally difficult (i.e. polymineralic) grains and for choosing grains for in situ chemical or isotopic analyses.

The occurrence and modal quantification of distinct HMC in till is of great importance in the definition of till dispersion trains in many ore exploration programs (i.e. gold); however, many HMC mounts are further characterized for individual mineral chemistry. Many HMC studies ((McClenaghan 2002b; Morris *et al.* 2002; Lehtonen *et al.* 2005 and references therein) have used the occurrence of HMC in bedrock sources coupled with the major and minor element chemistry to identify the provenance and fertility of the HMC.

The quantification of major elements can be obtained quickly for many elements from EDS software using a SEM with detection limits between 2000 and 10,000 ppm (Z>4). However, because EDS requires that individual X-Ray spectra be separated from other X-Ray spectra in a mineral analysis, some X-Ray energies cannot be separated from background radiation (high detection limit) or from X-Ray spectra of other elements (i.e. peak overlap). Most modern EDS detectors have an energy resolution of 130 to 160 eV (Full Width Half Max). For example, the quantitative analysis of molybdenite (MoS_2)

by EDS is not possible because the Mo L alpha line is at 2.2930 keV and overlaps with the S K alpha line at 2.3070 keV.

More commonly, indicator minerals are analyzed for major and minor elements using electron probe microanalyzer (EPMA). In principle, a EPMA is very similar to a SEM, as the electron source and focusing column are nearly identical. However, an EPMA and SEM collect X-Ray data differently. Both instruments collect chemical spectra using an EDS detector, but on a EPMA, spectra are also collected using wavelength dispersive spectroscopy (WDS). During the collection of WDS, spectra are separated by the mechanical diffraction of X-Rays into wavelengths that are individually measured by a detector. Most modern EPMA have up to 5 wavelength dispersive spectrometers, which allows the simultaneous measurement of five elements. EDS and WDS each have advantages and disadvantages. EDS can quickly collect a full X-Ray spectrum in 10s of seconds; whereas WDS is time consuming, requiring the movement of a diffraction crystal to measure each individual element. Much of the spectral interference encountered during EDS can be eliminated by the high-energy resolution of WDS (~10 eV). The biggest disadvantage of both EDS and WDS systems are the detection limits (~0.1 and 0.01%, respectively) for most elements in the characterization of mineral chemistry.

Mass spectrometry-based techniques

The use of laser ablation inductively coupled plasma mass spectrometry (LA-ICP-MS) for characterization of mineral chemistry has grown since its first application to geological media (Hale *et al.* 1984; Jackson *et al.* 1992). Conceptually the application of laser ablation for mineral chemical and isotopic analyses is a straightforward, albeit destructive, technique. A short-pulsed (femto- to nanosecond) laser ablates a small volume (~8000 um³) of a mineral sample over a period of 10s of seconds. During ablation the mineral is converted into vapour and aerosol components. This material is then continually transferred in an Ar or He carrier gas to be ionized in an inductively coupled plasma and mass analyzed in either a quadrupole or magnetic-sector mass spectrometer.

There are several instrument parameters that must be optimized to measure element and isotopic compositions of a mineral by LA-ICP-MS (Arevalo *et al.* 2010; Rogers *et al.* 2010; Koch & Gunther 2011); these include (1) laser pit size, (2) laser wavelength, (3) laser pulse-rate, (4) mass spectrometer, (5) matrix-match standards, and (6) curve calibration. Most laser ablation instruments are capable of adjusting the laser beam size from 1–2 to 300 microns, however, most analyses are completed at ~30 microns. If a laser pit is too small then not enough material is ablated to create a suitable signal in the mass spectrometer. If a laser pit is too large, the mass spectrometer detector may become saturated or go beyond the element calibration curve.

Numerous studies have examined the analyses of geological media using variable laser wavelengths (Motelica-Hieno & Donard 2001; Guillong *et al.* 2005; Jochum *et al.* 2007; Gaboardi & Humayun 2009) and laser pulse-rates (Poitrasson *et al.* 2003; Gonzalez *et al.* 2007; Horn 2008; Saetveit *et al.* 2008; Glaus *et al.* 2010), and collectively using similar laser energies. There is consensus that shorter wavelengths and higher laser pulse rates produce superior data that require fewer corrections for elemental and isotopic bias. In mineral analysis, a shorter

wavelength laser (i.e. 193 nm vs 213 nm) produces a flat-bottomed and sharp-walled ablation pit. The higher pulse rate (i.e. femtosecond vs nanosecond) of the mineral, the less thermal heating occurs with a lower abundance of secondary condensates (Gunther & Heinrich 1999; Gunther *et al.* 2000; Poitrasson *et al.* 2003; Hirata *et al.* 2004).

Ultimately, the ability of LA-ICP-MS to measure low-concentration elemental and isotopic data is a function of the mass spectrometer paired with the laser ablation system. There are three options for inductively coupled plasma mass spectrometers for use in laser ablation: 1) quadrupole, 2) high-resolution single collector, and 3) high-resolution multi-collector.

By far the most common mass spectrometer used in laser ablation studies of mineral chemistry is the quadrapole mass analyzer. These instruments filter ions created in the plasma by mass and charge (m/z) as they travel to the detector using variable DC voltages on four parallel stainless steel rods. By adjusting the DC voltage on the quadrupoles, the transient ions created in laser ablation can be filtered and analyzed for most of the periodic table in milliseconds (Hill 2007).

In high-resolution mass spectrometers, ions created in laser ablation and in the inductively coupled plasma are passed along a curved flight path through magnetic and electrical fields to disperse ions according to their momentum and translational energy (Willard 1988). By adjusting the magnetic and electrostatic fields, the transient ions arriving at the detector(s) can be varied on the basis of mass. Because of this geometry, the mass resolution of these instruments is superior to that of quadrupole instruments (e.g. ~10,000 versus ~600, respectively). As such, fractions of mass unit can be effectively separated during analysis, allowing for separation of polyatomic interferences (Hill 2007).

For effective ion transmission through both the magnetic and electrical sectors, ions are accelerated at much higher energies than in quadrapole instruments (e.g. 10 kV versus 10 eV, respectively). As such, less ion scattering is created and lower detection limits are observed using high-resolution instruments. For many mineral chemical applications, a high-resolution mass spectrometer commonly has only one detector. However, in applications where isotopic ratios are measured, high-resolution instruments commonly have several detectors (known as multi-collector). These instruments can measure individual isotopes (i.e. ^{204}Pb, ^{206}Pb, ^{207}Pb, ^{208}Pb) simultaneously, without adjustment of the magnetic or electric sectors, which yields superior isotopic ratios.

Quadrupole and high-resolution mass spectrometers each have advantages and disadvantages in mineral chemical analyses using laser ablation. In quadrapole instruments, a wide range of elements (i.e. m/z) can be analyzed very quickly, compared to magnetic and electrical field sector instruments. In high-resolution instruments, the magnetic sector must be adjusted and allowed to stabilize before analyzing of the next mass range (Giessmann & Greb 1994; Jakubowski *et al.* 1998). Given the transient nature of laser ablation analysis, a quadrapole instrument is much better suited for mineral analyses with varied element mass (i.e. rare earth elements, U, Pb). When there are narrow mass differences (<30%), very small laser ablation pits (<10 microns) or isotopic ratios are needed, for which high-resolution mass spectrometers offer vastly superior precision and detection limits.

Multi-element trace element analysis by LA-ICP-MS has not been universally adopted for mineral analysis because there is a
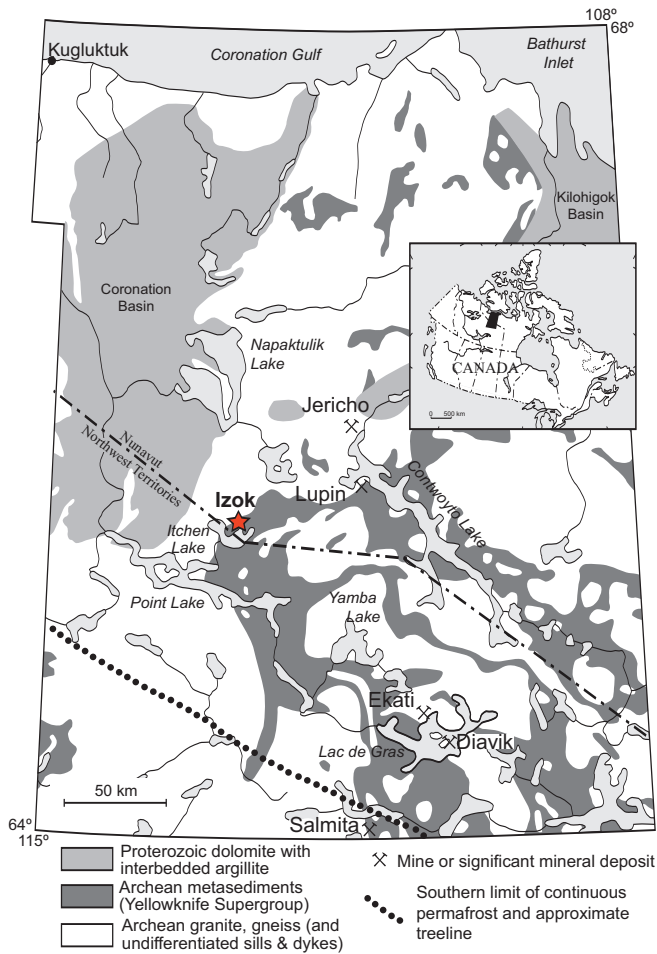
Fig. 4. Location map of the Izok Lake mineralization, Nunavut, Canada (modified after (Dredge *et al.* 1999; Hicken 2012; Hicken *et al.* 2013).
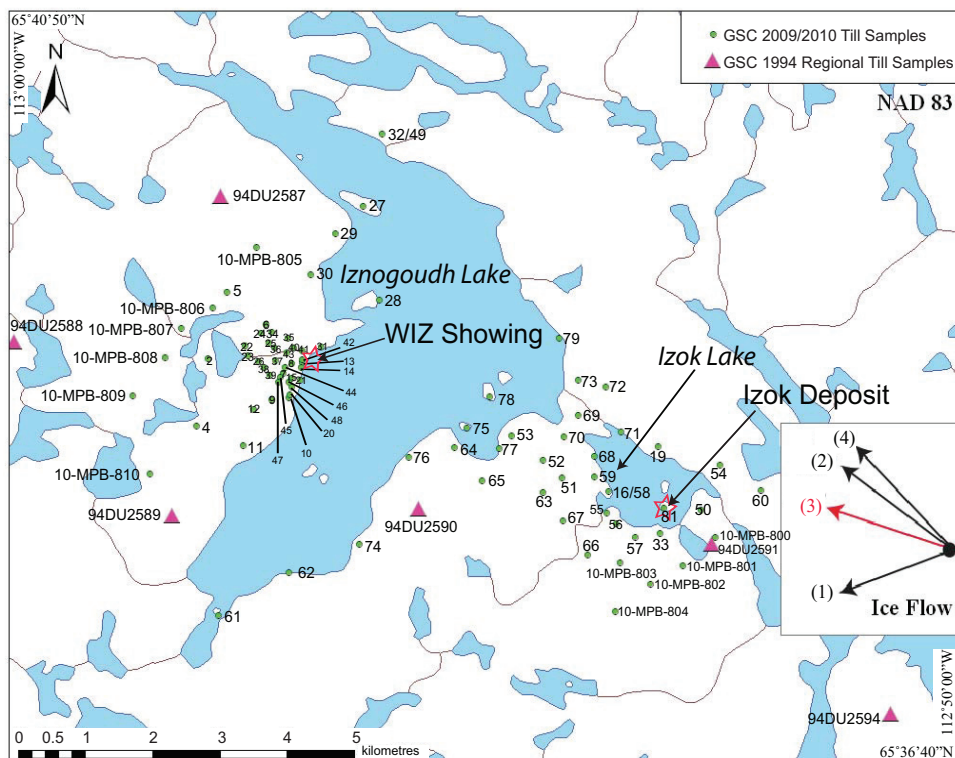
lack of suitable reference materials with similar matrix compositions. Furthermore, there has been a limited effort to find or create matrix-matched standards with variable concentrations of trace elements (i.e. 10, 100, 500 ppm), which is necessary to create standard calibration curves and element quantification. Recently there have been several geological glasses that have been created from rock powder standards (Jochum *et al.* 2000, 2006, 2012; Jochum & Nohl 2008) or by the doping of rock powder standards at variable concentrations (Guillong *et al.* 2005; Jochum *et al.* 2005; Kaiyun *et al.* 2013). The use of these standards in conjunction with EPMA data now allows the reliable quantification of many trace elements in minerals using LA-ICP-MS.

APPLICATIONS IN INDICATOR MINERAL STUDIES

During this workshop, several recent examples will outline the use of mineral chemistry in indicator mineral studies illustrating the methods described above. Due to brevity of an extended abstract, only one case study will be presented.

In exploration for volcanogenic massive sulphide (VMS) deposits in northern Canada, an indicator mineral survey was completed around the Izok Lake mineralization (Fig. 4) occurrence in Nunavut, Canada (McClenaghan *et al.* 2012b,c; McClenaghan *et al.* 2012c; McClenaghan 2013; Paulen *et al.* 2013). Ice-flow mapping in this area shows that glacial trajectories have undergone clockwise rotation from southwest to northwest, in a series of discrete ice-flow phases rather than as a continuous ice-flow change (Kerr *et al.* 1995; Dredge *et al.* 2003; Paulen *et al.* 2013). An early southwest ice-flow was followed by strong west- to west-northwest-trending flow. Surface morphology and ice-flow indicators (e.g. striations) within the Izok Lake area reflect this dominant northwest phase (Paulen *et al.* 2013).

Field documentation of ice-flow in the Izok Lake area, led to till sampling up- and down-ice (Fig. 5). Both bedrock and till

Fig. 5. Locations of till samples (green dots) 1994 Geological Survey of Canada regional samples (pink triangle) and bedrock mineralization (red star) near the Izok Lake deposit (Hicken 2012; Hicken *et al.* 2013).
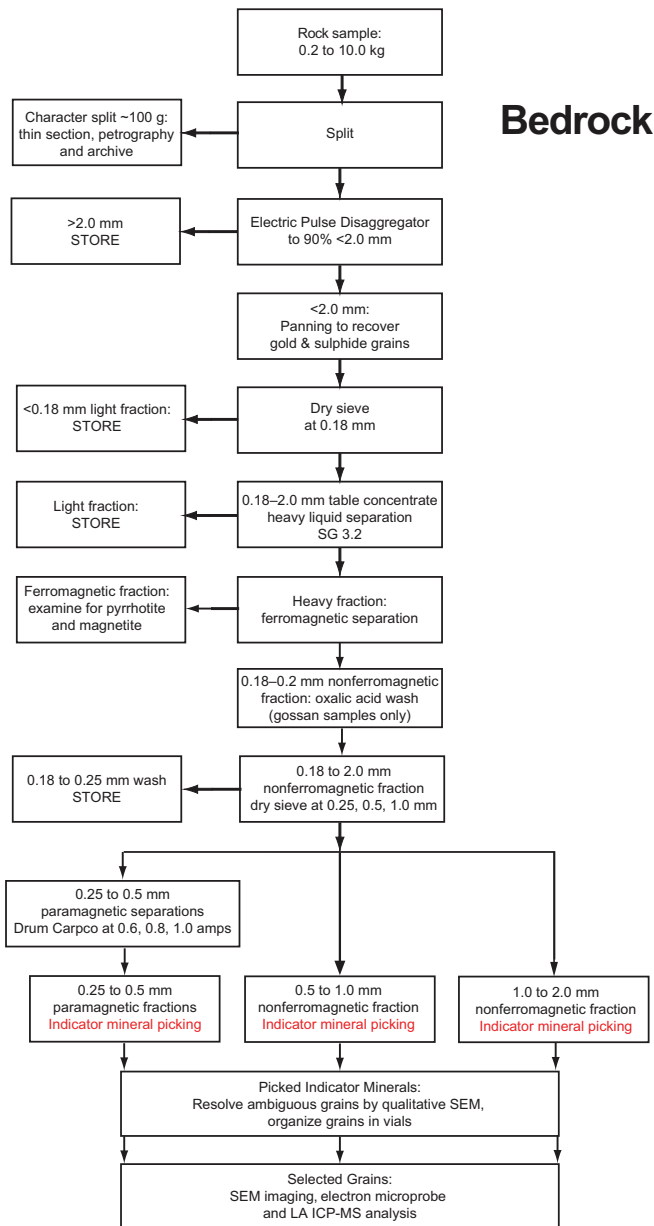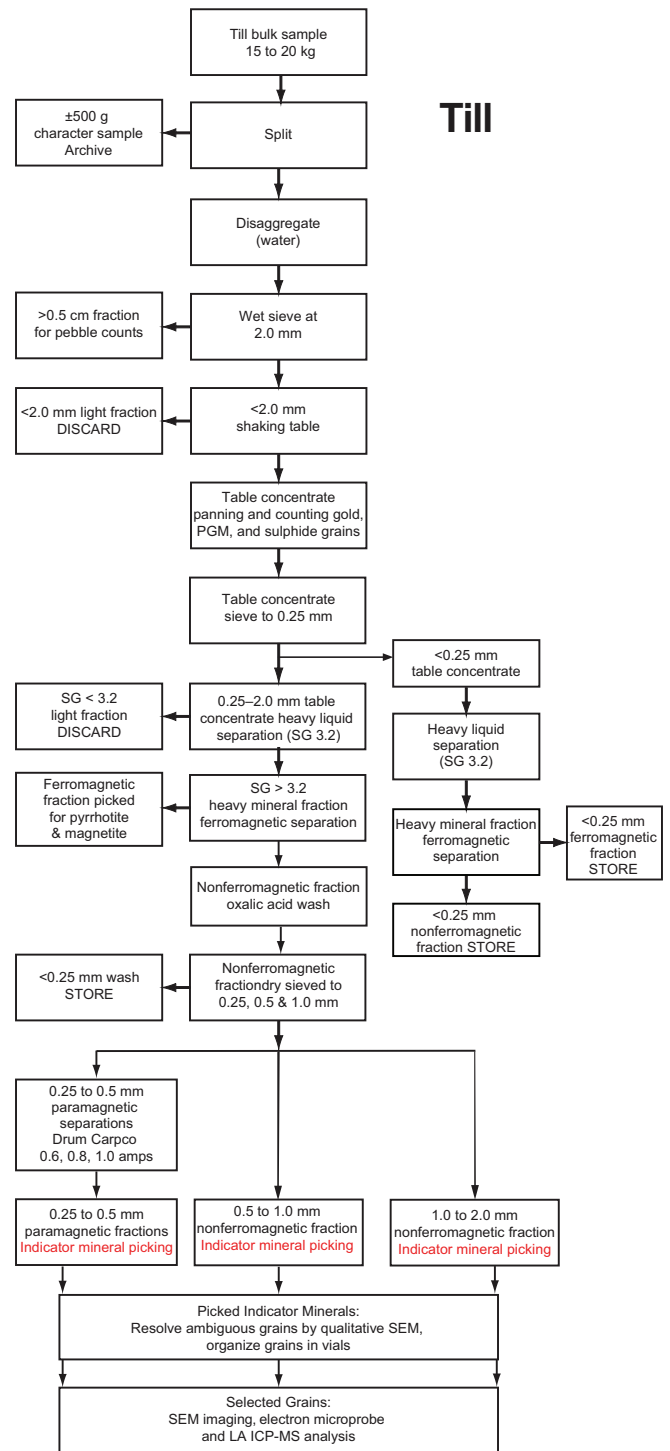
Bedrock

Rock sample: 0.2 to 10.0 kg

→ Split
- Character split ~100 g: thin section, petrography and archive

→ Electric Pulse Disaggregator to 90% <2.0 mm
- >2.0 mm STORE

→ <2.0 mm: Panning to recover gold & sulphide grains

→ Dry sieve at 0.18 mm
- <0.18 mm light fraction: STORE

→ 0.18–2.0 mm table concentrate heavy liquid separation SG 3.2
- Light fraction: STORE

→ Heavy fraction: ferromagnetic separation
- Ferromagnetic fraction: examine for pyrrhotite and magnetite

→ 0.18–0.2 mm nonferromagnetic fraction: oxalic acid wash (gossan samples only)

→ 0.18 to 2.0 mm nonferromagnetic fraction dry sieve at 0.25, 0.5, 1.0 mm
- 0.18 to 0.25 mm wash STORE

→ 0.25 to 0.5 mm paramagnetic separations Drum Carpco at 0.6, 0.8, 1.0 amps

- 0.25 to 0.5 mm paramagnetic fractions **Indicator mineral picking**
- 0.5 to 1.0 mm nonferromagnetic fraction **Indicator mineral picking**
- 1.0 to 2.0 mm nonferromagnetic fraction **Indicator mineral picking**

→ Picked Indicator Minerals: Resolve ambiguous grains by qualitative SEM, organize grains in vials

→ Selected Grains: SEM imaging, electron microprobe and LA ICP-MS analysis

Fig. 6. Flow-sheet outlining the sample processing and picking procedure for bedrock samples processed from the Izok Lake deposit area (Hicken 2012).

Till

Till bulk sample 15 to 20 kg

→ Split
- ±500 g character sample Archive

→ Disaggregate (water)

→ Wet sieve at 2.0 mm
- >0.5 cm fraction for pebble counts

→ <2.0 mm shaking table
- <2.0 mm light fraction DISCARD

→ Table concentrate panning and counting gold, PGM, and sulphide grains

→ Table concentrate sieve to 0.25 mm
→ <0.25 mm table concentrate

→ 0.25–2.0 mm table concentrate heavy liquid separation (SG 3.2)
- SG < 3.2 light fraction DISCARD

→ Heavy liquid separation (SG 3.2)

→ SG > 3.2 heavy mineral fraction ferromagnetic separation
- Ferromagnetic fraction picked for pyrrhotite & magnetite

→ Heavy mineral fraction ferromagnetic separation
- <0.25 mm ferromagnetic fraction STORE
- <0.25 mm nonferromagnetic fraction STORE

→ Nonferromagnetic fraction oxalic acid wash

→ Nonferromagnetic fraction dry sieved to 0.25, 0.5 & 1.0 mm
- <0.25 mm wash STORE

→ 0.25 to 0.5 mm paramagnetic separations Drum Carpco 0.6, 0.8, 1.0 amps

- 0.25 to 0.5 mm paramagnetic fractions **Indicator mineral picking**
- 0.5 to 1.0 mm nonferromagnetic fraction **Indicator mineral picking**
- 1.0 to 2.0 mm nonferromagnetic fraction **Indicator mineral picking**

→ Picked Indicator Minerals: Resolve ambiguous grains by qualitative SEM, organize grains in vials

→ Selected Grains: SEM imaging, electron microprobe and LA ICP-MS analysis

Fig. 7. Flow-sheet outlining the sample processing and picking procedure for till samples processed from the Izok Lake deposit area (Hicken 2012).

Table 1. Comparison of sizes (mm) of key indicator minerals observed in polished thin sections, heavy mineral concentrates, and pan concentrates.

Mineral	Size Range in Polished Thin Section (mm)	Size Range in Heavy Mineral Concentrate (mm)	Size Range in Pan Concentrate (µm)
Pyrite	0.1-6	0.25-1.0	25-200
Chalcopyrite	0.1-5	0.25-1.0	15-200
Sphalerite	0.2-5	0.25-1.0	15-100
Galena	0.01-0.6	0.25-0.50	15-100
Gahnite	0.2-3.0	0.25-1.0	n/a
Staurolite	0.2-1.3	0.25-0.50	n/a
Axinite	0.4-2.0	0.25-0.50	n/a

samples were processed for geochemistry, HMC mineral counts, and HMC mineral chemistry (Figs. 6, 7). The 0.25–0.5, 0.5–1.0, and 1.0–2.0 mm non-ferromagnetic fractions of the bedrock and till samples were examined using optical techniques (Fig. 8). Representative thin sections were made, in addition to mineral grain mounts based on indicator minerals counted/selected during optical examination (Table 1). Thin sections and grain mounts were examined using MLA-ESEM (Figs. 9, 10) to quantify modal mineralogy, mineral associations,
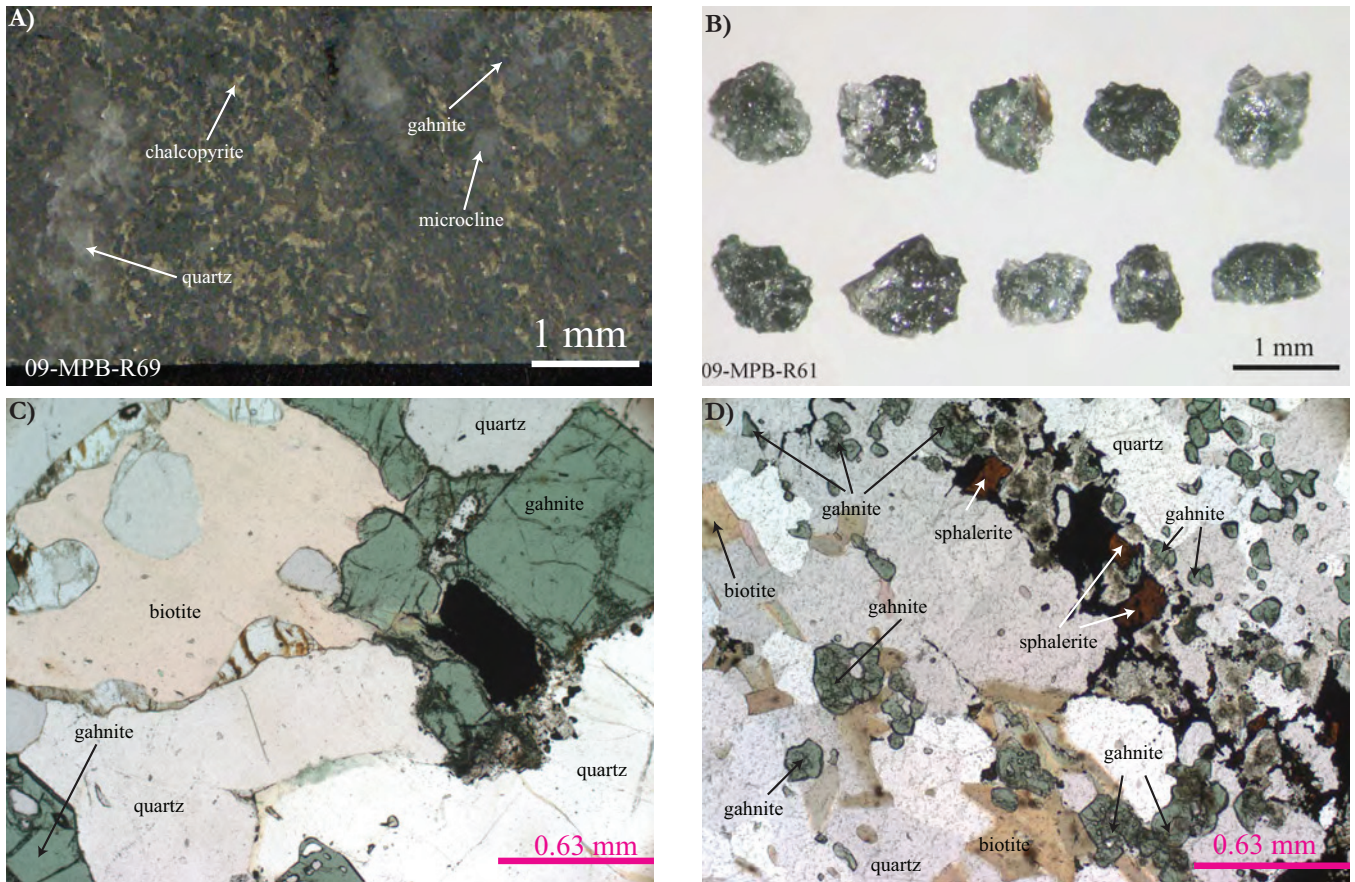
Fig. 8. Gahnite in **(A)** polished slab of drill core (sample 09-MPB-R69); **(B)** grains from a heavy mineral concentrate (sample 09-MPB-R61); **(C)** polished thin section (sample 09-MPB-R37); and **(D)** polished thin section (sample 09-MPB-R41B).
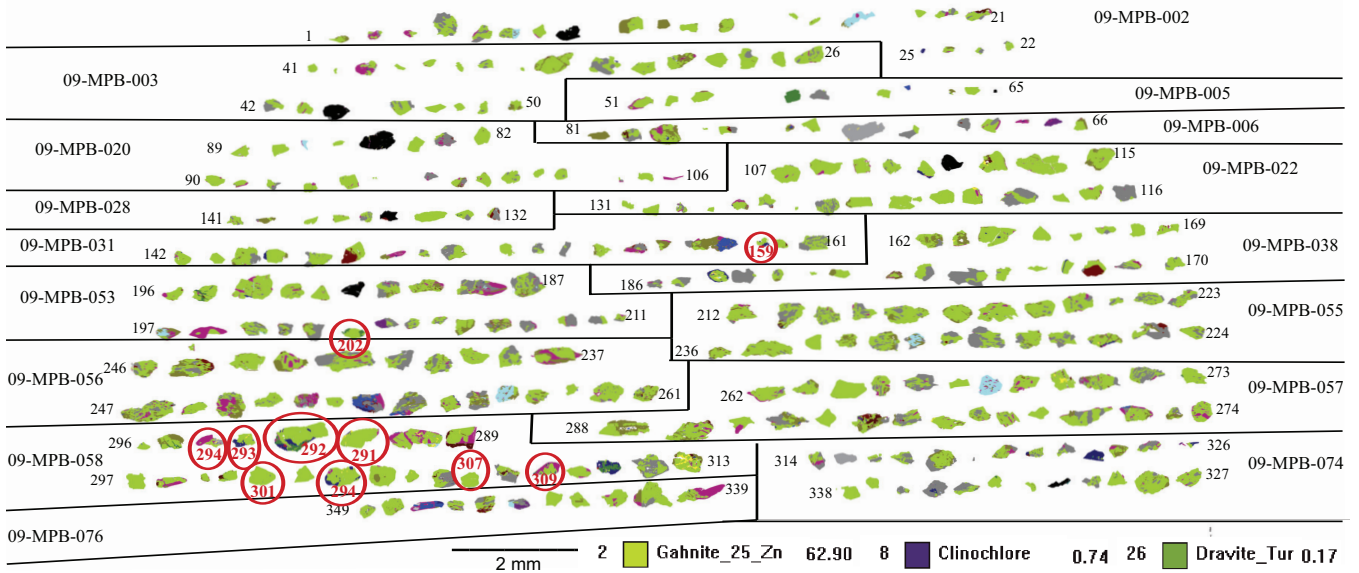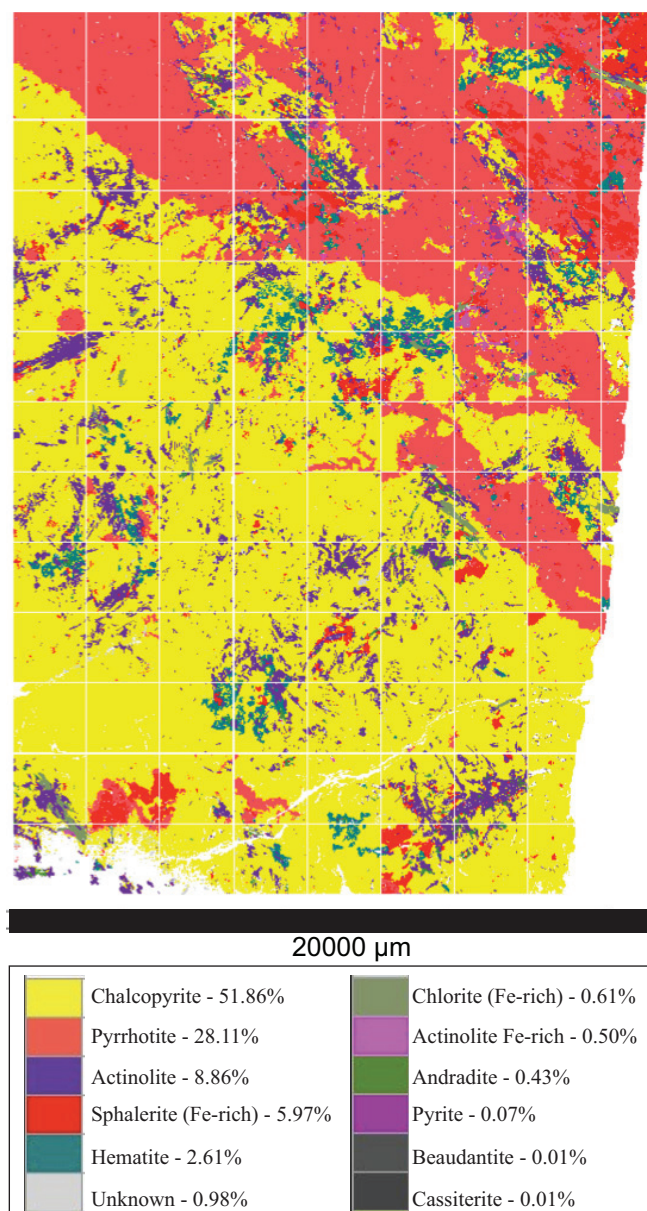

Fig. 9. MLA-SEM image of gahnite grain mount 10-0269-P01 from Izok Lake samples. Adhering gangue mineral compositions are indicated with various colours outlined in the legend. Till sample numbers are listed on the outer sides of the image and grain numbers are listed at the end of each row. Red circles indicate those grains for which the LA-ICP-MS/EPMA mineral chemistry is anomalous (Hicken 2012; Hicken *et al.* 2013).
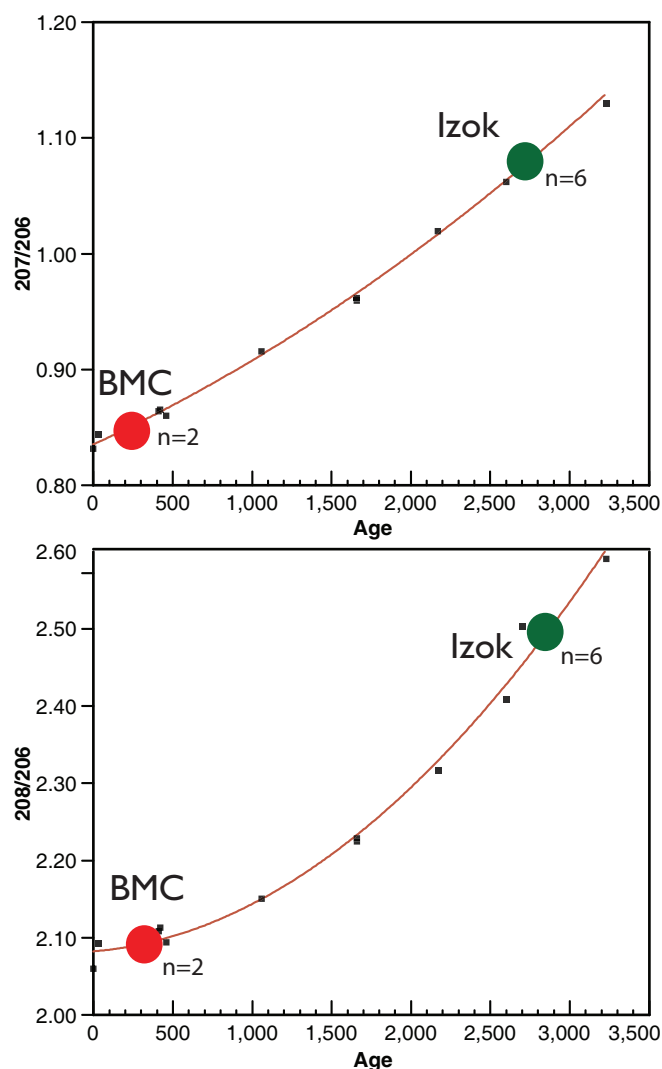
2	Gahnite_25_Zn	62.90	8	Clinochlore	0.74	26	Dravite_Tur	0.17
14	Quartz	15.67	1	Gahnite_35_Zn	0.72	29	Unknown	0.06
13	Muscovite	6.82	20	Ripidolite	0.56	15	Apatite	0.03
12	Biotite	5.52	9	Epidote	0.52	4	Spess_Alm	0.02
7	Ca_Amphibole	2.01	5	Sillimanite	0.33	18	Monazite	0.02
3	Gahnite_Crackle	1.46	21	Albite	0.32	17	Ilmenite	0.02
19	Spinel_loFe_tr_Zi	0.98	6	Corundum	0.28	28	Xenotime	0.01
11	Microcline	0.81						

Fig. 10. MLA image of 09-MPB-R60 (massive sulphide) from Izok Lake showing percentages of chalcopyrite, pyrrhotite, actinolite, sphalerite, hematite/magnetite, and trace minerals (Hicken 2012).

Fig. 11. LA-ICP-MS quadrupole Pb isotopic ratios for gahnite. **A)** $^{207}Pb/^{206}Pb$ age relations for Izok Lake (green circles) and Halfmile Lake (Bathurst Mining Camp, New Brunswick: red circles); **B)** $^{208}Pb/^{206}Pb$ age relations for Izok Lake (green circles) and Halfmile Lake (Bathurst Mining Camp, New Brunswick: red circles). Red line is an approximation of terrestrial lead isotopic evolution (Stacey & Kramers 1975). High-precision U/Pb ages for Halfmile Lake is 465 Ma (van Staal *et al.* 2003), for is Izok Lake is 2623 ± 20 Ma (Mortensen *et al.* 1988), and for Izok Lake is 2680.5 +7/-3 Ma (J. Gebert, unpub. 1995).

grain shape, and grain size. EPMA was completed on a selection of indicator minerals and LA-ICP-MS was conducted on a subset of gahnite grains (>50 microns) for trace element and Pb/Pb dating (Fig. 11).

FUTURE DIRECTIONS IN MINERAL CHEMISTRY

Need for novel methods

The identification of discrete indicator minerals in till has greatly influenced mineral exploration. There are well established methods for separation and identification of minerals in HMC. Indicator mineral chemistry has been used to identify bedrock sources and assess their fertility. The question then becomes, "Why do we need new techniques in the application of mineral chemistry to HMC?"

Successful mineral exploration using sediments and HMC requires a high degree of specialization. This type of work requires a person with not only a background in bedrock geology and ore deposits, but also a person with training in sample collection and preparation, mineralogy, analytical chemistry, and quaternary geology. Current exploration models use a team approach, where each individual contributes their own area of expertise. At present, mineral separation methods have been well established for size-fractions larger than 0.063 mm, but these methods are slow, expensive, and require a highly qualified mineralogist.

New HMC and mineral chemical methods are currently being developed to include a greater number of deposit types (e.g. volcanogenic massive sulphides, uranium, Ni-Cu-PGE, rare earth elements), to utilize the smaller size (i.e. <0.063 mm) and less dense fractions (i.e. <2.85 g/cm³) of samples, and

incorporate new, faster, and more accessible analytical instruments (i.e. hyperspectral, MLA express). Development of these new methods will decrease the need for extensive specialized training, decrease the time and cost of HMC characterization, extend the spatial footprint of dispersion trains (i.e. smaller and farther), and ultimately lead to the identification of new indicator minerals in uncharacterized mineralized systems.

REFERENCES

Arevalo, R., Bellucci, J. & McDonough, W.F. 2010. GGR Biennial review: Advances in laser ablation and solution ICP-MS from 2008 to 2009 with particular emphasis on sensitivity enhancements, mitigation of fractionation effects and exploration of new applications. *Geostandards and Geoanalytical Research*, **34**, 327–341.

Averill, S.A. 2011. Viable indicator minerals in surficial sediments for two major base metal deposit types; Ni-Cu-PGE and porphyry Cu. *Geochemistry Exploration, Environment, Analysis*, **11**, 279–291.

Averill, S.A. 2013. Discovery and delineation of the Rainy River gold deposit using glacially dispersed gold grains sampled by deep overburden drilling; a 20 year odyssey. *In:* Paulen, R.C. & McClenaghan, M.B. (eds.) *New Frontiers for Exploration in Glaciated Terrain*. Geological Survey of Canada, Open File **7374**, 37–46.

Averill, S.A. & Zimmerman, J.R. 1984. The riddle resolved; the discovery of the Partridge gold zone using sonic drilling in glacial overburden of Waddy Lake, Saskatchewan. *CIM Bulletin*, **77**, 88.

Burrows, D. & Gu, Y. 2006. JKMRC mineral liberation analyser – a modern tool for ore characterisation and plant optimization. *In:* Proceedings Metallurgical Plant Design and Operating Strategies 2006. Australasian Institute of Mining and Metallurgy, 125–139.

Butcher, A.R., Helms, T.A., Gottlieb, P., Bateman, R., Ellis, S. & Johnson, N.W. 2000. Advances in the quantification of gold deportment by QEM-SCAN®. *In:* Proceedings of 7th Mill Operators Conference, October 12–14 2000, Kalgoorlie, Australia 2000. Australasian Institute of Mining and Metallurgy, 267–271.

Craw, D., Youngson, J.H., Koons, P.O. & Minter, W.E.L. 1999. Gold dispersal and placer formation in an active oblique collisional mountain belt, Southern Alps, New Zealand. *Economic Geology*, **94**, 605–614.

Dredge, L., Kerr, D. & Ward, B. 2003. *Surficial geology, Point Lake, District of Mackenzie, Northwest Territories*. Geological Survey of Canada, Map 1890A.

Dredge, L.A., Kerr, D.E. & Wolfe, S.A. 1999. Surficial materials and related ground ice conditions, Slave Province, N.W.T., Canada. *Canadian Journal of Earth Sciences*, **36**, 1227–1238.

Eppinger, R.G., Kelley, K.D., Fey, D.L., Giles, S.A. & Smith, S.M. 2011. Exploration case study using indicator minerals in till at the giant Pebble porphyry Cu-Au-Mo deposit, southwest Alaska, USA. *Vuorimiesyhdistyksen Tutkimusseloste. Sarja B*, **92-4**, 41–48.

Gaboardi, M. & Humayun, M. 2009. Elemental fractionation during LA-ICP-MS analysis of silicate glasses: implications for matrix-independent standardization. *Journal of Analytical Atomic Spectrometry*, **24**, 1188–1197.

Giessmann, U. & Greb, U. 1994. High-resolution ICP-MS - a new concept for elemental mass-spectrometry. *Journal of Analytical Chemistry*, **350**, 186–193.

Glaus, R., Kaegi, R., Krumeich, F. & Gunther, D. 2010. Phenomenological studies on structure and elemental composition of nanosecond and femtosecond laser-generated aerosols with implications on laser ablation inductively coupled plasma mass spectrometry. *Spectrochimica Acta Part B-Atomic Spectroscopy*, **65**, 812–822.

Gonzalez, J.J., Liu, C.Y., Wen, S.B., Mao, X.L. & Russo, R.E. 2007. Metal particles produced by laser ablation for ICP-MS measurements. *Talanta*, **73**, 567–576.

Gottlieb, P., Butcher, A.R., Tun, E.H. & Sutherland, D.N. 2000. Applications of automated process mineralogy. *In: Proceedings*. International Congress on Applied Mineralogy, **6**, 321–323.

Gu, Y., Schouwstra, R. & Rule, C. 2012. The value of automated mineralogy. *In:* Innovative Processing for Sustainable Growth. 26th International Mineral Processing Congress, September 24–28 2012, New Delhi, India, 1726–1732.

Guillong, M., Hametner, K., Reusser, E., Wilson, S.A. & Guenther, D. 2005. Preliminary characterisation of new glass reference materials (GSA-1G, GSC-1G, GSD-1G and GSE-1G) by laser ablation-inductively coupled plasma-mass spectrometry using 193 nm, 213 nm and 266 nm wavelengths. *Geostandards and Geoanalytical Research*, **29**, 315–331.

Gunther, D. & Heinrich, C.A. 1999. Comparison of the ablation behaviour of 266 nm Nd: YAG and 193 nm ArF excimer lasers for LA-ICP-MS analysis. J*ournal of Analytical Atomic Spectrometry*, **14**, 1369–1374.

Gunther, D., Horn, I. & Hattendorf, B. 2000. Recent trends and developments in laser ablation-ICP-mass spectrometry. *Fresenius Journal of Analytical Chemistry*, **368**, 4–14.

Hale, M., Thompson, M. & Wheatley, M.R. 1984, Laser ablation of stream-sediment pebble coatings for simultaneous multi-element analysis in geochemical exploration. *Journal of Geochemical Exploration*, **21**, 361–371.

Hartner, R., Walters, S.G. & Berry, R. 2011. Optical and SEM-based microscopy integration for optimisation of geometallurgical modelling and ore deposit characterisation. *In:* Proceedings of 1st AusIMM International Geometallurgy Conference 2011, GeoMet 2011, September 5–7 2011, Brisbane, 157–162.

Hicken, A. 2012. Glacial Dispersal Of Indicator Minerals From The Izok Lake Zn-Cu-Pb-Ag Vms Deposit, Nunavut, Canada. M.Sc. thesis, Queen's University, Kingston, Ontario.

Hicken, A.K., McClenaghan, M.B., Paulen, R.C., Layton-Matthews, D., Averill, S.A. & Crabtree, D. 2013. *Indicator mineral signatures of the Izok Lake Zn-Cu-Pb-Ag volcanogenic massive sulphide deposit, Nunavut: Part 2 till*. Geological Survey of Canada, Open File **7343**. doi:10.4095/293033

Hill, S.J. 2007. *Inductively Coupled Plasma Spectrometry and its Applications*. Wiley-Blackwell.

Hirata, T., Asada, Y., Apinya, T., Ohno, T., Iizuka, T., Hayano, Y., Tanimizu, M. & Orihashi, Y. 2004. Improvements in the precision and accuracy of elemental and isotopic analyses of geochemical samples by a laser ablation-ICP-mass spectrometer. *Bunseki Kagaku*, **53**, 491–501.

Horn, I. 2008. Comparison of femtosecond and nanosecond laser interactions with geologic matrices and their influence on accuracy and precision of LA-ICP-MS data. In: Sylvester, P. (ed.) Laser Ablation ICP–MS in the Earth Sciences: Current Practices and Outstanding Issues. Mineralogical Association of Canada, Short Course **40**, 53–65.

Jackson, S.E., Longerich, H.P., Dunning, G.R. & Fryer, B.J. 1992. The application of laser-ablation microprobe - inductively coupled plasma-mass spectrometry (LAM-ICP-MS) to in situ trace-element determinations in minerals. *Canadian Mineralogist*, **30**, 1049–1064.

Jakubowski, N., Moens, L. & Vanhaecke, F. 1998, Sector field mass spectrometers in ICP-MS. *Spectrochimica Acta Part B-Atomic Spectroscopy*, **53**, 1739–1763.

Jochum, K.P., Dingwell, D.B., Rocholl, A., Stoll, B., Hofmann, A.W., Becker, S., Besmehn, A., Bessette, D., Dietze, H. J., Dulski, P., Erzinger, J., Hellebrand, E., Hoppe, P., Horn, I., Janssens, K., Jenner, G. A., Klein, M., McDonough, W.F., Maetz, M., Mezger, K., Muenker, C., Nikogosian, I.K., Pickhardt, C., Raczek, I., Rhede, D., Seufert, H.M., Simakin, S.G., Sobolev, A.V., Spettel, B., Straub, S., Vincze, L., Wallianos, A., Weckwerth, G., Weyer, S., Wolf, D. & Zimmer, M. 2000. The preparation and preliminary characterisation of eight geological MPI-DING reference glasses for in-situ microanalysis. *Geostandards and Geoanalytical Research*, **24**, 87–133.

Jochum, K.P. & Nohl, U. 2008, Reference materials in geochemistry and environmental research and the GeoReM database. *Chemical Geology*, **253**, 50–53.

Jochum, K.P., Nohl, U., Rothbarth, N., Schwager, B., Stoll, B. & Weis, U. 2012. Geostandards and Geoanalytical Research Bibliographic Review 2011. *Geostandards and Geoanalytical Research*, **36**, 415–419.

Jochum, K.P., Stoll, B., Herwig, K. & Willbold, M. 2007. Validation of LA-ICP-MS trace element analysis of geological glasses using a new solid-state 193 nm Nd: YAG laser and matrix-matched calibration. *Journal of Analytical Atomic Spectrometry*, **22**, 112–121.

Jochum, K. P., Stoll, B., Herwig, K., Willbold, M., Hofmann, A. W., Amini, M., Aarburg, S., Abouchami, W., Hellebrand, E., Mocek, B., Raczek, I., Stracke, A., Alard, O., Bouman, C., Becker, S., Duecking, M., Braetz, H., Klemd, R., de Bruin, D., Canil, D., Cornell, D., de Hoog, C.-J., Dalpe, C., Danyushevsky, L., Eisenhauer, A., Gao, Y., Snow, J. E., Groschopf, N., Guenther, D., Latkoczy, C., Guillong, M., Hauri, E.H., Hoefer, H.E., Lahaye, Y., Horz, K., Jacob, D.E., Kasemann, S.A., Kent, A.J.R., Ludwig, T., Zack, T., Mason, P.R.D., Meixner, A., Rosner, M., Misawa, K., Nash, B.P., Pfaender, J., Premo, W.R., Sun, W.D., Tiepolo, M., Vannucci, R., Vennemann, T., Wayne, D. & Woodhead, J.D. 2006, MPI-DING reference glasses for in situ microanalysis; new reference values for element concentrations and isotope ratios. *Geochemistry, Geophysics, Geosystems G^3*, **7**. doi:10.1029/2005GC001060

Jochum, K.P., Willbold, M., Raczek, I., Stoll, B. & Herwig, K. 2005. Chemical characterisation of the USGS reference glasses GSA 1G, GSC-1G, GSD-1G, GSE-1G, BCR-2G, BHVO-2G and BIR-1G using EPMA, Id-Tims, ID-ICP-MS and LA-ICP-MS. *Geostandards and Geoanalytical Research*, **29**, 285–302.

Kaiyun, C., Honglin, Y., Zhian, B., Chunlei, Z. & Mengning, D. 2013. Precise and accurate in situ determination of lead isotope Ratios in NIST, USGS, MPI-DING and CGSG glass reference materials using Femtosecond laser

ablation MC-ICP-MS. *Geostandards and Geoanalytical Research*, doi:10.1111/j.1751-908X.2013.00223.x

Kelley, K.D., Lang, J. & Eppinger, R.G., 2010. Exploration geochemistry at the giant Pebble porphyry Cu-Au-Mo deposit, Alaska. *SEG Newsletter*, **80**, 18–23.

Kerr, D.E., Dredge, L.A., Ward, B.C. & Gebert, J.S. 1995. Quaternary geology and implications for drift prospecting in the Napaktulik Lake, Point Lake, and Contwoyto Lake map areas, Northwest Slave Province, Northwest Territories. *In: Current Research*. Geological Survey of Canada, Paper **1995-E**, 201–209.

Koch, J. & Gunther, D. 2011. Review of the state-of-the-art of laser ablation inductively coupled plasma mass spectrometry. *Applied Spectroscopy*, **65**, 155A–162A.

Lehtonen, M.L., Marmo, J.S., Nissinen, A.J., Johanson, B.S. & Pakkanen, L.K. 2005. Glacial dispersal studies using indicator minerals and till geochemistry around two eastern Finland kimberlites. *Journal of Geochemical Exploration*, **87**, 19–43.

McClenaghan, M.B. 2002, Indicator mineral and till geochemical methods for kimberlite exploration in glaciated terrain. *CIM Bulletin*, **95**, 79–84.

McClenaghan, M.B. 2005. Indicator mineral methods in mineral exploration. *Geochemistry: Exploration, Environment, Analysis*, **5**, 233–245.

McClenaghan, M.B. 2013. Volcanogenic massive sulphide exploration in glaciated terrain using till geochemistry and indicator minerals. *In:* Paulen, R.C. (ed.) *New Frontiers for Exploration in Glaciated Terrain*. Geological Survey of Canada, Open-File **7374**, 53–64.

McClenaghan, M.B. & Kjarsgaard, B.A. 2001. Indicator mineral and geochemical methods for diamond exploration in glaciated terrain in Canada. *In:* McClenaghan, M.B. (ed.) *Drift Exploration in Glaciated Terrain*. Geological Society, Special Publication **185**, p. 83-123.

McClenaghan, B. & Kjarsgaard, B.A. 2007. Indicator mineral and surficial geochemical exploration methods for kimberlite in glaciated terrain: examples from Canada. *In:* Goodfellow, W.D. (ed.) *Mineral Deposits of Canada: A Synthesis of Major Deposit Types, District Metallogeny, the Evolution of Geological Provinces, and Exploration Methods*. Geological Association of Canada, Mineral Deposits Division, Special Publication **5**, 983–1006.

McClenaghan, M.B. & Peter, J. 2013. Volcanogenic massive sulphide exploration in glaciated terrain using till geochemistry and indicator minerals. *In:* Paulen, R.C. (ed.) *New Frontiers for Exploration in Glaciated Terrain*. Geological Survey of Canada, Open-File **7374**, 53–64.

McClenaghan, M.B., Thorleifson, L.H. & Dilabio, R.N.W. 2000. Till geochemical and indicator mineral methods in mineral exploration. *Ore Geology Reviews*, **16**, 145–166. doi:10.1016/S0169-1368

McClenaghan, M.B., Ward, B.C., Kjarsgaard, I.M., Kjarsgaard, B.A., Kerr, D.E. & Dredge, L.A. 2002. Indicator mineral and till geochemical dispersal patterns associated with the Ranch Lake kimberlite, Lac de Gras region, NWT, Canada. *Geochemistry - Exploration, Environment, Analysis*, **2**, 299–319.

McClenaghan, M.B., Averill, S.A., Kjarsgaard, I.M., Layton-Matthews, D. & Matile, G. 2011. Indicator mineral signatures of magmatic Ni-Cu deposits, Thompson Nickel Belt, central Canada. *Vuorimiesyhdistyksen Tutkimusseloste, Sarja B*, **92-4**, 67–72.

McClenaghan, B., Budulan, G., Averill, S., Layton-Matthews, D. & Parkhill, M.A. 2012a. *Indicator mineral abundance data for bedrock and till samples from the Halfmile Lake Zn-Pb-Cu volcanogenic massive sulphide deposit, Bathurst Mining Camp, New Brunswick*. Geological Survey of Canada, Open File **7076**.

McClenaghan, B., Hicken, A.K., Averill, S., Paulen, R. & Layton-Matthews, D. 2012b. *Indicator mineral abundance data for bedrock and till samples from the Izok Lake Zn-Cu-Pb-Ag volcanogenic massive sulphide deposit, Nunavut*. Geological Survey of Canada, Open File **7075**.

McClenaghan, B., Hicken, A.K., Paulen, R. & Layton-Matthews, D. 2012c. *Indicator mineral counts for regional till samples around the Izok Lake Zn-Cu-Pb-Ag VMS deposit, Nunavut*. Geological Survey of Canada, Open File **7029**.

McMartin, I. and McClenaghan, M.B. 2001, Till geochemistry and sampling techniques in glaciated shield terrain; a review. *In:* McClenaghan, M.B. (ed.) *Drift Exploration in Glaciated Terrain*. Geological Society. Special Publications, 185, 19–43.

Morris, T.F., Sage, R.P. Ayer, J.A. & Crabtree, D.C. 2002. A study in clinopyroxene composition: implications for kimberlite exploration. *Geochemistry - Exploration, Environment, Analysis*, **2**, 321–331.

Mortensen, J.K., Thorpe, R.I., Padgham, W.A., King, J.E. & Davis, W.J. 1988. U-Pb zircon ages for felsic volcanism in Slave Province, N.W.T. *In: Radiogenic Age and Isotopic Studies: Report 2*. Geological Survey of Canada, Paper **88-2**, 85–95.

Motelica-Hieno, M. & Donard, O.F.X. 2001. Comparison of UV and IR laser ablation ICP-MS on silicate reference materials and implementation of normalisation factors for quantitative measurements. *Geostandards Newsletter-the Journal of Geostandards and Geoanalysis*, **25**, 345–359.

Paulen, R.C., McClenaghan, B. & Hicken, A.K. 2013. Regional and local ice-flow history in the vicinity of the Izok Lake Zn-Cu-Pb-Ag deposit, Nunavut. *Canadian Journal of Earth Sciences*. doi:10.1139/cjes-2013-0064

Pirrie, D., Butcher, A.R., Power, M.R., Gottlieb, P. & Miller, G.L. 2004. Rapid quantitative mineral and phase analysis using automated scanning electron microscopy (QEMSCAN®); potential applications in forensic geoscience. *In:* Pye, K. & Croft, D.J. (eds.) *Forensic Geoscience, Principles, Techniques and Applications*. Geological Society, Special Publication **232**, 123–136.

Pirrie, D. & Rollinson, G. 2009. Use of automated mineral analysis using QEMSCAN® in the characterisation of mine tailings. *Applied Earth Science*, **118**, 32.

Poitrasson, F., Mao, X.L., Mao, S.S., Freydier, R. & Russo, R.E. 2003. Comparison of ultraviolet femtosecond and nanosecond laser ablation inductively coupled plasma mass spectrometry analysis in glass, monazite, and zircon. *Analytical Chemistry*, **75**, 6184–6190.

Rogers, R.R., Fricke, H.C., Addona, V., Canavan, R.R., Dwyer, C.N., Harwood, C.L., Koenig, A.E., Murray, R., Thole, J.T. & Williams, J. 2010. Using laser ablation-inductively coupled plasma-mass spectrometry (LA-ICP-MS) to explore geochemical taphonomy of vertebrate fossils in the upper cretaceous two medicine and Judith River formations of Montana. *Palaios*, **25**, 183–195.

Saetveit, N.J., Bajic, S.J., Baldwin, D.P. & Houk, R.S. 2008. Influence of particle size on fractionation with nanosecond and femtosecond laser ablation in brass by online differential mobility analysis and inductively coupled plasma mass spectrometry. *Journal of Analytical Atomic Spectrometry*, **23**, 54–61.

Sarala, P. & Peuraniemi, V. 2007. Exploration using till geochemistry and heavy minerals in the ribbed moraine area of southern Finnish Lapland. *Geochemistry - Exploration, Environment, Analysis*, **7**, 195–205.

Sauerbrei, J.A., Pattison, E.F. & Averill, S.A. 1987. Till sampling in the Casa-Berardi gold area, Quebec: a case history in orientation and discovery (Canada). *Journal of Geochemical Exploration*, **28**, 297–314.

Stacey, J.S. & Kramers, J.D. 1975, Approximation of terrestrial lead isotope evolution by a two-stage model. *Earth Planet. Science Letters*, **26**, 207–221.

Sylvester, P.J. 2012. Use Of the mineral liberation analyzer (MLA) for mineralogical studies of sediments and sedimentary rocks. *In:* Sylvester, P.J. (ed.) *Quantitative Mineralogy and Microanalysis of Sediments and Sedimentary Rocks*. Mineralogical Association of Canada, Short Course **42**, 285.

Thorleifson, L.H. 1993. Kimberlite indicator mineral tracing on the Canadian Prairie. *Canadian Mining and Metallurgical Bulletin*, **86**, 70.

van Staal, C.R., Wilson, R.A., Rogers, N., Fyffe, L.R., Langton, J.P., McCutcheon, S.R., McNicoll, V. & Ravenhurst, C.E. 2003. Geology and tectonic history of the Bathurst Supergroup, Bathurst mining camp, and its relationships to coeval rocks in southwestern New Brunswick and adjacent mine; a synthesis. *In:* Goodfellow, W.D., McCutcheon, S.R. & Peter, J.M. (eds.) *Massive Sulfide Deposits of the Bathurst Mining Camp, New Brunswick, and Northern Maine*. Economic Geology, Monograph **11**, 37–60.

Ward, B.C., Dredge, L.A., Kerr, D.E. & Kjarsgaard, I.M. 1996. Kimberlite indicator minerals in glacial deposits, Lac de Gras area, NWT. In: LeCheminant, A.N., Richardson, D.G., DiLabio, R.N.W. & Richardson, K.A. (eds.) *Searching for Diamonds in Canada*. Geological Survey of Canada, Open File **3228**, 191–195.

Willard, H.H. 1988. *Instrumental Methods of Analysis*. Wadsworth Publishing Company, 895 p.

Quality assurance and quality control measures applied to indicator mineral studies of glacial sediments at the Geological Survey of Canada

A. Plouffe*, M.B. McClenaghan, R.C. Paulen, I. McMartin, J.E. Campbell & W.A. Spirito

Geological Survey of Canada, 601 Booth Street, Ottawa, Ontario, Canada K1A 0E8
Corresponding author e-mail: aplouffe@nrcan.gc.ca

Fig. 1. Two hoe-picks of the same brand. The top one is nearly new and the bottom one has been used for three field seasons. Note that the old one has visibly lost metallic mass (distance between the white lines), which has, in part, ended up in sediment samples collected.

There are a number of ongoing research projects at the Geological Survey of Canada (GSC) with the objective of enhancing exploration success through the identification of new indicator minerals hosted within, or associated with, a variety of mineral deposit types. These indicator minerals can be recovered from glacial sediments and traced back to their bedrock source as an effective mineral exploration method in glaciated terrain. As research on indicator minerals evolves, quality assurance and quality control (QA/QC) measures must be implemented to ensure that 1) in the field, samples are not contaminated from external sources or from other samples; 2) during sample processing and indicator mineral picking, loss of indicator mineral grains is minimized (close to zero), cross-contamination before and among sample batches does not occur, and minerals are correctly identified; and 3) all reported indicator mineral data include adequate metadata for future reference and comparison. To fulfill these needs, protocols have been developed for ongoing and future research projects at the GSC to ensure indicator mineral data are of the highest quality. These protocols satisfy the requirements of National Instrument 43-101 (2005), which specifies that technical information reported by exploration and mining companies in Canada (such as indicator mineral data) must include details of the quality assurance program being implemented.

These short course notes have been prepared specifically for short course SC07 *Application of Indicator Mineral Methods to Mineral Exploration* offered at the 26th International Applied Geochemistry Symposium, November 2013, in Rotorua, New Zealand. The notes have been presented in a similar workshop offered at the Prospectors and Developers Association of Canada (PDAC) Conference, March 2013 in Toronto, Canada (Plouffe *et al.* 2013) but have been revised based upon constructive comments received at PDAC workshop, and more recent results obtained as part of on-going GSC projects. These notes contain summary and key points addressed in Plouffe *et al.* (in press) and Spirito *et al.* (2011).

FIELD PROCEDURES

Detailed field procedures to accurately locate sample sites, record field notes, and identify the type of glacial sediments being sampled are addressed by Spirito *et al.* (2011). Metallic tools (shovels, picks, hammers, etc.) are generally used for the sampling of glacial sediments. At the onset of a field program, tools should be examined and thoroughly cleaned in order to reduce their role as potential sources of contamination. Paint, varnish, and other types of surface coatings should be removed as they are a potential source of contamination to heavy mineral concentrates. Sampling tools do wear with usage (Fig. 1), and produce metal shavings of various unnatural

forms that should be expected and recognized in heavy mineral concentrates (Fig. 2). Glacial sediment samples collected from diamond drill core can be contaminated with industrial diamonds from the drill bit (Fig. 3). Tools should also be cleaned properly in between samples to avoid cross-contamination (Fig. 4A and 4B). As much as possible, samples should not be manipulated by bare hands or with dirty work gloves, which also represent a potential source of contamination (Fig. 4C). Finally, those collecting the samples should not wear hand jewellery because rings are known sources of contamination (Kontas 1991) and could impact geochemical analyses of heavy mineral concentrates.

© D.G. Paré, 1986
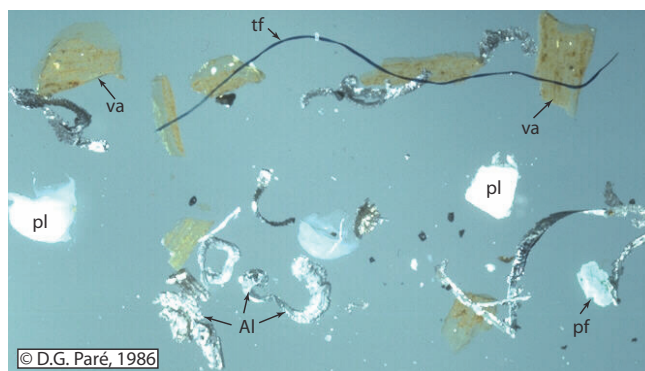
Fig. 2. Examples of contamination in heavy mineral concentrates including plastic from vial cover (pl), textile fibre (tf), aluminum shavings (Al), varnish flakes with traces of wood fibre (va), and paint flakes (pf); photographs from D.G. Paré, Consorminex Incorporated, Gatineau, QC (www.consorminex.com).
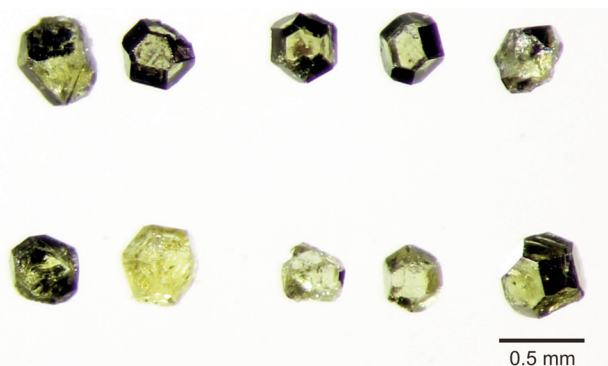
Fig. 3. Industrial diamonds recovered from the heavy mineral fraction of a till sample that was collected from diamond drill core.

Anthropogenic contamination of glacial sediments at sample sites may also affect the indicator mineral component and should be expected in areas proximal to present and past producing mines and related infrastructure (Bajc & Hall 2000; McMartin *et al.* 2002; Hozjan & Averill 2009; Michaud & Averill 2009). For example, gold spheres can be expected in samples collected close to gold mines with assay facilities (DiLabio *et al.* 1988). Although smelter particles can be small (for example 5 to 100 mm in Knight & Henderson 2006), larger particles (0.25 to 0.5 mm) can be expected near smelter sites (Fig. 5 and examples in Henderson *et al.* 1998; McClenaghan *et al.* 2013). At least in one instance, airborne smelter particles are suspected to have been introduced into till samples at the time of sampling (McClenaghan *et al.* 2013). Therefore, near anthropogenic sites, sample bags should be kept closed until the last moment of sample collection and samples should be collected at a minimum depth of 0.5 m (where possible) even if fresh unoxidized and undisturbed till is exposed at surface. All sites where anthropogenic contamination is suspected should be sampled with extreme caution and noted accordingly (Fig. 6). Near-surface till that appears to be undisturbed can actually be highly contaminated in these areas (McMartin *et al.* 1999). Knowledge of the sedimentological properties of till (cf. Evans *et al.* 2006) is essential to identify sediment genesis properly near anthropogenic deposits.

Samples should be collected in new plastic bags (>6 mil), plastic pails, or in metal pails lined with large plastic bags. Rice or cloth bags are not suitable for till or glaciofluvial sediment sampling as they are porous and easily torn, allowing the loss of fine-grained material and/or possible contamination of the sample. Care must be taken when transporting samples from field sites to the laboratory to avoid puncturing the sample bags which could also lead to loss of sample material and/or contamination. The chain of custody of all samples must be monitored and documented to prevent contamination or tampering.

Sample size suitable for recovery of indicator minerals is largely dependent on glacial sediment texture. To obtain an adequate number of sand-sized indicator mineral grains, a sample must contain an average of 5 to 10 kg of sand-sized material (0.063 to 2 mm) (Clifton *et al.* 1969; Averill 2001). Sample size may also be dictated by the range and type of analyses to be performed. In the field, a consistent sample size is collected based on volume, for example a full pail or full sample bag, knowing that a full pail or bag represents an approximate weight of material. The weight of the sediment

Fig. 4. A) A dirty pick with sediment stuck to it after the collection of a sample, and therefore unsuitable for the collection of the next sample. **B)** A cleaned pick ready for the collection of a sample. **C)** Work gloves represent a potential source of contamination.

will vary according to moisture content, sediment compaction, and composition. As a general guide, 10 to 20 kg of sandy-silty till, 20 to 40 kg of clayey till, and 12 to 25 kg of glaciofluvial sediment is required to obtain a representative heavy mineral sand-sized concentrate. At the GSC, samples are often not screened in the field to remove coarse clasts because silt and clay adhering to the larger clasts would be lost from the sample (in other words, potentially losing silt-sized indicator min-
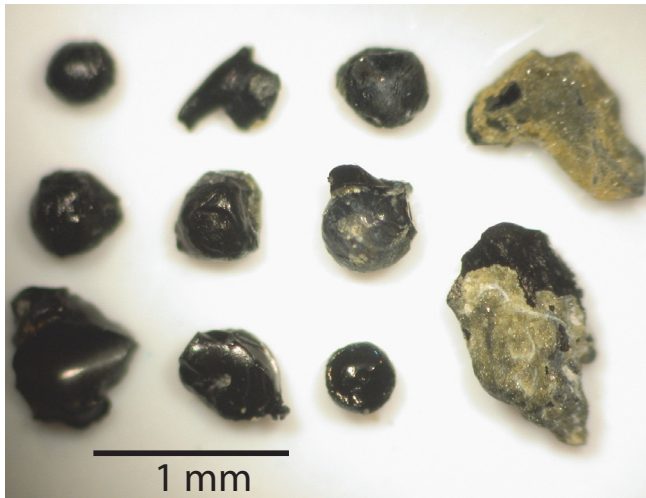
Fig. 5. Smelter particles recovered from till samples collected proximal to the Thompson Ni-Cu mine site in central Canada (McClenaghan *et al.* 2013).

erals such as gold and platinum group minerals), and sieves may represent an additional source of cross-contamination.

Field duplicate samples may be collected to serve two purposes. First, they provide some indication of sediment heterogeneity and site variability. In this case, the duplicate sample can be collected 5 to 10 m away from the original sample hole (site variability) (Fig. 7) or from the exact same sample hole (sediment heterogeneity). For example, duplicate samples collected 300 m down ice of the Izok Lake Zn-Cu-Pb-Ag volcanogenic massive sulphide deposit in Nunavut, Canada, demonstrate till heterogeneity near mineralization (McClenaghan

et al. 2012). The original sample (09-MPB-016: 12.2 kg of <2 mm processed) contains no sphalerite grains and the duplicate sample (09-MPB-058: 11.8 kg of <2 mm processed), collected 5 m from the original site, contains 1500 sphalerite grains in the 0.25 – 0.5 mm fraction. Such a significant difference in mineralogical composition between samples could be a result of either 1) a weathered sphalerite-rich clast in the duplicate sample that was disaggregated during sample processing, or 2) sampling of a discontinuous layer of metal-rich till at the duplicate sample collection. On the other hand, at six field stations not located close to known mineralization, duplicate and matching original samples, collected approximately 10 m apart, were found to contain comparable mineralogy (McMartin *et al.* 2013). The sampling procedures for the duplicate samples need to be clearly stated with the reported results.

Second, field duplicate samples can be used to measure precision for the entire laboratory process — from heavy mineral separation to identification — if both samples (the original and duplicate) are completely homogenized. However, field or laboratory methods for homogenizing unconsolidated sediment samples that will then be used to measure laboratory precision for indicator mineral analysis need to be tested. Glacial sediment heterogeneity and site variability (as exemplified above with till), especially near mineralization, eliminates the possibility of using unmixed samples to measure laboratory precision. An incremental sampling methodology (www.itrcweb.org/ISM-1/Executive_Summary.html; see also their list of references) consisting of taking small sample increments and placing them alternatively in two separate sampling bags, as utilized for the sampling of contaminated soils, could be further tested as a means of collecting homogenized sediment samples for indicator mineral study.

Fig. 6. A till sample site in a region heavily disturbed by anthropogenic activity at the old Pine Point Pb-Zn Mississippi Valley-type mining district, Northwest Territories. Till samples were collected in a former open pit mine, below the original natural land surface (Rice *et al.* 2013), and away from mine waste piles, which consisted of till excavated from the former open pit, mixed with other mine debris.

Fig. 7. Example of a till sampling site with a routine (black arrow) and field duplicate (white arrow) sample collected in the same sedimentary unit and at approximately the same depth.

Fig. 8. A) Sample site of the unconsolidated weathered Silurian-Devonian granite (grus) used for GSC blank heavy mineral samples. **B)** Close-up view of the blank sample material. **C)** Close-up view of the 2–4 mm fraction of the blank material.

PREPARING SAMPLES PRIOR TO INDICATOR MINERAL PROCESSING

Blank and spiked samples should be introduced into a sample batch prior to being shipped to an indicator mineral processing laboratory. Blank samples consist of unconsolidated earth materials devoid of indicator minerals of interest. Currently, the GSC utilizes as a blank a weathered granite (grus) collected from a Silurian-Devonian intrusion of the South Nepisiguit River Plutonic Suite (Wilson 2007) located approximately 66 km west of Bathurst, New Brunswick (Fig. 8). A blank is introduced as the first sample in a batch to monitor cross-contamination potentially derived from previously processed samples. A blank sample should also be introduced immediately after a sample known to contain large abundances of indicator minerals of interest (e.g. collected near known mineralization). In a large sample batch (N>200), a blank sample can be introduced randomly every 50 samples. Blank samples serve to detect cross-contamination, but cannot necessarily prevent it. For example, a blank sample of weathered granite introduced at the beginning of a sample batch at an external processing laboratory, detected the presence of pyrite contamination (10 grains) from another client's previously processed samples (McClenaghan *et al.* 2012). Similarly, contamination (chromite, ruby corundum, cinnabar, pyrite, and chalcopyrite) was detected in quartz blanks introduced at the beginning and throughout a batch of bedrock samples crushed by an electric pulse disaggregator and processed for indicator minerals (Normandeau & McMartin 2013). Again, the contamination was derived from another client's previously processed mineralized samples.

Spiked samples consist of base material into which spiking grains are voluntarily introduced. They are used to quantitatively monitor the effectiveness of a processing laboratory at recovering and identifying specific indicator minerals (Michaud & Averill 2009). These spiked samples are the equivalent to the secondary standards with known elemental concentrations used to monitor accuracy of geochemical analyses (McClenaghan *et al.* in press). The base material should be similar in texture to the rest of the routine samples and its mineralogy known as a result of repetitive indicator mineral separations and analyses. Currently, the GSC uses till recovered from a borrow pit near Almonte, Ontario as its base material for spiking. The material is texturally typical of till derived from the southern Canadian Shield and has an established average mineralogical composition based on repetitive indicator minerals analyses (Plouffe *et al.* in press). The spiking grains should be mineral grains of interest that have been either laser etched (Whiteford 2003) or photographed so that they can be recognized. The spiking grains should be carefully selected to ensure that they are not fractured or well-cleaved, as they could break into smaller particles during the sample processing (Hozjan & Averill 2009; Michaud & Averill 2009). If possible, spiking grains should be ones that have been recovered from other sediment samples. Spiking grains from crushed or disaggregated bedrock may differ in morphology compared to natural grains present in the sample and could bias the assessment of processing and picking recovery. Artificial density beads or cubes with specific size ranges and densities are commercially available and can also be used for spiking (Baumgartner 2006; Gent *et al.* 2011; McClenaghan 2011) with some limitations outlined in Plouffe *et al.* (in press). As part of the protocols implemented at the GSC, it is recommended that 2% of a sample batch be spiked samples.

Blank, spiked, and duplicate samples should have numbers similar to the routine samples so that they cannot be easily recognized by the processing laboratory as quality control inserts. A processing order for all samples should be communicated to the laboratory. For instance, to avoid carry-over contamination, samples known to potentially contain large amounts of indicator minerals of interest (e.g. collected near known mineralization) should be processed last.

LABORATORY PROCEDURES FOR THE RECOVERY OF INDICATOR MINERALS

Towie & Seet (1995), Gent *et al.* (2011), and McClenaghan (2011) provide a summary of several processing methods available for the recovery of indicator minerals from unconsolidated sediments. It should be emphasized that different processing methods will produce concentrates optimized for varying mineral species. Therefore, it is important to ensure that the method used in the laboratory is appropriate for the recovery of the target minerals. Furthermore, as part of the laboratory selection, Doherty (2009) recommends visiting the facility to identify potential steps in the processing where contamination might occur or mineral grains may be lost.

Plouffe *et al.* (in press) describe the heavy mineral processing methods adopted by the GSC. These methods have been utilized by the GSC in various geological settings with glacial sediments of varying textures for more than 25 years with satisfactory results. GSC methods include 1) pre-concentration of the <2 mm size fraction of a large sediment sample using a shaking table (material >2 mm is retained for the identification of clast lithologies); 2) micro-panning of the table concentrates for the counting and determination of the size of small mineral grains with high density (e.g. gold grains, platinum group minerals, uranium, and sulphide minerals); 3) further density concentration of the table concentrate with heavy liquids (typically specific gravity of 3.2 but can also be done at 2.8 and 3.0 depending on the minerals of interest); 4) extraction of the ferromagnetic fraction from the heavy mineral concentrates with a hand magnet; and 5) examination and identification of indicator minerals in three different size fractions: 1.0–2.0 mm, 0.5–1.0 mm, and 0.25–0.50 mm. Electromagnetic separations at precise amperages are used to further separate minerals in the 0.25–0.50 mm fraction as per their magnetic properties that facilitates mineral identification (e.g. McClenaghan 2011). The ferromagnetic fraction can also be examined for the presence of specific indicator minerals, such as pyrrhotite, and the recovery of magnetite (e.g. McMartin *et al.* 2011). Sample weights should be recorded at each step of the processing. Visual identification of potential indicator minerals is carried out using a binocular microscope and is aided by using a scanning electron microscope (SEM) and ultraviolet light.

AFTER RECEIVING DATA AND INDICATOR MINERALS FROM A PROCESSING LABORATORY

Once data are received from the mineral processing and identification laboratory, all QA/QC results should be examined and evaluated. The QA/QC results should then be communicated to the laboratory. Satisfactory results indicate to the lab-

oratory that their procedures are adequate for the recovery and identification of the reported minerals. In the case of perceived errors, laboratory procedures may need to be adjusted.

To verify the precision of the indicator mineral identification, approximately 10% of the mineral concentrates should be re-submitted (Doherty 2009; McClenaghan 2011). Picked mineral grains are usually not recombined with the heavy mineral concentrates, especially if they will be used for further analyses. Those samples should be re-labelled so that they cannot be identified by laboratory personnel.

The chemical composition of indicator minerals provides key information about the genesis of the mineralization, alteration, or bedrock lithology and, in some cases, the mineral fertility of a potential deposit (e.g. diamond grade of a kimberlite). A number of instruments and analytical methods are available to assess and/or determine the composition of mineral grains, including scanning electron microscopy equipped with an energy dispersive X-ray spectrometer (SEM-EDS), electron microprobe (EMP) analysis, laser ablation-inductively coupled plasma mass spectrometry (LA ICP-MS) (Jackson 2009), and secondary ion mass spectrometry (SIMS). Regardless of the selected analytical method, certified mineral reference standards and duplicate grain analyses should be used to monitor analytical accuracy and precision (de Souza 2006; Doherty 2009).

At the GSC, all indicator mineral data including original laboratory reports and mineral chemistry, as well as sample heavy mineral concentrates, unmounted picked grains, and grain mounts are permanently archived, using specific guidelines, for future reference (Spirito *et al.* 2011, 2013).

REPORTING INDICATOR MINERAL DATA

As a minimum, all GSC published reports with indicator mineral data include the following (from Plouffe *et al.* 2013, in press; Spirito *et al.* 2013):
- Sample medium: till, glaciofluvial sediments, stream sediments, etc.;
- Name of the processing laboratory;
- Name of the mineral identification laboratory (if different from the processing laboratory);
- Weights of material processed for recovery of indicator minerals (original sample weight, weight of table feed - <2 mm);
- List of blank samples and their type;
- List of duplicate samples and sampling methodology;
- List of spiked samples and their spiking grain content (size, morphology, and mineralogy);
- Pre-concentration method (e.g. panning, hydro-separator, shaking table, dense media separator, Knelson concentrator, jig, rotary spinal concentrator, other);
- Heavy liquid separation: name of liquid, and density;
- Magnetic separation: type of magnet used (e.g. hand magnet, Frantz, roll magnet, or other methods) and amperages if an electromagnet is used;
- List of all size and density fractions prepared and their individual weights;
- Weight and size range of fraction(s) examined for indicator minerals and percentage of concentrate examined for each sample if the complete concentrate was not examined;
- Mineral identification or characterization method: visual scan under the binocular microscope, MLA, quantitative evaluation of material by scanning electron microscopy (QEMSCAN), SEM-EDS, cathodoluminescence (CL), or other methods;
- Mineral chemistry determination method, machine operating conditions, and laboratory name for EMP, SEM-EDS, LA ICP-MS, other;
- Raw indicator mineral count data as reported by the picking laboratory;
- Indicator mineral count data as confirmed by EMP, SEM-EDS, or other methods;
- Indicator mineral count data as values normalized to total sediment weight processed (e.g. number of grains per 10 kg table feed of the <2 mm fraction).

Note: the total indicator mineral grain counts for an individual sample are never added together and reported as one number; they are reported separately for each size fraction.

CONCLUSIONS

Indicator mineral sampling surveys represent a significant investment and, as such, implementation of proper QA/QC measures at all stages of surveys, from field to archive, will ensure that the data generated are of the highest quality possible. The GSC protocols presented in these short course notes will continue to be improved over time as more samples are processed, and as mineral separation and identification procedures at commercial laboratories evolve and improve.

ACKNOWLEDGEMENTS

REFERENCES

Averill, S.A. 2001. The application of heavy indicator mineralogy in mineral exploration with emphasis on base metal indicators in glaciated metamorphic and plutonic terrains. *In*: McClenaghan, M.B., Bobrowsky, P.T., Hall, G.E.M. & Cook, S.J. (eds) *Drift Exploration in Glaciated Terrain*. Geological Society, London, 69–81.

Bajc, A.F. & Hall, G.E.M. 2000. *Geochemical responses of surficial media, north and East Ranges, Sudbury Basin*. Ontario Geological Survey, Open File **6033**.

Baumgartner, M. 2006. Industry leading laboratory services for diamond explorers. *Explore*, **133**, 5–10.

Clifton, H.E., Hunter, R.E., Swanson, F.J. & Phillips, R.L. 1969. *Sample size and meaningful gold analysis*. United States Geological Survey, Professional Paper **625-C**.

de Souza, H. 2006. Indicator mineral processing at SGS Mineral Services. *Explore*, **133**, 13–15.

DiLabio, R.N.W., McIvor, D.F. & Newsome, J.W. 1988. The spherical form of gold: Man-made or secondary?. *Economic Geology*, **83**, 153–162.

Doherty, M. 2009. Quality control in indicator mineral methods. *In*: *Workshop B: Indicator Mineral Methods in Mineral Exploration*. The Association of Applied Geochemists, 24th International Applied Geochemistry Symposium, 1-4 June, 2009, New Brunswick, Canada, 35–36.

EVANS, D.J.A., PHILLIPS, E.R., HIEMSTRA, J.F. & AUTON, C.A. 2006. Subglacial till: formation, sedimentary characteristics and classification. *Earth Science Reviews*, **78**, 115–176.

GENT, M., MENENDEZ, M., TORAÑO, J. & TORNO, S. 2011. A review of indicator minerals and sample processing methods for geochemical exploration. *Journal of Geochemical Exploration*, **110**, 47–60.

HENDERSON, P.J., MCMARTIN, I., HALL, G.E.M., PERCIVAL, J.B. & WALKER, D.A., 1998. The chemical and physical characteristics of heavy metals in humus and till in the vicinity of the base metal smelter at Flin Flon, Manitoba, Canada. *Environmental Geology*, **34**, 39–58.

HOZJAN, D.J. & AVERILL, S.A. 2009. Quality control in indicator mineral sampling and processing. *In*: PAULEN, R.C. & MCMARTIN, I. (eds) *Application of till and stream sediment heavy mineral and geochemical methods to mineral exploration in western and northern Canada*. Geological Association of Canada, Short Course Notes **18**, 141–151.

JACKSON, S. 2009. Mineral chemistry: modern techniques and applications to exploration. *In*: *Workshop B: Indicator Mineral Methods in Mineral Exploration*. Association of Applied Geochemists, 24th International Applied Geochemistry Symposium, 1-4 June, 2009, New Brunswick, Canada, 21–26.

KNIGHT, R.D. & HENDERSON, P.J. 2006. Smelter dust in humus around Rouyn-Noranda, Québec. Geochemistry: *Exploration, Environment, Analysis*, **6**, 203–214.

KONTAS, E. 1991. Gold contamination of the fine fraction of till during sampling and sample preparation. *Journal of Geochemical Exploration*, **39**, 289–284.

MCCLENAGHAN, M.B. 2011. Overview of common processing methods for recovery of indicator minerals from sediment and bedrock in mineral exploration. *Geochemistry: Exploration, Environment, Analysis*, **11**, 265–278.

MCCLENAGHAN, M.B., HICKEN, A.K., AVERILL, S A., PAULEN, R.C. & LAYTON-MATTHEWS, D. 2012. *Indicator mineral abundance data for bedrock and till samples from the Izok Lake Zn-Cu-Pb-Ag volcanogenic massive sulphide deposit, Nunavut*. Geological Survey of Canada, Open File **7075**.

MCCLENAGHAN, M.B., KJARSGAARD, I.M., AVERILL, S.A., LAYTON-MATTHEWS, D., CRABTREE, D., MATILE, G., MCMARTIN, I. & PYNE, M. 2013. *Indicator mineral signatures of magmatic Ni-Cu deposits, Thompson Nickel Belt, Manitoba: Part 2- till data*. Geological Survey of Canada, Open File **7200**.

MCCLENAGHAN, M.B., PLOUFFE, A., MCMARTIN, I., CAMPBELL, J.E., SPIRITO, W., PAULEN, R.C., GARRETT, R.G. & HALL, G.E.M. in press. Till sampling and geochemical analytical protocols used by the Geological Survey of Canada. *Geochemistry: Exploration, Environment, Analysis*.

MCMARTIN, I., HENDERSON, P.J. & NIELSEN, E. 1999. Impact of a base metal smelter on the geochemistry of soils of the Flin Flon region, Manitoba and Saskatchewan. *Canadian Journal of Earth Sciences*, **36**, 141–160.

MCMARTIN, I., HENDERSON, P.J., PLOUFFE, A. & KNIGHT, R.D. 2002. Comparison of Cu-Hg-Ni-Pb concentrations in soils adjacent to anthropogenic point sources: examples from four Canadian sites. *Geochemistry: Exploration, Environment, Analysis*, **2**, 57–73.

MCMARTIN, I., CORRIVEAU, L. & BEAUDOIN, G. 2011. An orientation study of the heavy mineral signature of the NICO Co-Au-Bi deposit, Great Bear magmatic zone, Northwest Territories, Canada. *Geochemistry: Exploration, Environment, Analysis*, **11**, 293–307.

MCMARTIN, I., CAMPBELL, J.E., DREDGE, L.A. & MCCURDY, M.W. 2013. *Till composition and ice-flow indicators West of Repulse Bay: 2010 and 2011 results from the GEM Wager Bay Surficial Geology Activity*. Geological Survey of Canada, Open File **7288**.

MICHAUD, M.D.J. & AVERILL, S.A. 2009. Introduced particles in indicator mineral processing: considerations in preparing test samples for QA/QC and examples of anthropogenic contamination. *In*: *Workshop B: Indicator Mineral Methods in Mineral Exploration*. 24th International Applied Geochemistry Symposium, 1-4 June, 2009, New Brunswick, Canada. Association of Applied Geochemists, 67–70.

NATIONAL INSTRUMENT 43-101, 2005. Standards of Disclosure for Mineral Projects, 19 p. (http://www.cim.org/committees/NI_43-101_Dec_30.pdf)

NORMANDEAU, P.-X. & MCMARTIn, I. 2013. *Composition of till and bedrock across the Great Bear magmatic zone: Quaternary field database and analytical results from the GEM IOCG-Great Bear Project*. Geological Survey of Canada, Open File **7307**.

PLOUFFE, A., MCCLENAGHAN, M.B., PAULEN, R.C., MCMARTIN, I., CAMPBELL, J.E. & SPIRITO, W.A. 2013. Quality assurance and quality control measures applied to indicator mineral studies at the Geological Survey of Canada. *In*: PAULEN, R.C. & MCCLENAGHAN, M.B. (eds) *New Frontiers for Exploration in Glaciated Terrain*. Geological Survey of Canada, Open File **7374**.

PLOUFFE, A., MCCLENAGHAN, M.B., PAULEN, R.C., MCMARTIN, I., CAMPBELL, J.E. & SPIRITO, W., in press. Processing of glacial sediments for the recovery of indicator minerals: protocols used at the Geological Survey of Canada. *Geochemistry: Exploration, Environment, Analysis*.

RICE, J.M., PAULEN, R.C., MENZIES, J.M., MCCLENAGHAN, M.B. & OVIATT, N.M. 2013. *Glacial stratigraphy of the Pine Point Pb-Zn mine site, Northwest Territories*. Geological Survey of Canada, Current Research **2013-5**. doi:10.4095/292184

SPIRITO, W.A., MCCLENAGHAN, M. B., PLOUFFE, A., MCMARTIN, I., CAMPBELL, J.E., PAULEN, R.C., GARRETT, R.G. & HALL, G.E.M. 2011. *Till sampling and analytical protocols for GEM projects: from field to archive*. Geological Survey of Canada, Open File **6850**.

SPIRITO, W.A., ADCOCK, S.W. & PAULEN, R.C. 2013. Managing geochemical data: challenges and best practices. *In*: PAULEN, R.C. & MCCLENAGHAN, M.B. (eds) *New Frontiers for Exploration in Glaciated Terrain*. Geological Survey of Canada, Open File **7374**.

TOWIE, N.J. & SEET, L.H. 1995. Diamond laboratory techniques. *Journal of Geochemical Exploration*, **53**, 205–212.

WHITEFORD, S. 2003. QA/QC within a indicator mineral laboratory. *In*: *Indicator mineral methods in mineral exploration*. Prospectors and Developers Association of Canada, Short course proceedings, CD-ROM.

WILSON, R.A. 2007. *Bedrock geology of the Nepisiguit Lakes area (NTS 21O/7), Restigouche and Northumberland counties, New Brunswick*. New Brunswick Department of Natural Resources, Minerals, Policy and Planning Division, Plate **2007-32**.

Morphology of placer gold grains as a predictive tool in placer and primary source exploration

John Youngson

Youngson & Associates Ltd., Box 5284, Dunedin 9016, New Zealand
(e-mail: john@placerglobal.com)

Morphological changes to gold particles during fluvial transport occur in response to interaction with other sedimentary particles and/or the substrate. The changes are a function of transport distance and reflect changes in fluvial gradient, bed roughness, turbulence, velocity, and bed load in the river. Particle size, outline (2-D), shape (3-D), and texture are all modified by abrasion, flattening, folding, and breakage during transport. Resultant morphological characteristics can be used to predict transport distance, source type (primary/palaeoplacer), and source location, as well as the origin and dispersal patterns of gold in palaeoplacers remnants where transport history is unclear.

In physical-weathering regimes, gold commonly enters fluvial systems as inclusions within relatively easily transported ore clasts. Maximum particle size may increase for the first few kilometres downstream from the entry point(s) as ore clasts are comminuted and gold is released; however, further downstream the particle size progressively decreases. Conversely, in chemical-weathering regimes, gold typically enters fluvial systems as free particles; maximum particle size occurs near the entry point(s) and decreases progressively downstream.

In the moderate-to-high-gradient (upper reach) catchments, a moderate amount of particle rounding occurs and is focussed initially on grain extremities and protrusions between grain re-entrants. Brittle inclusions of gangue material are typically removed in such reaches but cavities from which inclusions were 'plucked' are commonly preserved into the transition zone to more typical trunk river gradients downstream, albeit with some smearing or abrasion of adjacent surfaces. Thus, the texture of gold particles in proximal reaches changes from pristine surfaces between inclusions (if present), to rounded and abraded protrusions between inclusions or cavities from which they were plucked, to more rounded, abraded, and smeared particle surfaces with relict cavities plus or minus remnant inclusions.

Preservation of 'pluck-cavities' into the transition zone between proximal (tributary) and more typical trunk river gradients indicates that little or no flattening, folding, or breakage of gold particles occurs in the proximal reaches. The Flatness Index [F.I. = (a+b)/2c] of gold particles upstream of the transition typically ranges from c.1 to 10 and reflects flatness inherited from primary source(s) rather than particle flattening during transport. Flattening, folding, and breakage of gold particles increases markedly through the transition zone and middle reaches of the trunk river. Flatness Index maxima (F.I. up to c.30), roundness, and the proportion of folded particles all increase and remaining inclusions and cavities from which they were plucked are effectively eliminated. Flattened-discoid-, cylindrical, and folded particles become more common, and surface textures become progressively more smoothed as the grain size of the associated fluvial sediment decreases. Distal trunk placer gold has a relatively high Flatness Index (F.I. up to 40), is typically well rounded and smoothed, and is dominated by discoid and cylindrical particles, up to 50% of which may be folded or multiply folded.

The Flatness Index of gold particles, the proportion of folded particles, and particle roundness in a given sample are useful indicators of source type (primary/palaeoplacer/till), additional gold inputs along the transport route, and fluvial transport distance. A reliable and predictable relationship between F.I. maxima and fluvial transport distance defines a critical F.I., above which gold is entrained and transported, and below which it is incorporated into a placer. Particle F.I. is increased by flattening, but is decreased by breakage and especially so by folding. Gold particles entering a system with subcritical F.I. must be flattened to supercritical F.I. before further transport can occur.

The relationships between maximum F.I. maxima, mean F.I., and particle folding can distinguish first-cycle, multi-cycle, and multi-source placers. F.I. maxima relate to downstream changes in fluvial dynamics in the last transport cycle, whereas F.I. mean is sensitive to additional gold inputs en route and particle folding. Mean F.I. can be markedly decreased by local inputs from relatively proximal placer, palaeoplacer, or primary sources, but can be increased by incorporation of gold recycled from relatively distal placer or palaeoplacer sources. Flattened and/or folded particles in moderate-to-high gradient tributary valleys generally indicate a more distal palaeoplacer source rather than a primary source. Abundant non-folded gold with subcritical F.I. in trunk placers typically indicates local primary and/or relatively proximal palaeoplacer sources en route.

Major and trace element chemistry of gahnite in metamorphosed massive sulphide deposits: discrimination diagrams to determine provenance

Joshua J. O'Brien[1*], **Paul G. Spry**[1], **Graham S. Teale**[2], **Simon Jackson**[3] **& Dean Rogers**[4]

[1]*Department of Geological and Atmospheric Sciences, 253 Science I, Iowa State University, Ames, Iowa, USA 50011-3212*
[2]*Teale and Associates, P.O. Box 740, North Adelaide, South Australia 5006, Australia*
[3]*Natural Resources Canada, Geological Survey of Canada, 601 Booth Street, Ottawa, Ontario, Canada K1A 0E8*
[4]*Perilya Limited, P.O. Box 5001, Broken Hill, New South Wales 2880, Australia*
(*e-mail: jjobrien@iastate.edu)

Zincian spinel, or gahnite ($ZnAl_2O_4$), occurs in and around a variety of metamorphosed massive sulphide deposits, including Broken Hill-type (BHT) Pb-Zn-Ag, volcanogenic massive sulphide (VMS) Cu-Zn-Pb, and sedimentary exhalative (Sedex) Pb-Zn deposits. The empirical association of gahnite-rich rocks with ores of this type has been recognized as a potential exploration guide by several workers (e.g. Sheridan & Raymond 1984), and has previously led mining companies to target gahnite-rich rocks with expensive drilling programs, which have led to mixed success in ore discoveries. Efforts to distinguish gahnite in prospective or sulphide-rich rocks, from comparatively sulphide-poor ones, have focused on evaluating the major element chemistry of gahnite as a targeted exploration guide (e.g. Spry & Scott 1986; Heimann *et al.* 2005; Spry & Teale 2009). However, O'Brien *et al.* (2012) conducted the first trace element study of gahnite (measured using laser ablation-inductively coupled plasma-mass spectrometry (LA-ICP-MS)), and proposed that the major-trace element chemistry of gahnite constitutes an exploration guide to high-grade Broken Hill-type Pb-Zn-Ag mineralization, in the Broken Hill domain, Australia. Although great attention had been paid to determining the variability of gahnite chemistry within a single ore field (i.e. the Broken Hill domain), little has been done to characterize the trace element chemistry of gahnite from various types of ore deposits.

The composition of gahnite from various ore fields and deposit types will provide insight into the natural range of gahnite chemistry. Within the past decade, advances in analytical equipment have improved the ability of geoscientists to measure in situ concentrations of trace elements. Studies requiring high-precision, in situ measurements of trace elements have benefitted from wider availability and increased use of LA-ICP-MS and electron probe microanalyzers (EPMA). Laser ablation-ICP-MS facilitates the measurement of many elements (e.g. concentrations of 52 elements were measured in gahnite by O'Brien *et al.* (2012)) at low concentrations (i.e. parts per billion) (e.g. Jackson *et al.* 1992).

Using trace element compositions of magnetite, Dupuis & Beaudoin (2011) developed a series of discrimination diagrams to identify compositional differences among magnetite originating from various types of ore deposits. Like magnetite, gahnite is an indicator mineral that is resistant to erosion and weathering due to its physicochemical properties (McClenaghan 2005). Therefore, detrital gahnite can be transported, and has been found to persist in a variety of unconsolidated sediments, which include glacial till (e.g. Morris *et al.* 1997), beach sands (e.g. Kaye & Mrose 1965), soil (e.g.

Nachtegaal *et al.* 2005), and stream sediments (e.g. Crabtree 2003). Using previously developed discrimination plots, the major-trace element chemistry of detrital gahnite may be used by explorationists conducting resistate mineral studies to determine its provenance, deposit type, and aid in the location and discovery of metamorphosed massive sulphide deposits in greenfield and brownfield terranes.

The major-trace element chemistry of gahnite in Broken Hill-type deposits (i.e. Broken Hill, Australia; Broken Hill, South Africa; Melbourne Rockwell, Australia; and Mutooroo, Australia), volcanogenic massive sulphide deposits (i.e. Bleikvassli, Norway; Mamandur, India; Moskosel, Stollberg, Sweden; several small Proterozoic Cu-Zn deposits, Colorado (i.e. Bon Ton, Caprock, Cotopaxi, Independence, and Sedalia)), and sedimentary exhalative deposits (i.e. Angas, Australia; Foster River, Saskatchewan) is used to determine the range in trace element compositions of gahnite in metamorphosed ore deposits and to develop a series of discrimination diagrams that can be used to distinguish among gahnite in BHT, Sedex, and VMS deposits.

METHODS

Major element compositions of gahnite (MgO, Al_2O_3, SiO_2, TiO_2, MnO, FeO, ZnO) were measured using EPMA at the University of Minnesota, operated with an accelerating voltage of 15 kV, a beam current of 20 nA, and a spot size of 1–2 μm, and using a range of mineral standards including gahnite (Zn, Al), pyrope (Si, Mg), hornblende (Ti), ilmenite (Fe), and spessartine (Mn). The beam time for background and peaks were 10 seconds each.

Concentrations of 52 elements were measured at the Geological Survey of Canada using a LA-ICP-MS, with a Photon Machines "Analyte 193" excimer (Ar-F) laser that has a UV wavelength of 193 nm, which undergoes a high degree of absorption by most minerals. This instrument was connected to an Agilent 7700 Series ICP-MS with a second rotary pump that doubles instrument sensitivity. Data reduction was performed using the computer program GLITTER!, which allowed for the integration of inclusion-free analyses through visual recognition of anomalous peaks from time resolved graphical profiles of the data (Van Achterberg 2001).

GAHNITE CHEMISTRY

Major element compositions of gahnite. The major element chemistry of gahnite (AB_2O_4) comprises varying proportions
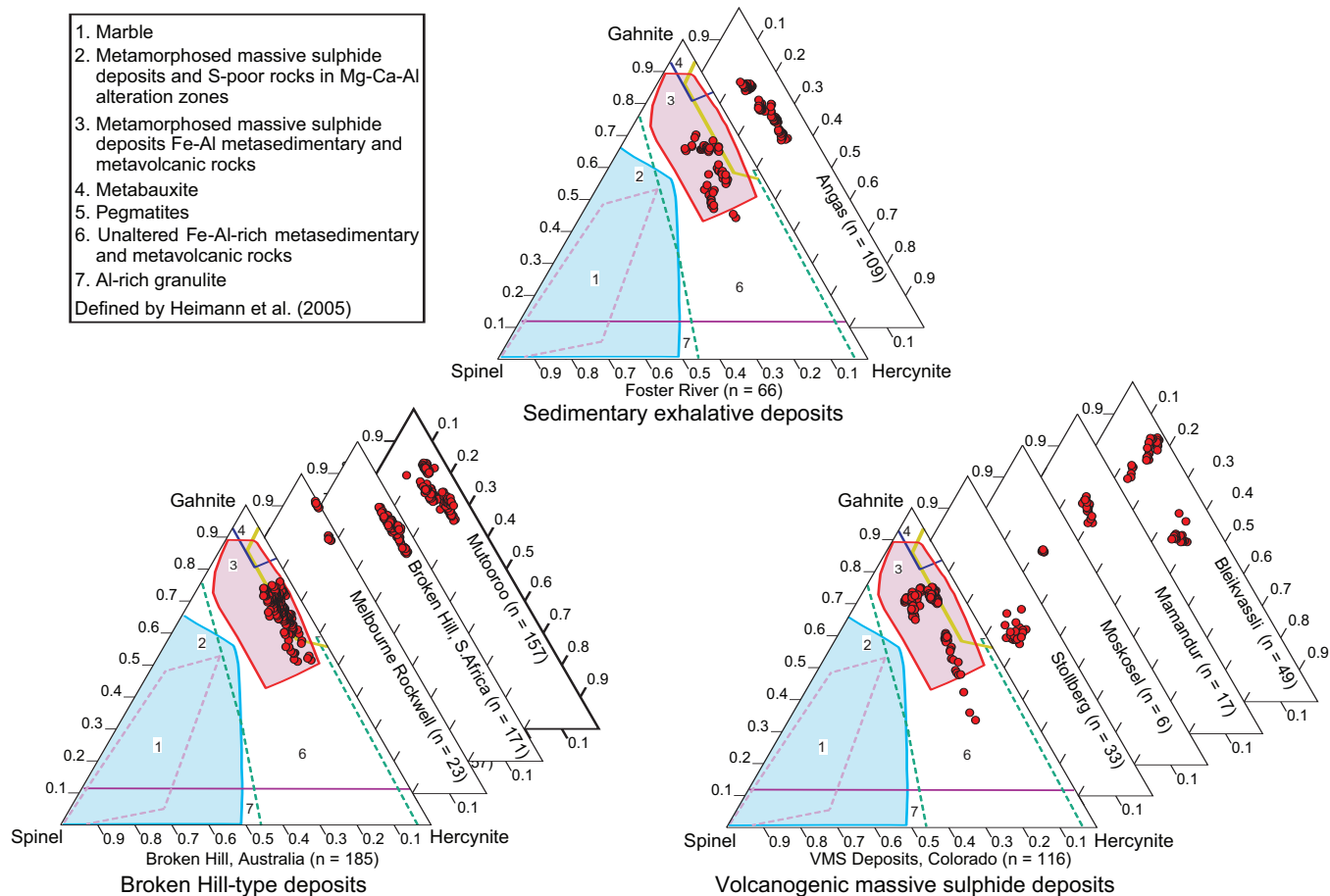
Fig. 1. Ternary plots of gahnite compositions from various ore fields grouped by deposit type, in terms of the gahnite(Zn)-hercynite(Fe)-spinel sensu stricto (Mg) spinel end members. Numbers correspond to compositional ranges of gahnite from different geological settings defined by Heimann *et al.* (2005). The number of analyses obtained from each location is given in brackets.

of Zn^{2+}, Fe^{2+}, Mg^{2+} and lesser amounts of Mn^{2+} in the tetrahedral site (A) with Al^{3+} and to a lesser extent Fe^{3+} in the octahedral site (B). Using the same components as Spry & Scott (1986) and Heimann *et al.* (2005) (i.e. gahnite ($ZnAl_2O_4$), hercynite ($FeAl_2O_4$), and spinel sensu stricto ($MgAl_2O_4$)), relative proportions of Zn, Fe, and Mg for each analysis are presented here in a series of ternary plots (Fig. 1). For the purposes of comparison, separate plots were created for each deposit type and overlain by compositional fields of gahnite from different geological settings (identified by Heimann *et al.* 2005). Gahnite mostly plots within the field for metamorphosed massive sulphide deposits hosted by hydrothermally altered Fe–Al-rich metasedimentary and metavolcanic rocks (gahnite$_{45-85}$hercynite$_{15-45}$spinel$_{0-20}$). However, some gahnite from the Foster River and Colorado Cu-Zn deposits contain a higher proportion of Fe, and plot within the field of unaltered Fe-Al-rich metasedimentary and metavolcanic rocks. Gahnite in VMS deposits and Sedex deposits mostly contains a higher Mg content than gahnite from BHT deposits.

Different physicochemical conditions (e.g. fO_2, fS_2, temperature, pressure, and host rock composition) affect the major element chemistry of gahnite in sulphide-bearing rocks (e.g. Spry *et al.* 1986; Heimann *et al.* 2005). Experiments by Spry *et al.* (1986) showed that the composition of zincian spinel in the gahnite-hercynite solid solution is strongly dependent upon fS_2 and fO_2, which is dictated by the a_{FeS} content of Fe-bearing sulphides (i.e. sphalerite, pyrite, and pyrrhotite) that coexist

with gahnite. For the broad range of metamorphic conditions (the upper greenschist to the granulite facies) at which gahnite is stable, the composition of gahnite in the gahnite-hercynite solid solution is buffered and fixed (i.e. ~65–85 mole % $ZnAl_2O_4$) by coexisting Fe-bearing sulphides (Spry & Scott, 1986).

Because the gahnite:hercynite ratio is buffered by the presence of these sulphides, the major element chemistry of gahnite can be used to determine whether or not sulphides were present during gahnite formation. The abundance of pyrrhotite, sphalerite, and pyrite must comprise more than ~1 volume % for the composition of gahnite to be buffered by Fe-sulphides in the host rock (Spry & Teale 2009) and produce a characteristic major element composition (i.e. gahnite$_{45-85}$hercynite$_{15-45}$spinel$_{0-20}$) for gahnite in sulphide-bearing assemblages, which may contain as little as 1 to 3 volume % sulphides. Therefore, major element chemistry may serve as a first-order indicator of whether or not detrital gahnite originally coexisted with sulphides. However, this diagnostic compositional range is not indicative of the modal percentage of sulphides present and is, therefore, incapable of distinguishing sulphide-poor from sulphide-rich rocks.

Trace element chemistry of gahnite

Like other members of the spinel group (e.g. magnetite and chromite), the trace element chemistry of gahnite is dominated

Table 1. Compositions of gahnite from different types of metamorphosed ore deposits measured by LA-ICP-MS.

Trace Elements (ppm)			Ti	V	Cr	Mn	Co	Ni	Ga	Cd
Sedimentary Exhalative Deposits	Angas n = 10	Min.	1	58	30	1841	8	1	62	2
		Max.	4	114	464	3067	17	3	173	5
		Med.	2	87	253	2268	9	1	92	3
		Mean	2	84	219	2346	11	2	108	3
	Foster River n = 53	Min.	3	27	2	3124	19	1	94	1
		Max.	29	131	692	12276	130	17	571	6
		Med.	10	57	25	4776	42	3	188	3
		Mean	12	65	70	5675	55	4	255	3
Broken Hill-type Deposits	Broken Hill Australia n = 95	Min.	1	15	1	481	12	0	111	1
		Max.	161	706	403	3119	145	30	425	13
		Med.	56	160	55	1001	57	4	247	4
		Mean	60	173	107	1199	59	7	252	4
	Broken Hill S. Africa n = 56	Min.	6	10	0	3429	19	2	76	1
		Max.	52	378	741	6106	112	11	244	6
		Med.	14	62	11	4122	61	4	135	3
		Mean	18	109	124	4437	59	4	137	3
	Melbourne Rockwell n = 19	Min.	9	149	40	1518	45	25	62	3
		Max.	47	195	186	2486	73	48	105	16
		Med.	18	176	117	2072	67	30	80	7
		Mean	22	177	110	2049	64	34	85	8
	Mutooroo n = 54	Min.	1	45	1	370	39	1	84	2
		Max.	43	194	490	1687	109	28	167	12
		Med.	3	133	7	840	65	7	109	5
		Mean	11	118	65	928	64	11	113	5
Volcanogenic Massive Sulphide Deposits	Bleikvassli n = 19	Min.	1	3	1	558	1	0	94	2
		Max.	17	9	23	1621	20	3	168	10
		Med.	5	6	3	1074	8	1	108	4
		Mean	6	5	6	1107	8	1	113	5
	Colorado Cu-Zn Deposits n = 72	Min.	1	1	0	318	7	0	109	1
		Max.	102	144	257	6749	114	10	1275	11
		Med.	9	38	4	2045	31	4	182	5
		Mean	17	51	35	2651	33	5	316	5
	Mamandur n = 34	Min.	15	15	1	1800	14	42	124	2
		Max.	77	112	31	3745	22	62	249	11
		Med.	26	28	3	2464	17	53	141	3
		Mean	31	43	5	2639	17	51	174	4
	Moskosel n = 3	Min.	2	0	0	391	2	1	292	4
		Max.	1	1	0	462	3	1	441	5
		Med.	2	1	0	431	2	1	419	5
		Mean	2	1	0	428	2	1	384	5
	Stollberg n = 10	Min.	8	1	2	779	2	1	114	1
		Max.	15	3	6	1243	3	1	169	2
		Med.	9	1	4	1028	2	1	144	1
		Mean	10	2	4	1022	2	1	144	1

by the first series transition metals (i.e. Ti, V, Cr, Mn, Co, Ni), Ga, and Cd (Pagé & Barnes 2009; Nehring *et al.* 2010; Dupuis & Beaudoin 2011; Nadoll *et al.* 2012). Unlike major element chemistry, little is known about the factors controlling the trace element chemistry of gahnite. However, concentrations of trace elements in gahnite likely depend upon several factors, which include bulk rock chemistry, the partitioning of elements between gahnite and other minerals in the matrix, temperature, pressure, fO_2, fS_2, fH_2O, crystal-chemical controls (i.e. the major element chemistry), and the composition of precursor minerals (e.g. sphalerite, garnet, pyrrhotite).

The minimum, maximum, median, and mean trace element compositions of gahnite from each deposit are reported in Table 1, which allows for comparison among deposits within each deposit type. Compositions of gahnite in Sedex deposits contain similar concentrations of V, Ni, and Cd. Gahnite in the Foster River Zn deposit contain more Ti, Co, Ga, Mn, and lesser amounts of Cr than gahnite in the Angas Zn-Pb-Ag deposit, which are among the most Cr-rich in this study.

Gahnite in different BHT Pb-Zn-Ag deposits contain similar concentrations of V, Cr, Co, and Cd. Concentrations of Ga and Ti are higher in gahnite from Broken Hill (Australia), than in gahnite from Broken Hill (South Africa), Melbourne Rockwell, and Mutooroo; whereas elevated Ni content distinguishes gahnite from Melbourne Rockwell from the other three deposits. Gahnite in the Broken Hill deposit (South Africa) contains the highest concentration of Mn for gahnite in BHT deposits.

Gahnite in different VMS deposits contains similar amounts of Cd, but the concentrations of other trace elements are variable and not as uniform as those in Sedex and BHT deposits. With the exception of gahnite in the Independence Cu-Zn deposit in Colorado, which contains 2 to 257 ppm Cr, the Cr content of gahnite in VMS deposits is generally less than 30 ppm. Vanadium, Co, and, to a lesser extent, Mn occur in comparatively lower concentrations (less than 3 ppm, 20 ppm, and 1621 ppm, respectively) in gahnite in the Bleikvassli, Moskosel, and Stollberg deposits than in gahnite from the Mamandur deposit and some Cu-Zn deposits in Colorado. Gahnite from the Mamandur deposit contains the highest Ti content among VMS deposits, and the highest amount of Ni in gahnite measured in this study. With exception of this deposit, gahnite in other VMS deposits contains comparable concentrations of Ni and Ti. The Ga content of gahnite in the Moskosel deposit is among the highest measured in this study.

Gahnite in BHT deposits generally contains similar amounts of Mn and Cd, more Ti, V, Co, Ga, Ni, and less Cr than gahnite in Sedex deposits, and similar amounts of Ni and Cd, more Ti (with the exception of some Colorado Cu-Zn deposits and Mamandur), V, Cr, Co, and less Mn, and Ga than gahnite in VMS deposits. Gahnite in Sedex deposits generally contains similar quantities of Cd, less Mn, Ni, and Ga, and more Ti, V, Cr, and Co (with the exception of Mamandur and some Cu-Zn deposits in Colorado) than gahnite in VMS deposits.

DISCRIMINATION DIAGRAMS

A series of discrimination plots were created to demonstrate variability in gahnite chemistry for the three types of metamorphosed massive sulphide deposits, to identify specific combinations of elements that can be used as discriminators to these ore types, and to compositionally fingerprint detrital gahnite (Fig. 2).

A scatter plot of Mg (ppm) versus V (ppm) shows that gahnite in BHT deposits contain less Mg and comparable to slightly higher V contents than that in VMS and Sedex deposits (Fig. 2). Because the spinel *sensu stricto* component does not take part in gahnite-forming desulphidation reactions, its MgO content is generally related to the bulk MgO composition of the host rocks (i.e. Sedex and VMS host rocks are generally more MgO-rich relative to the host rocks of BHT deposits; Heimann *et al.* 2005).

A bivariate plot of Co (ppm) versus V (ppm) shows that the composition of gahnite in BHT and Sedex deposits can be distinguished from the composition of gahnite in VMS deposits,
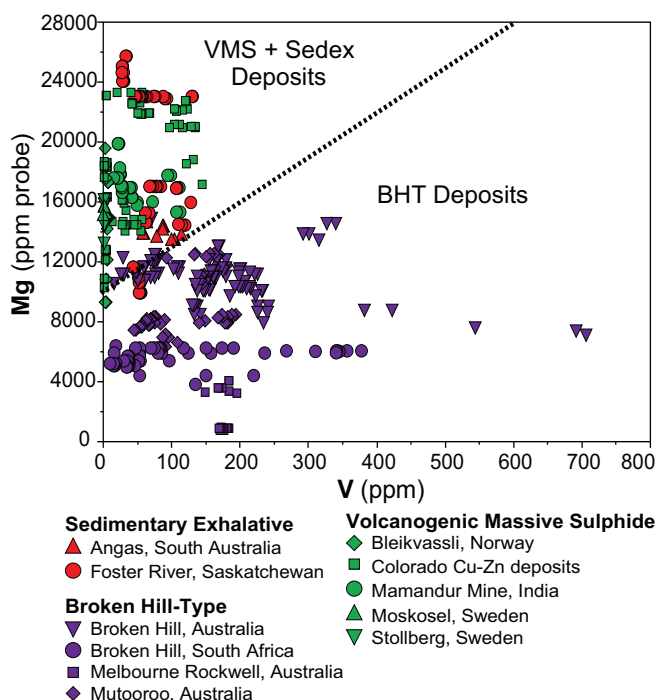
Fig. 2. Bivariate plot of Mg versus V for gahnite from different deposit types, which include sedimentary exhalative (Sedex) Pb-Zn-Ag deposits (Angas, South Australia; Foster River, Saskatchewan), volcanogenic massive sulphide (VMS) Cu-Zn-Pb deposits (Cotopaxi, Sedalia, Cinderella, Bon Ton, and Independence, Colorado; Bleikvassli, Norway; Mamandur, India; Moskosel and Stollberg, Sweden), and Broken Hill-type deposits (BHT) (Broken Hill, Australia; Broken Hill, South Africa; Mutooroo and Melbourne Rockwell, Australia). Note that gahnite from BHT deposits can be distinguished from those in Sedex and VMS deposits, which mostly overlap.

which mostly contain less than 30 ppm Co and 140 ppm V (Fig. 3). Exceptions include Co- and V-rich gahnite from some Colorado Cu-Zn deposits (i.e. Bonton, Cotopaxi, Independence, and Sedalia). The compositions of some gahnite from the Angas and Foster River deposits overlap the compositional field identified for gahnite in VMS deposits in Figure 3.

Gahnite in BHT deposits are excluded from Figures 4 (Mn versus Ti) and 5 (Co versus Ti) for two reasons: (1) because the composition of gahnite in BHT deposits are easily distinguished from gahnite in the other two classes of metamorphosed sulphide deposits using Figure 2; and (2) to highlight compositional differences between gahnite in Sedex and VMS deposits. Gahnite in Sedex deposits generally contains more Mn, but less Ti than most gahnite in VMS deposits (Fig. 4). However, gahnite in some Colorado Cu-Zn deposits plot within the Sedex field; moreover, the Mn content of gahnite in the Angas deposit and in some gahnite from the Foster River deposit overlaps with gahnite in VMS deposits. The Co content of gahnite in Sedex deposits is higher than that for gahnite in VMS deposits, which, when plotted against Ti, allows them to be distinguished from each other (Fig. 5).
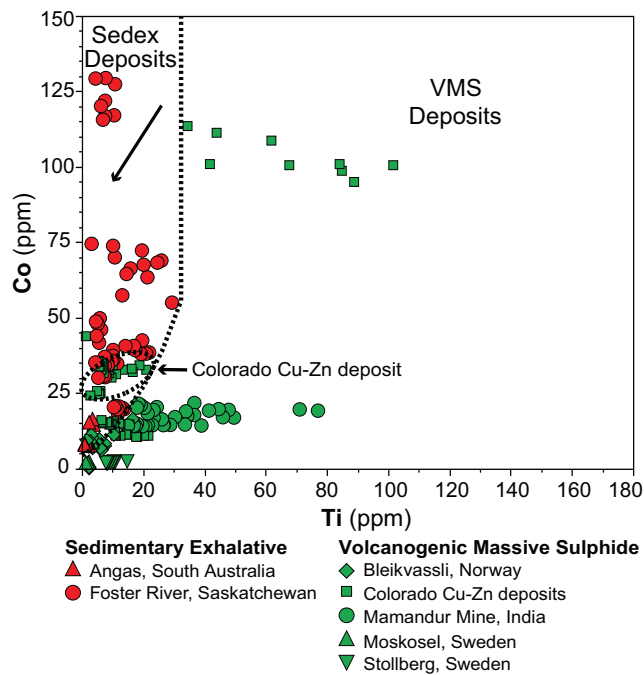
CONCLUSIONS

1) The trace element chemistry of gahnite in VMS, Sedex, and BHT deposits is dominated by Ti, V, Cr, Mn, Co, Ni, Ga, and Cd.
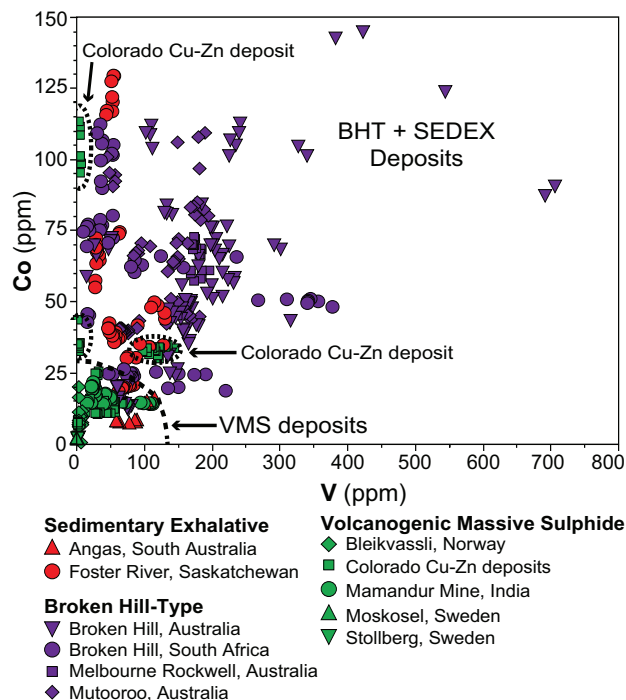
Fig. 3. Bivariate plot (Co versus V) of gahnite from BHT, VMS, and Sedex deposits. Note gahnite from the Stollberg, Bleikvassli, Moskosel, and Mamandur deposits mostly contain less than 30 ppm Co and 140 ppm V, where as those from the Colorado Cu-Zn deposits are comparatively enriched in these elements and overlap with gahnite from BHT and Sedex deposits.
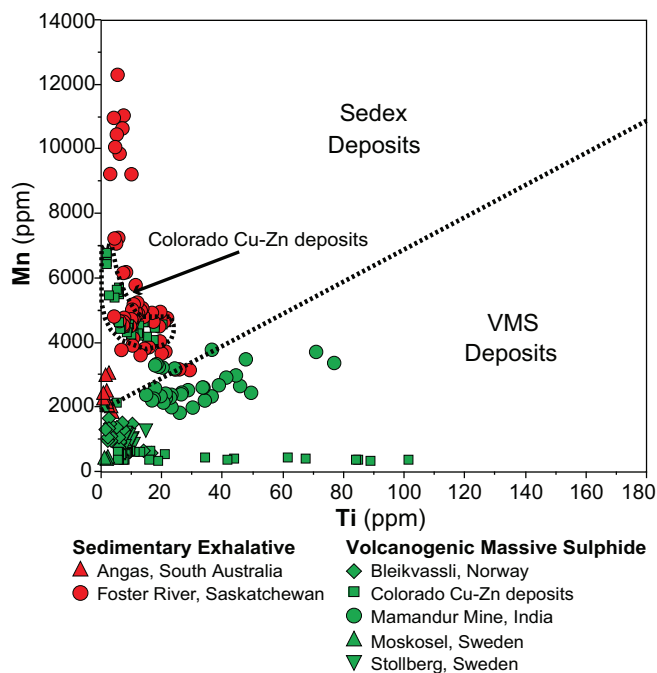
Fig. 4. Bivariate plot (Mn versus Ti) of gahnite from Sedex and BHT deposits. Compositional fields identified for gahnite in Sedex deposits and gahnite in VMS deposits are denoted by a dashed line. Note gahnite in Sedex deposits mostly contains higher Mn and lower Ti contents than gahnite in VMS deposits. Compositions of gahnite in Sedex deposits are overlapped by gahnite in the Colorado Cu-Zn deposits.

Co versus V, Mn versus Ti, and Co versus Ti.

5) The major and trace element composition of gahnite can be used as an exploration guide to metamorphosed massive sulphide deposits in productive ore camps and in greenfield terranes where it occurs as a resistate mineral in unconsolidated sediments.

REFERENCES

CRABTREE, D.C. 2003. *Preliminary results from the James Bay lowland indicator mineral sampling program*. Ontario Geological Survey, Open File Report **6108**.

DUPUIS, C. & BEAUDOIN, G. 2011. Discriminant diagrams for iron oxide trace element fingerprinting of mineral deposit types. *Mineralium Deposita*, **46**, 319–335.

HEIMANN, A., SPRY, P.G. & TEALE, G.S. 2005. Zinc-rich spinels associated with Proterozoic base metal sulfide occurrences, Colorado, and their use as guides to metamorphosed massive sulphide deposits. *Canadian Mineralogist*, **43**, 601–622.

JACKSON, S.E., LONGERICH, H.P., DUNNING, G.R. & FREYER, B.J. 1992. The application of laser-ablation microprobe; inductively coupled plasma-mass spectrometry (LAM-ICP-MS) to in situ trace-element determinations in minerals. *Canadian Mineralogist*, **30**, 1049–1064.

KAYE, C.A. & MROSE, M.E. 1965. *Magnetic spherules, colored corundum, and other unusual constituents of a heavy beach sand, Martha's Vineyard, US*. United States Geological Survey, Professional Paper **P0525-D**.

McCLENAGHAN, M.B. 2005. Indicator mineral methods in mineral exploration. Geochemistry: *Exploration, Environment, Analysis*, **5**, 233–245.

MORRIS, T.F., BREAKS, F.W., AVERILL, S.A., CRABTREE, D.C. & McDONALD, A. 1997. Gahnite composition: implications for base metal and rare-element exploration. *Exploration and Mining Geology*, **6**, 253–260.

NACHTEGAAL, M., MARCUS, M.A., SONKE, J.E., VANGRONSVELD, J., LIVI, K.J.T., VAN DER LELIE, D. & SPARKS, D.L.. 2005. Effects of in situ remediation on the speciation and bioavailability of zinc in smelter contaminated soil. *Geochemica et Cosmochimica Acta*, **69**, 4649–4664.

NADOLL, P., MAUK, J.L., HAYES, T.S., KOENIG, A.E. & BOX, S.E. 2012. Geochemistry of magnetite from hydrothermal ore deposits and host rocks of the Mesoproterozoic Belt Supergroup, United States. *Economic Geology*, **107**, 1275–1292.

NEHRING, F., FOLEY, S.F. & HÖLTTÄ, P. 2010. Trace element partitioning in the granulite facies. *Contributions to Mineralogy and Petrology*, **159**, 493–519.

O'BRIEN, J.J., SPRY, P.G., TEALE, G.S., JACKSON, S. & ROGERS, D. 2012. Gahnite ($ZnAl_2O_4$) as a potential exploration guide to metamorphosed massive sulfide deposits (Broken Hill Type, SEDEX and VMS): Major and trace element compositions. *In: Fe-oxide Workshop: Processes that Control the Composition of Fe-Oxides in Ore Deposits*. 22nd Goldschmidt Conference, 30th June 2012, Montreal, Canada, 10.

PAGÉ, P., AND BARNES, S.-J. 2009. Using trace elements in chromites to constrain the origin of podiform chromitites in the Thetford mines ophiolite, Québec, Canada. *Economic Geology*, **104**, 997–1018.

SHERIDAN, D.M. AND RAYMOND, W. 1984. *Precambrian deposits of zinc-copper-lead sulfides and zinc spinel (gahnite) in Colorado*. U.S. Geological Survey Bulletin, **1550**.

SPRY, P.G. & SCOTT, S.D. 1986. The stability, synthesis, origin and exploration significance of zincian spinels. *Economic Geology*, **81**, 1446–1463.

SPRY, P.G. & TEALE, G.S. 2009. Gahnite composition as a guide in the search for metamorphosed massive sulfide deposits. *In: Indicator Mineral Workshop B*. International Association of Applied Geochemists, May 2009, Fredericton, New Brunswick, 27–34.

VAN ACHTERBERGH, E. RYAN, C.G. JACKSON, S.E. & GRIFFIN, W. 2001. *Data reduction software for LA-ICP-MS*. Mineralogical Association of Canada, Series **29**, 239–243.

Fig. 5. Bivariate plot (Co versus Ti) of gahnite from Sedex and BHT deposits. Compositional fields identified for gahnite in Sedex deposits and gahnite in VMS deposits are denoted by a dashed line Note gahnite in Sedex deposits mostly contains higher Co and lower Ti contents than gahnite in VMS deposits. Compositions of gahnite in Sedex deposits are overlapped by gahnite from the Colorado Cu-Zn deposits.

2) Gahnite in BHT deposits contains similar amounts of Mn and Cd, higher Ti, V, Co, Ni, and Ga content, and less Cr than gahnite in Sedex deposits, and similar amounts of Ni and Cd, more V, Cr, Co, and less Mn and Ga than gahnite in VMS deposits.

3) Gahnite grains in Sedex deposits contain similar amounts of Cd, less Mn, Ni, and Ga, and more V, Cr, and Co than gahnite in VMS deposits.

4) Trace element compositions of gahnite in VMS deposits are variable. Gahnite from Bleikvassli, Moskosel, and Stollberg contains lower V, Co, and Mn contents than that from the Mamandur deposit and some of the Colorado Cu-Zn deposits and gahnite in Sedex and BHT deposits; whereas, the compositions of gahnite in Mamandur and some of the Colorado Cu-Zn deposits partially overlap the other two deposit types (BHT and Sedex). Gahnite in BHT deposits can be distinguished from that in Sedex and VMS deposits based on a plot of Mg (ppm) versus V (ppm); whereas, the composition of gahnite in Sedex deposits is distinct from that in VMS deposits on the basis of plots of

Indicator mineral fingerprints in surficial sediments near Cu-Au deposits of the porphyry-epithermal-volcanogenic suite

Stuart A. Averill

Overburden Drilling Management Limited, 107-15 Capella Court, Nepean, Ontario, Canada, K2E 7X1
(e-mail: odm@storm.ca)

An indicator mineral, in the sense used herein, is a mineral whose dispersed grains in surficial sediments are of practical use for detecting, from afar, a specific type of rock, mineralized zone, or hydrothermal alteration zone. To detect the intended target from afar, the minerals must be visually discernible at concentrations as low as 5 grains per billion. Therefore the grains must be of a sufficient specific gravity — generally >3.2 g/cm³ — to be further concentrated by heavy mineral separation, and also generally coarser than 0.25 mm. However, gold and a few other minerals are sufficiently dense and visually distinctive that grains of any size can be used.

Cu-Au deposits of the porphyry-epithermal-volcanogenic suite are a source of many potential indicator minerals but the utility of some of these minerals depends on climate (both past and present), depth of sampling, and the degree of interference from visually similar background heavy minerals. This will be illustrated using examples from glaciated Cu, Cu-Au, and Au deposits in the metamorphosed Archean craton and younger, unmetamorphosed Western Cordillera of Canada and Alaska, as well as unglaciated deposits in the southern hemisphere.

GENETIC RELATIONSHIPS BETWEEN PORPHYRY Cu, EPITHERMAL Au AND VOLCANOGENIC Au DEPOSITS

Porphyry Cu (and Cu-Au), epithermal Au and volcanogenic Au deposits are genetically related, being differentiated mainly on their depth of formation (Fig. 1) and thus, indirectly, on the temperatures and compositions of their associated hydrothermal fluids. Porphyry deposits are the deepest, forming ~5 km below surface within or adjacent to high-level porphyritic intrusions of a felsic to intermediate composition in terrestrial volcanic belts. Most preserved porphyry deposits are geologically young, either of Mesozoic or Cenozoic age, and occur in areas of recent uplift because older terrestrial belts tend to be so deeply eroded that any former porphyry deposits have been erased. Epithermal deposits form in the overlying volcanic rocks at crustal depths sufficiently shallow to allow boiling of hydrothermal fluids, typically <1 km. Volcanogenic Au deposits, in contrast, are mainly submarine. They form either directly on the seafloor or in permeable volcaniclastic rocks below the seafloor, with an underlying porphyry intrusion commonly providing the heat source to drive subsurface circulation of metal-scavenging seawater. Being better protected from erosion than terrestrial deposits, they are preserved in volcanic belts of all ages, with known occurrences in Canada ranging from the Archean deposits at Bousquet, Quebec (Dubé *et al.* 2007b) and Rainy River, Ontario (Averill 2013) in the Canadian Shield to the Cretaceous Blackwater deposit (Simpson *et al.* 2012) in the interior of British Columbia in the Western Cordillera (Fig. 2).
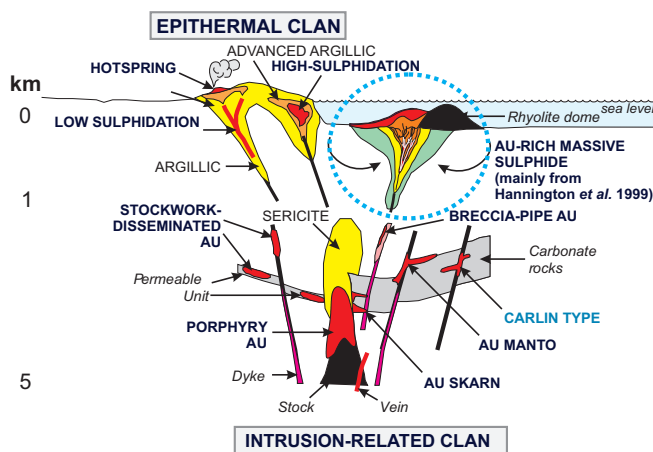

Fig. 1. Inferred crustal levels of gold deposition in porphyry, epithermal, volcanogenic. and other related deposits. Modified from Dubé *et al.* (2007a) and Sillitoe & Bonham (1990).

RANGE OF INDICATOR MINERALS

Each of the above deposits is a source of visually recognizable and deposit-specific heavy minerals coarser than 0.25 mm, many of which form useful indicator minerals under favourable conditions. All but the porphyry Cu deposits are also a source of gold grains. While most gold grains are much finer than 0.25 mm, with ~90% being silt-sized or <0.063 mm (Averill 2001), the grains are visually distinct and their high specific gravity of ~19 g/cm³ permits their separation from the other heavy minerals in the concentrate. Consequently each recovered gold grain, no matter how small, can be physically identified and studied.

GOLD AS AN INDICATOR MINERAL

A key feature of gold grains is their ability to survive both physical transport and post-depositional weathering. Only a few other heavy minerals — principally ilmenite, rutile, zircon, chromite, kyanite, and staurolite commonly found in residual soils and heavy mineral sands — have this capability. In the deeply weathered Cenozoic colluvial cover at the Big Spring and Ellendale olivine lamproite fields in arid Western Australia, for example, chromite and picroilmenite are often the only durable kimberlite/lamproite indicator minerals. Most or all grains of olivine and other silicate indicator minerals, including the key Cr-pyrope garnet grains that are needed to assess diamond prospectivity, have been degraded (Jaques *et al.* 1986). To the east in the more tropical Northern Territory, Hutchison (2013) notes that a "large majority" of the surviving grains are chromite and in many cases diamond is the most abundant mineral present even though in kimberlite and lamproite it is
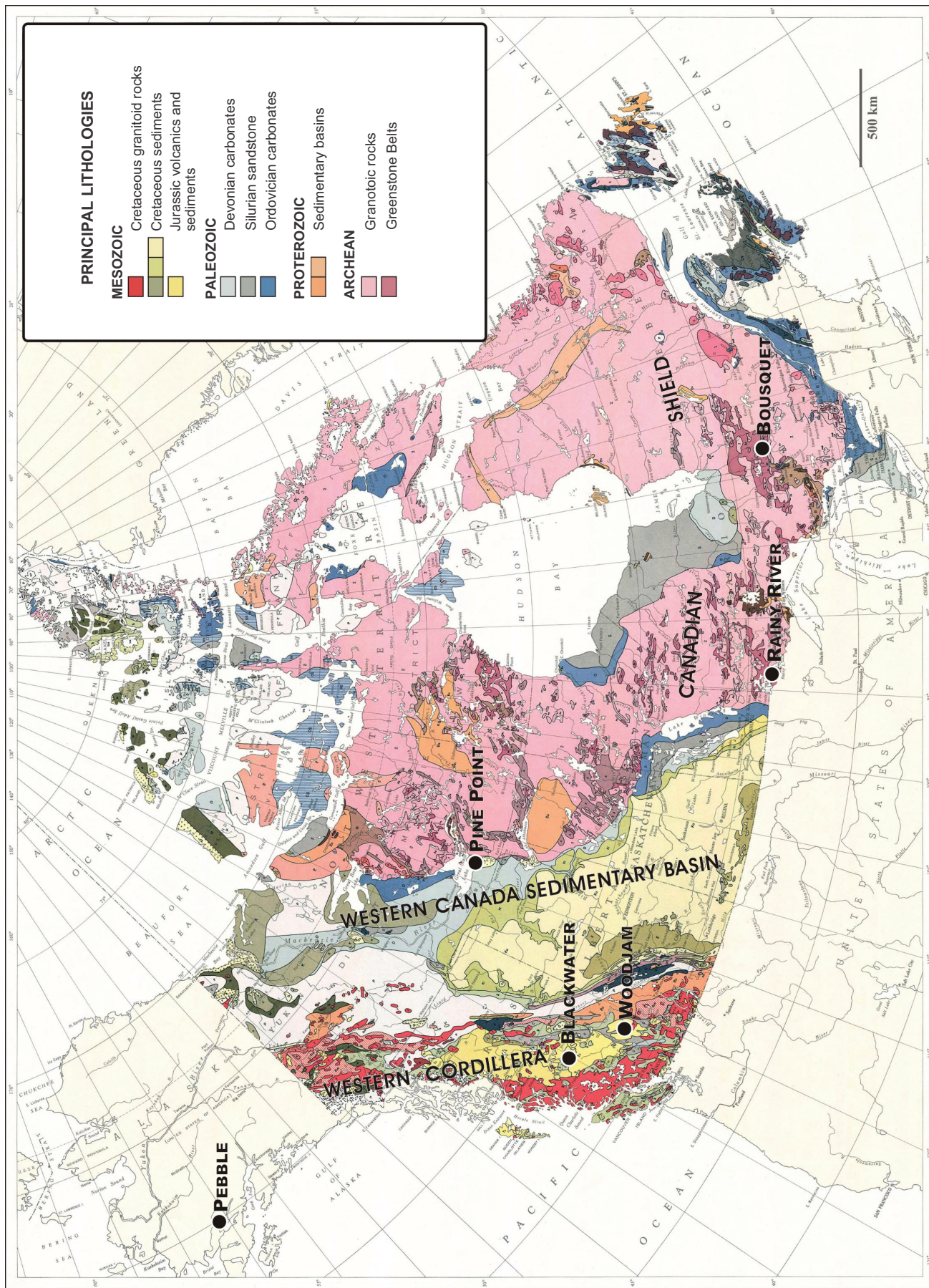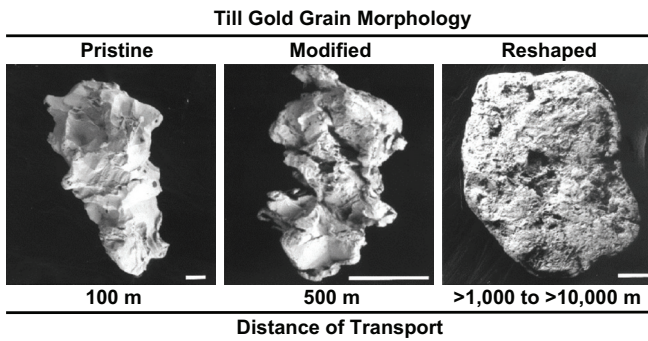
S.A. Averill

Figure 2. Geological setting of Canadian and Alaskan mineral deposits discussed in the text. Map source: Geological Survey of Canada (1957).

Till Gold Grain Morphology

Pristine	Modified	Reshaped

| 100 m	500 m	>1,000 to >10,000 m

Distance of Transport

Fig. 3. Backscatter electron images of gold grains from till illustrating the relationship between grain wear and distance of transport. The wear processes are compressional (infolding and compaction) and do not reduce the mass of the gold grain. Scale bars = 50 μm. Source: Averill (2001).

several orders of magnitude less abundant than the other indicator minerals.

The physical resistance of gold is a result of its malleability. This property also results in the grains being moulded systematically during transport, a feature that can be used to gauge their distance of transport as exemplified by the progressive modification and eventual reshaping of pristine grains during glacial transport (Fig. 3; Averill 2001).

Throughout the glaciated regions of Canada (Fig. 4), exposed till sections are significantly oxidized to a depth of 2 to 3 m (Fig. 5), below which drilling has consistently shown that the till is as fresh as when it was deposited 10,000 to 15,000 years ago (Fig. 6). All gold grains from the oxidized zone of the till that have been analyzed by the author and his associates at Overburden Drilling Management (ODM) have been found to completely retain their primary, alloyed silver whereas grains from the cold-
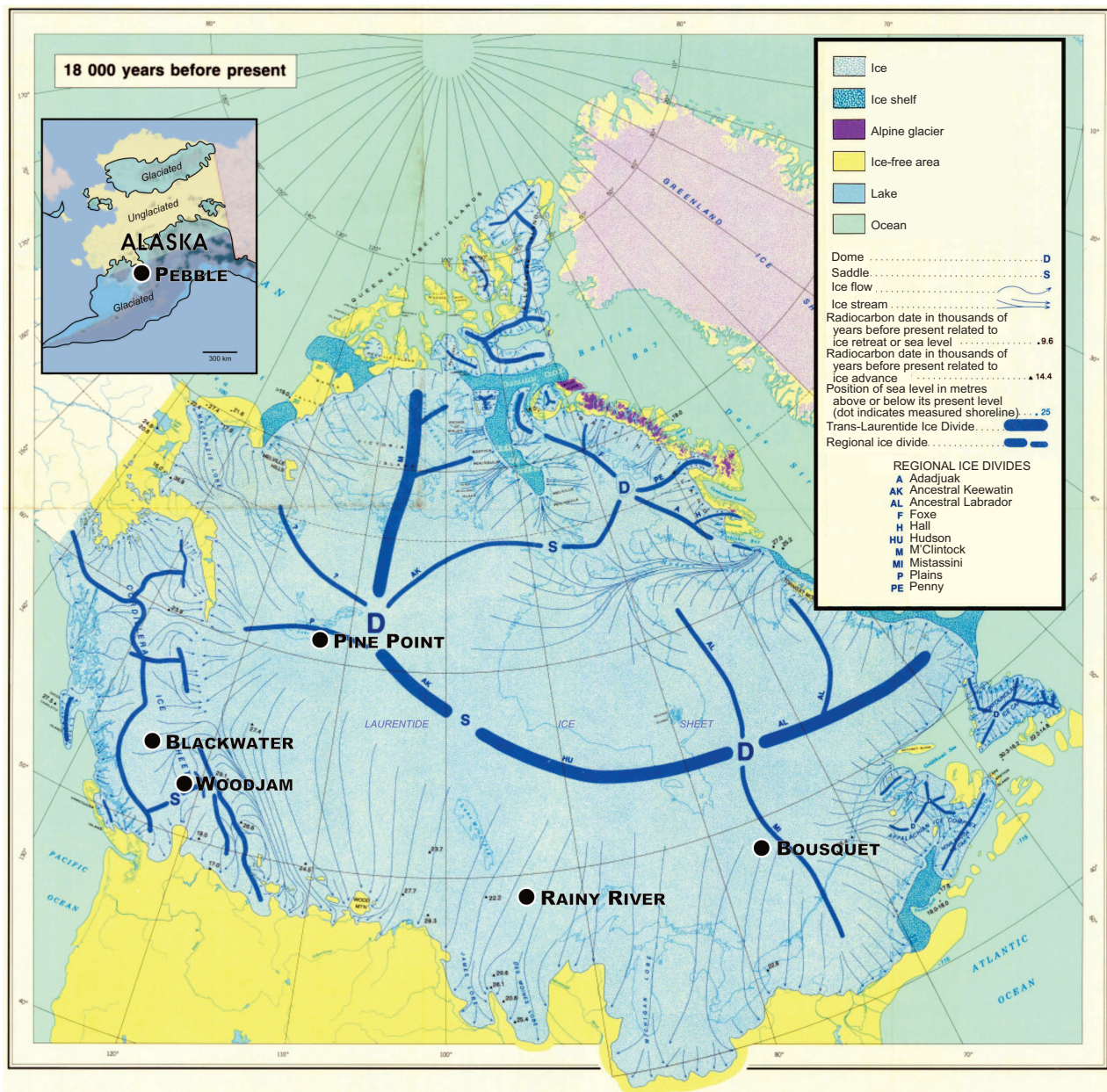
Fig. 4. Locations of the Canadian and Alaskan mineral deposits discussed in the text in relation to the Laurentide and Cordilleran ice sheets during glaciation approximately 18,000 years ago. Map source: Dyke & Prest (1987).

Fig. 5. Typical sample pit in oxidized till in Canada. Till excavated from the B- and C-horizons of the overprinted soil profile has been piled separately to illustrate their different oxidization states. Ideally, the sample is obtained from the weakly oxidized, pale yellow-ochre C-horizon below the highly oxidized, dark red-ochre B-horizon, generally at a depth of 0.5 to 1 m. The insert shows the heavy mineral fraction of the till in which most of the original sulphide grains have been consumed by oxidation.
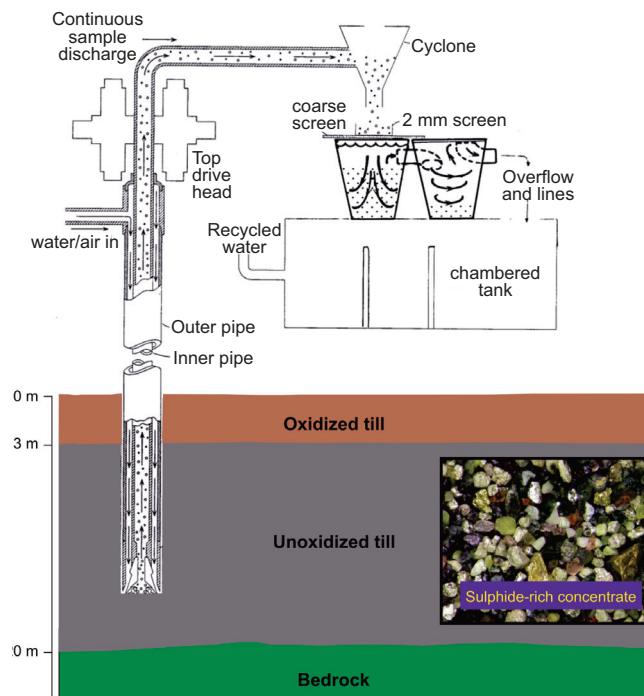

Fig. 6. Schematic diagram of a typical reverse circulation rotary drill specifically designed for sampling thick till in Canada. In holes drilled by these and other drill rigs, fresh, unoxidized till is typically encountered below a depth of 2 to 3 m. As illustrated in the inset, this fresh till retains all of its original sulphide mineral grains, precluding mobility of metals from or through the till to the overlying soil.

climate alluvial placers of the Klondike have Ag-depleted rims (Knight *et al*. 1999) and those from more mature placers elsewhere are depleted to the core (Desborough *et al*. 1970). In French Guiana, where most placers contain only fully Ag-depleted gold grains, Kelley (2007) used remnant alloyed silver and small sulphide inclusions to identify a less mature, actively forming placer having a potentially significant lode source. This example raises the further possibility that the types of sulphide inclusions present in gold grains might be used to distinguish porphyry, epithermal, and volcanogenic gold sources

LIMITATIONS OF SULPHIDES AS INDICATOR MINERALS

The coarse, >0.25 mm heavy minerals in most porphyry, epithermal, and volcanogenic Au deposits that have not been affected by supergene alteration include at least one primary sulphide mineral in addition to pyrite. The sulphide species vary with deposit type, with porphyry deposits typically containing chalcopyrite and possibly also bornite and molybdenite, epithermal deposits containing As sulphides such as realgar, and volcanogenic deposits containing chalcopyrite, sphalerite, and possibly galena.

In till samples collected in Canada by reverse circulation or rotasonic drilling below the 2 to 3 m depth of post-glacial weathering, all sulphide mineral grains are perfectly preserved (Fig. 6). In areas of thick till cover, therefore, most base metal anomalies obtained from surface soil geochemistry surveys simply reflect leaching of glacially dispersed sulphide minerals from the top 2 to 3 m of the till, regardless of the analytical method employed, and are not indicative of mineralization in the subjacent bedrock.

In the top 2 to 3 m of non-calcareous till, such as that found over the Canadian Shield, grains of only two sulphide minerals, molybdenite and chalcopyrite, are significantly resistant to oxidation (Table 1). The rate of molybdenite survival appears to be 100 percent as no transported grains with visibly leached

surfaces have been observed by ODM in many years of study. The rate of chalcopyrite survival is much lower, apparently just a few percent, and most of the surviving grains are of a dull bronze colour with deeply furrowed surfaces (Fig. 7A). With pyrite normally being much more abundant than chalcopyrite even in significant Cu deposits, pyrite grains were correspondingly more abundant in the till before it was oxidized. Due to the lag in chalcopyrite degradation relative to pyrite degradation, the survival of just a few tens to hundreds of chalcopyrite grains unaccompanied by pyrite grains indicates a once-stronger and potentially significant chalcopyrite anomaly. Sphalerite and galena grains have been found to survive to a significant extent only in carbonate-rich, sulphide-buffering till such as that found over the Western Canada Sedimentary Basin (Fig. 2), where they form a significant dispersal train glacially down-ice from the Mississippi Valley-type Zn-Pb deposit at Pine Point (Oviatt *et al*. 2013).

In the deeply weathered lateritic soils of the tropics and the thick, mature colluvium/alluvium covering ancient, low-relief landscapes in arid regions such as Western Australia, sulphide leaching is normally complete, precluding the use of any sulphide minerals as indicator minerals. In geologically younger,

Table 1. Relative stabilities of sulphide and arsenide mineral grains in oxidized till in Canada. Stabilities were determined by comparing grain abundances in shallow, oxidized till samples to those in deeper, unoxidized samples. Modified from Averill (2011).

| Stable	Unstable	Parastable
Molybdenite	Pyrrhotite	Chalcopyrite
Cinnabar	Pyrite	Sphalerite } in carbonate-rich till
Sperrylite	Pentlandite	Galena
Loellingite	Arsenopyrite	
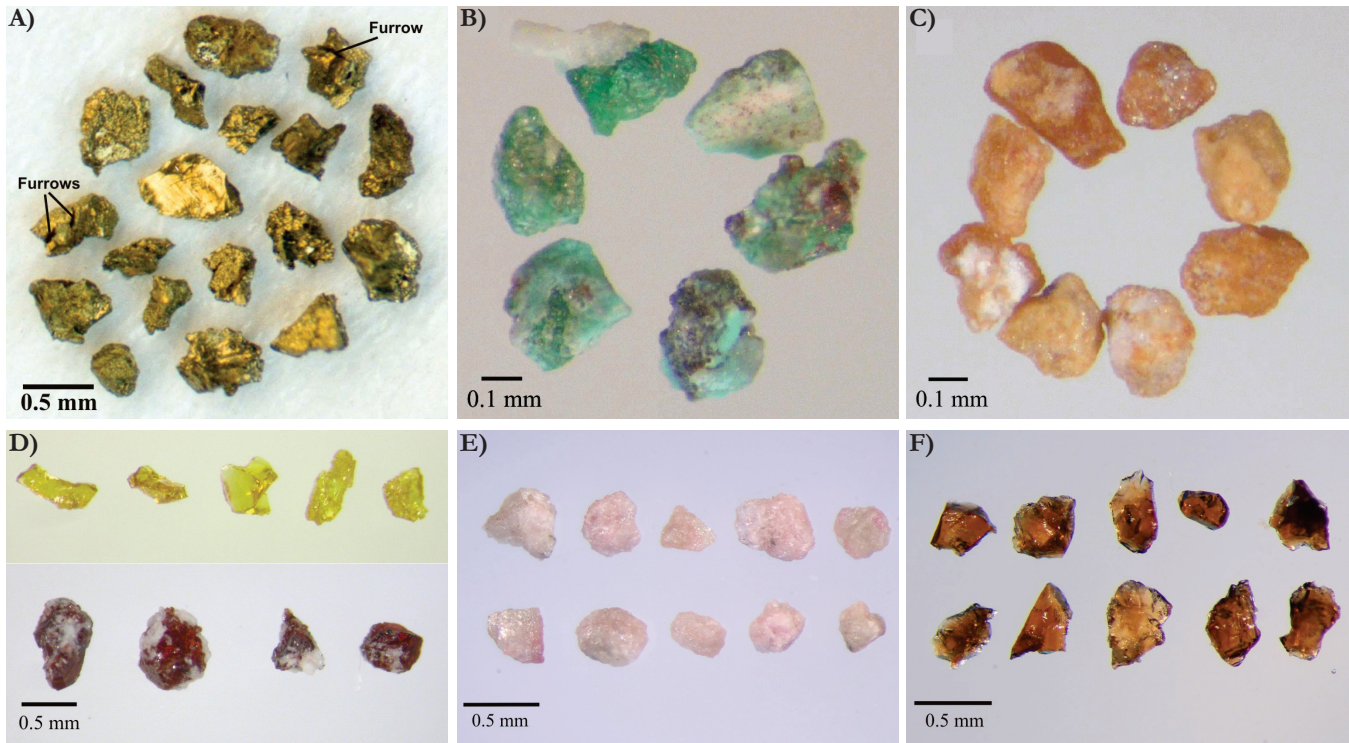
Fig. 7. Examples of transported indicator mineral grains recovered from oxidized surficial sediments near porphyry Cu and volcanogenic Au deposits. **A)** Surviving chalcopyrite grains from a shallow till sample in Canada. The original bright metallic surfaces have been oxidized to a dull bronze colour and deep furrows have developed along some cleavage planes. **B)** Atacamite grains from sheet wash gravel, Chile. **C)** Jarosite grains from sheet wash gravel, Chile. **D)** Andradite garnet grains from alluvium, Arizona porphyry Cu belt, USA. The colour of the grains ranges from yellow-orange (top row) to red-orange (lower row; garnet is intergrown with finer grained quartz alteration) or orange-brown. **E)** Ruby-pink Mn-epidote grains from a shallow till sample, Woodjam porphyry Cu district, British Columbia, Canada. **F)** Orange-brown spessartine garnet grains from a shallow till sample, Blackwater volcanogenic Au district, British Columbia, Canada. All photos by Overburden Drilling Management Limited.

recently uplifted, high-relief regions with similarly arid climates such as the Atacama Desert and Arizona in the Western Cordillera of the Americas, however, most porphyry Cu and Cu-Au deposits have a supergene blanket in which the original chalcopyrite has been transformed into secondary sulphide minerals such as chalcocite and "oxide" minerals such as turquoise $(CuAl_6(PO_4)_4(OH)_8 \cdot 5H_2O)$ and atacamite $(Cu_2Cl(OH)_3$; Fig.

7B). Exploration samples collected from the thin, dry soil or *chusca* developed on alluvial gravel downslope from porphyry Cu deposits in Chile and Arizona and tested by ODM have consistently shown high survival of dispersed grains of supergene Cu-oxide minerals whereas supergene Cu-sulphides are absent. For example, a distinct turquoise anomaly, defined by sampling at a density of ~1 sample per km² (Fig. 8), is present
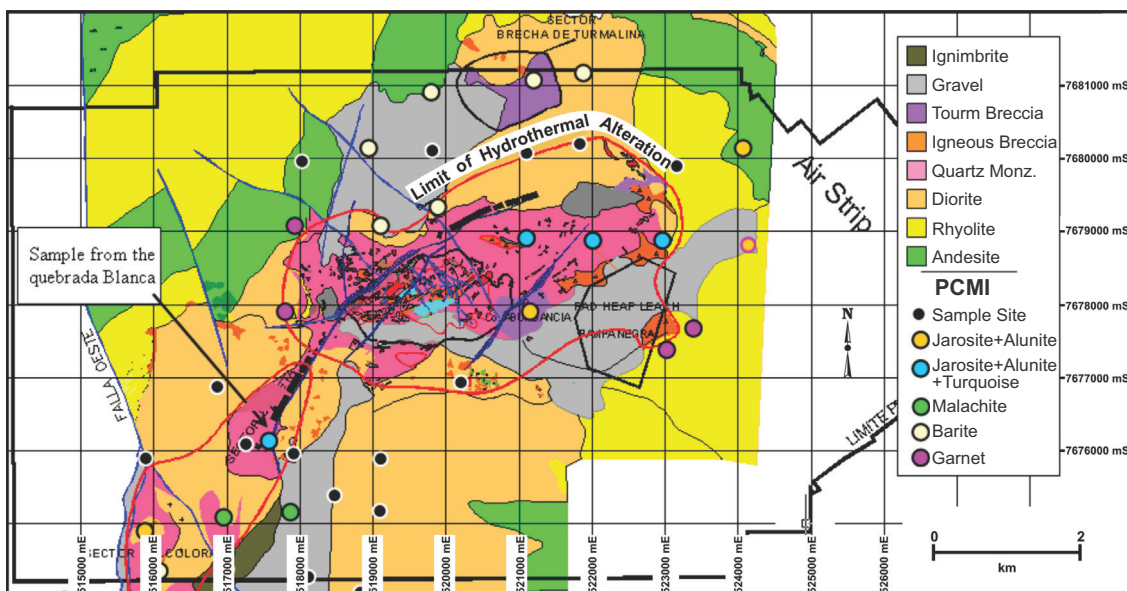
Fig. 8. Distribution of porphyry Cu indicator minerals in weathered alluvium near the Quebrada Blanca deposit, Chile. Source: Averill (2011).
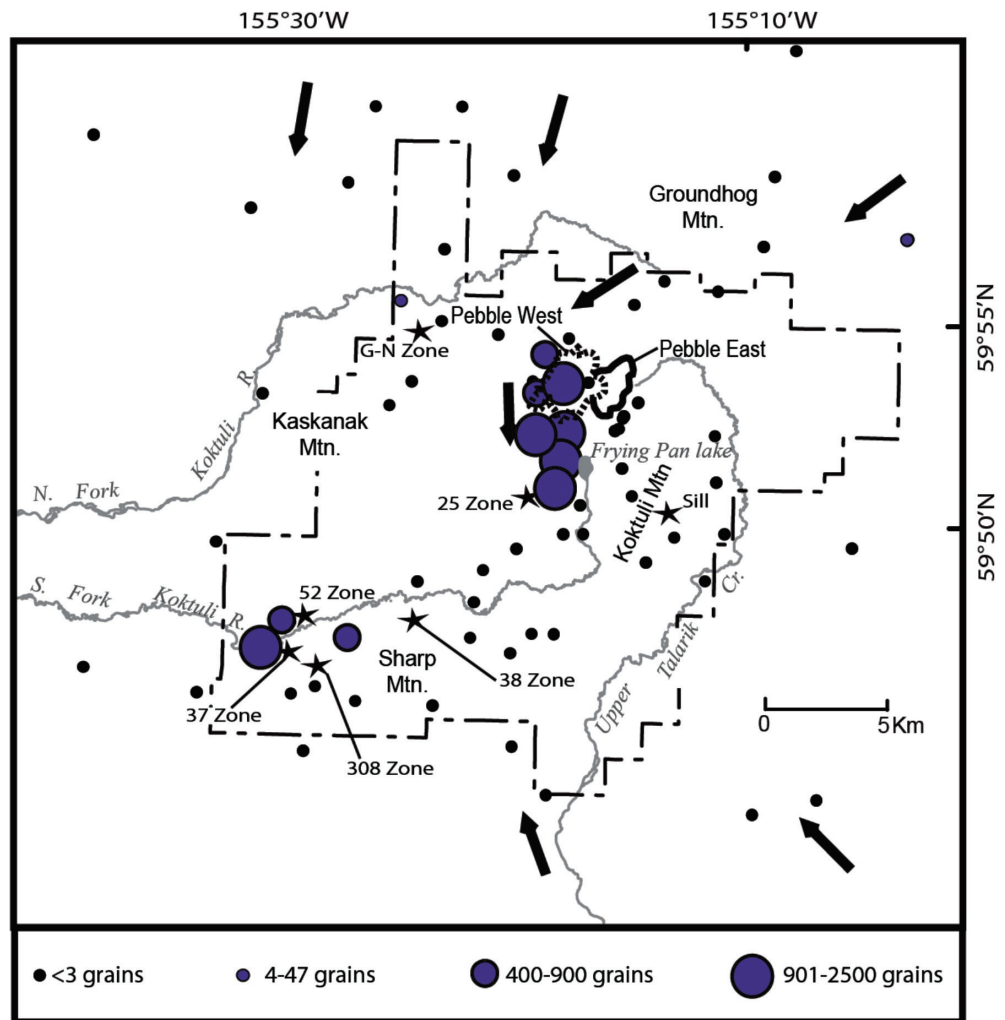
Fig. 9. Jarosite abundance in the 0.25 to 0.5 mm heavy mineral fraction of 10 kg till samples collected near the Pebble porphyry Cu-Au deposit, Alaska. The direction of glacial ice flow is shown by the black arrows. Source: Kelley *et al.* (2011).

in the alluvium over and downslope from the Quebrada Blanca porphyry Cu deposit (Averill 2011). Similarly, the primary realgar and other As-bearing sulphides of epithermal Au deposits have been partly transformed to the more stable and useful As-oxide mineral scorodite ($FeAsO_4 \cdot 2H_2O$). Some of the oxide minerals have a specific gravity of <3.2 g/cm^3 and thus become useful indicator minerals only if a lower density separation is performed to recover them (Averill 2011).

The hyperarid weathering in Chile has been beneficial not only in transforming hypogene chalcopyrite and realgar into stable secondary oxide minerals that can be used effectively as indicator minerals; it has also transformed pyrite into jarosite ($KFe_3(SO_4)_2(OH)6$; Fig. 7C), which is similarly stable and distinctly anomalous in the *chusca* at Quebrada Blanca (Fig. 8). While an arid climate combined with a recently uplifted terrane such as the Western Cordillera of the Americas is necessary for the formation of secondary sulphurous minerals such as jarosite, today's climate need not be arid in order for these minerals to be used as indicator minerals. For example, the Pebble porphyry Cu-Au deposit occurs in an area of Alaska that has been glaciated (Fig. 3) and presently has a subarctic climate but the preglacial climate was arid and glaciation was sufficiently light that part of the supergene blanket of the deposit is preserved. Recognizing this, Kelley *et al.* (2011) performed an indicator mineral survey at Pebble specifically directed at recovering both gold grains and a Chilean-type suite of porphyry Cu-

Au indicator minerals and successfully identified a strong, 5 km long jarosite dispersal train leading directly down-ice from the Pebble deposit (Fig. 9). The jarosite content of the anomalous samples ranged up to 2500 grains per 10 kg till sample versus background of just 0 to 3 grains per sample

ALTERATION INDICATOR MINERALS

The very limited survival of sulphide mineral grains in surficial sediments near sulphide-rich mineral deposits greatly increases the dependence of indicator mineral surveys on more chemically stable minerals derived from the hydrothermal alteration zones of these deposits. The alteration systems associated with porphyry Cu and Cu-Au deposits tend to be concentrically zoned (Lowell & Guilbert 1970) and, as shown by Averill (2011) and summarized in Table 2, at least one hypogene mineral from each alteration zone can be used as an indicator mineral. The most useful minerals identified to date include diaspore and magnesian tourmaline (dravite), derived from the highly aluminous, advanced argillic core of the alteration system, and andradite garnet, derived from the outer propylitic zone, as illustrated by the central tourmaline and peripheral andradite anomalies at Quebrada Blanca (Fig. 8). If, as at Quebrada Blanca, the porphyry mineralization grades upward to epithermal mineralization, significant barite can also be expected.

Table 2. Principal hypogene porphyry Cu and epithermal Au indicator minerals found in oxidized surficial sediments in recently uplifted arid regions of the Western Cordillera of the Americas. Modified from Averill (2011).

| Mineral	Composition	Principal Provenance (alteration zone)				
		Potassic	Argillic	Phyllic	Propylitic	Epithermal Au
Diaspore	$AlO(OH)$		———			
Alunite	$KAl_3(SO_4)_2(OH)_6$		———————			
Dravite	$NaMg_3Al_6(BO_3)_3(Si_6O_{18})(OH)_4$		———			
Andradite	$Ca_3Fe_2(SiO_4)_3$				———	
Barite	$BaSO_4$					———

The chemical composition of andradite $(CaFe_2(SiO_4)_3)$ reflects the Ca+Fe metasomatism that is characteristic of propylitic alteration. This metasomatism is further indicated by the presence within propylitic zones of other, more abundant Ca and/or Fe-rich minerals, principally calcite, epidote $(Ca_2(Al,Fe)_3(Si_3O_{12})(OH))$, and pyrite (Lowell & Guilbert 1970). While epidote is sufficiently heavy and resistant to weathering to be a potential indicator mineral, the surficial sediments near most porphyry deposits contain abundant epidote derived from unaltered intrusive and volcanic rocks, impeding the recognition of any propylitic epidote grains. In the glaciated Woodjam porphyry district (Fig. 2) in the Western Cordillera of Canada, however, the unaltered rocks contain

minimal epidote and Plouffe *et al.* (2013) have shown that the propylitic alteration zones of the porphyry deposits are reflected by a significant increase in the overall epidote content of the till (Fig. 10). Some of the epidote grains contain sufficient manganese to change their colour from the usual pistachio green to ruby pink (Fig. 7E) but overall epidote abundance rather than epidote colour is the best indicator of propylitic alteration at Woodjam.

The hydrothermal alteration envelopes of the volcanogenic gold deposits in the Bousquet, Rainy River, and Blackwater districts in Canada also contain garnet but of a spessartine $(MnFe_2(SiO_4)_3)$ rather than andradite composition, reflecting Mn enrichment in the fluids associated with the formation of volcanogenic deposits. Spessartine is abundant at each deposit but is a useful indicator mineral only in the Blackwater district. Blackwater is located in the Western Cordillera (Fig. 2) where the till contains no almandine garnet to impede identification of the spessartine grains, which are of a rather bland orange-brown colour (Fig. 7F). The absence of almandine in the till is due to (a) the underlying volcanic rocks being unmetamorphosed; and (b) the Blackwater area, during glaciation, being only 100 km down-ice form the ice divide in the high mountains of the Coast Range to the west (Fig. 3) and most of the intervening rock formations also being unmetamorphosed.
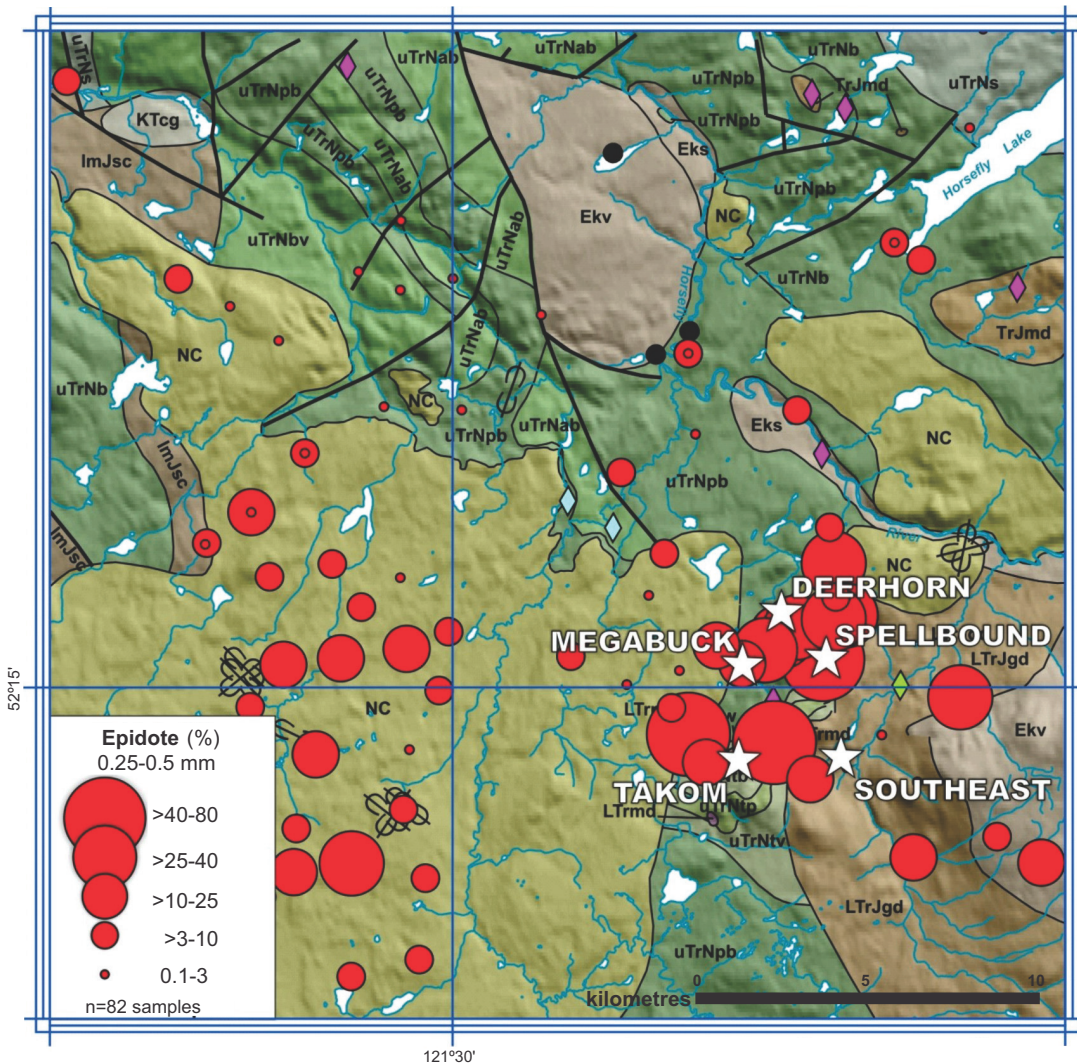
Fig. 10. Percent epidote in the 0.25 to 0.5 mm heavy mineral fraction of the till near the porphyry Cu and Cu-Au deposits of the Woodjam district, British Columbia, Canada. Source: Plouffe *et al.* (2013).
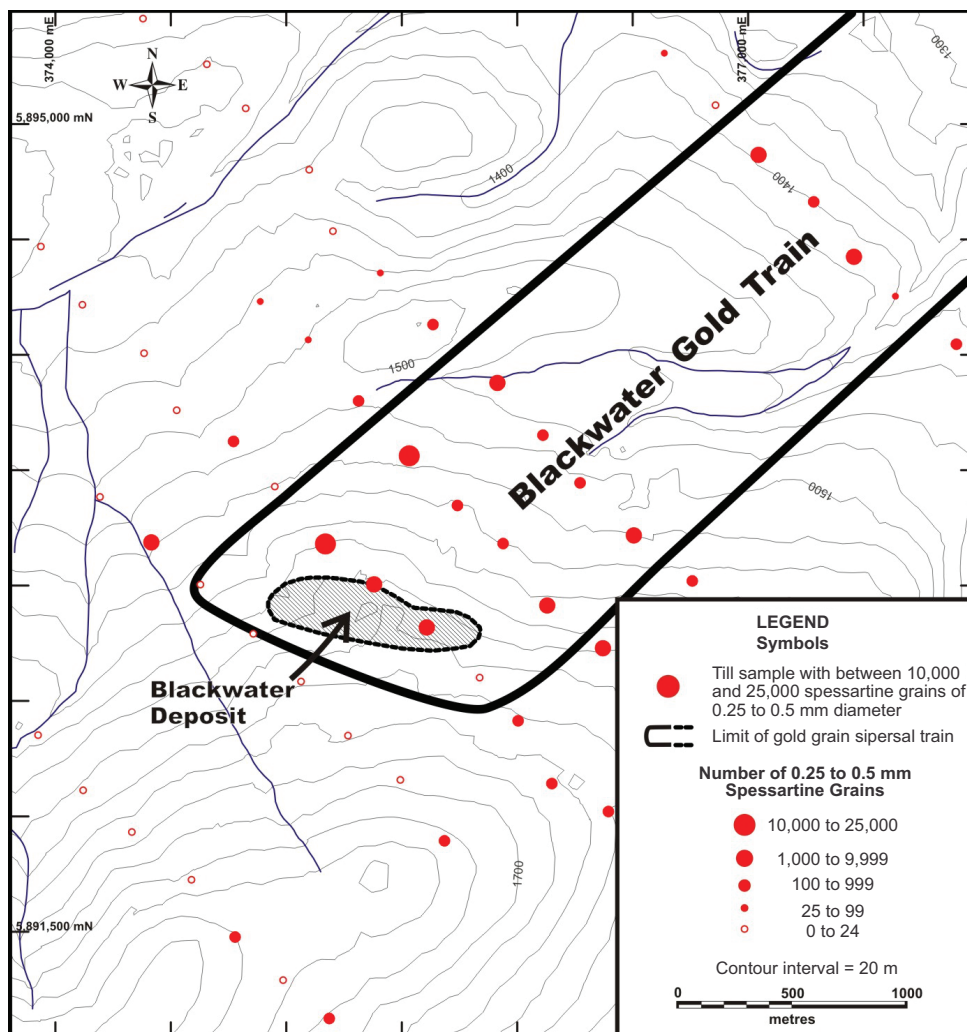
Fig. 11. Spessartine abundance in the 0.25 to 0.5 mm heavy mineral fraction of 10 kg till samples collected in the area of the Blackwater gold grain dispersal train, British Columbia. Courtesy of New Gold Inc.

The till in the Bousquet and Rainy River districts of the Canadian Shield, in contrast, is very almandine rich, commonly containing hundreds of thousands of grains of >0.25 mm size per 10 kg sample even though the underlying volcanic rocks are almandine-free greenstone. This is because these districts, when glaciated by the Laurentide ice sheet, were >1000 km down-ice from the ice centre to the northeast and the intervening Archean rocks consist mainly of garnetiferous gneiss. The alteration zones of both deposits are so aluminous that they also contain kyanite (Al_2SiO_5), a mineral that would not normally be expected in greenschist-facies rocks. At the Rainy River deposit, the presence of kyanite in the alteration zone was recognized only after a kyanite dispersal train was identified in the till (Averill 2013).

At Blackwater, surface till sampling, mostly at a density of 2 to 3 samples per km^2 compared to the 1 sample per km^2 commonly used in porphyry Cu exploration programs such as Quebrada Blanca (Fig. 8), has identified a strong, 1.2 km wide gold grain dispersal train (Fig. 11) and traced it 2.5 km down-ice to the limit of sampling. Gold grain counts obtained from 10 kg till samples collected within the train ranged from tens to hundreds of grains per sample, compared to a very low background of 0 to 5 grains per sample. The same till samples yielded up to 25,000 spessartine grains compared to very low background levels of 0 to 20 grains per sample. In view of the sharp, up to 1000:1 contrast between anomalous and back-

ground spessartine values and the considerable strength of the anomaly in the most distal till samples, 2.5 km down-ice from Blackwater, the total detectable length of the train probably exceeds 10 km.

DISCUSSION AND CONCLUSION

Porphyry Cu (and Cu-Au), epithermal Au, and volcanogenic Au deposits all contain minerals that are heavy, coarse-grained, visually distinctive, and specifically indicative of these deposits. When dispersed into surficial sediments, however, not all of these minerals form useful indicator minerals in all situations. The utility of a mineral depends mainly on its susceptibility to oxidation, the degree of oxidation of the host sediments, the climate under which this oxidation occurred, and also the climate at the time the deposit was formed, as witnessed by the jarosite dispersal train in the till at Pebble, Alaska (Fig. 9). Most sulphide indicator minerals are susceptible to oxidation whereas many indicators of hydrothermal alteration zones are stable in oxidized sediments. In gold grains, which are mostly finer than the other indicator minerals and are extracted separately, only the alloyed silver is normally subject to oxidation, although Hough *et al.* (2008) have identified minute crystals of secondary gold deposited by saline groundwater in regolith at a gold deposit in Western Australia. Noble *et al.* (2013) tested various size fractions of anomalous soil samples from this

region and in some samples obtained much higher Au analyses from the -0.2 μm nanoparticulate fraction than from the coarser particulate fractions, suggesting that ultrafine secondary gold particles may also be present in the soil.

In recently glaciated regions such as Canada, all indicator minerals are preserved in unoxidized till below a depth of 2 to 3 m. At this depth, every sulphide grain remains as fresh as it was when the till deposited (Fig. 6), and the specific sulphide mineral assemblage within a dispersal train can be used to distinguish the type of source. For example, a pyrite-chalcopyrite-sphalerite-galena anomaly in the >0.25 mm fraction of the till accompanied by gold grains in the finer fractions normally indicates a volcanogenic Au deposit. A consequence of the freshness of sulphides at depth is that soil surveys in areas of thick till cover primarily detect metals leached from the top 2 to 3 m of the till. Since no metals have been leached from the underlying fresh, sulphide-bearing till, no geochemical method can be expected to see into this till or through it to bedrock.

In unglaciated areas, the most complete range of indicator minerals occurs at deposits in geologically young, recently uplifted terranes with arid climates, such as those of Arizona and the Atacama Desert. In the upper parts of these deposits, supergene oxidation has transformed some of the hypogene sulphide minerals into secondary oxide minerals that, following dispersal into the surficial environment, remain resistant to further oxidation and form very useful indicator minerals. Porphyry Cu and Cu-Au deposits tend to have particularly large and diagnostic indicator mineral signatures, especially in arid regions, because (1) both the deposits and their alteration envelopes are large; (2) the alteration is concentrically zoned with different indicator minerals present in each zone; and (3) being in geologically young terranes, there are no metamorphic minerals in the surficial sediments to dilute and impede the recognition of indicator minerals, such as the key andradite garnet grains derived from the propylitic alteration zone. Epithermal Au deposits associated with the porphyry deposits in arid regions of the Americas appear to have a more restricted suite of available indicator minerals, principally barite and scorodite.

In Canada, spessartine garnet is commonly present in the alteration zones of volcanogenic Au deposits but is a useful indicator mineral only for deposits such as Blackwater that are hosted by the unmetamorphosed volcanic rocks of the Western Cordillera (Fig. 2). While spessartine grains are also present in till near similar gold deposits in the Canadian Shield, such as those of the Bousquet and Rainy River districts, the spessartine signature tends to be overwhelmed by almandine garnet derived from Archean gneiss that comprises much of the shield. And in the most deeply weathered and thickly covered parts of Western Australia, most heavy mineral grains in the surficial sediments, including those of spessartine and other garnets, have been consumed by oxidation, as illustrated by the very limited lamproite indicator mineral suite in the colluvium at Big Spring and Ellendale (Jaques *et al.* 1986). In most other regions, however, indicator minerals derived from porphyry Cu (and Cu-Au) and epithermal and volcanogenic Au deposits are sufficiently diverse and abundant in the surficial environment to distinguish between and explore effectively and efficiently for these closely related types of mineral deposits.

REFERENCES

AVERILL, S.A. 2001. The application of heavy indicator mineralogy in mineral exploration with emphasis on base metal indicators in glaciated metamorphic and plutonic terrains. *In:* MCCLENAGHAN, M.B., BOBROWSKY, P.T., HALL, G.E.M. & COOK, S.J. (eds) *Drift Exploration in Glaciated Terrains.* Geological Society, London, Special Publications, 185, 69–81.

AVERILL, S.A. 2011. Viable indicator minerals in surficial sediments for two major base metal deposit types: Ni-Cu-PGE and porphyry Cu. *Geochemistry: Exploration, Environment, Analysis,* 11, 279–292.

AVERILL, S.A. 2013. Discovery and delineation of the Rainy River gold deposit using glacially dispersed gold grains sampled by deep overburden drilling: A 20 year odyssey. *In:* PAULEN, R.C. & MCCLENAGHAN, M.B. (eds) *New Frontiers for Exploration in Glaciated Terrain.* Geological Survey of Canada, Open File 7374, 37–46.

DESBOROUGH, G.A., RAYMOND, W.H. & IAGMIN, P.J. 1970. Distribution of silver and copper in placer gold derived from the northeastern part of the Colorado Mineral Belt. *Economic Geology,* 65, 937–944.

DUBÉ, B., GOSSELIN, P., MERCIER-LANGEVIN, P., HANNINGTON, M. & GALLEY, A. 2007a. Gold-rich volcanogenic massive sulphide deposits. *In:* GOODFELLOW, W.D. (ed) *Mineral Deposits of Canada.* Geological Association of Canada, Mineral Deposits Division, Special Publication No. 5, 75–94.

DUBÉ, B., MERCIER-LAGNEVIN, P., HANNINGTON, M., LAFRANCE, B., GOSSELIN, G. & GOSSELIN, P. 2007b. The LaRonde Penna world-class Au-rich volcanogenic massive sulphide deposit, Abitibi, Quebec: mineralogy and geochemistry of alteration and implications for genesis and exploration. *Economic Geology,* 102, 633–666.

DYKE, A.S. & PREST, V.K. 1987. *Paleogeography of northern North America, 18,000-5,000 years ago.* Geological Survey of Canada, Map 1703A.

GEOLOGICAL SURVEY OF CANADA 1957. *Bedrock geology.* Atlas of Canada, 3rd edition.

HANNINGTON, M.D., POULSEN, K.H., THOMPSON, J.F.H., AND SILLITOE, R.H. 1999. Volcanogenic gold in the massive sulfide environment. *In:* Barrie, C.T. and Hannington, M.D. (eds.) *Volcanic-Associated Massive Sulfide Deposits: Processes and Examples in Modern and Ancient Settings.* Reviews in Economic Geology, 8, 325–356.

HOUGH, R.M., NOBLE, R.R.P., HITCHEN, G.J., HART, R., REDDY, S.M., SAUNDERS, M., CLODE, P., VAUGHAN, D., LOWE, J., GRAY, D.J., ANAND, R.R., BUTT, C.R.M. & VERRALL, M. 2008. Naturally occurring transparent gold nanoplates and particles. *Geology,* 36, 571–574.

HUTCHISON, M.T. 2013. Diamond exploration and prosectivity of the Northern Territory of Australia. *In:* PEARSON, D.G., GRUTTER, H.S., HARRIS, J.W., KJARSGAARD, B.A. O'BRIEN, H., CHALAPATHI RAO, N.V. & SPARKS, S. (eds) *Proceedings.* 10th International Kimberlite Conference. 2, 257–280.

JAQUES, A.L., LEWIS, J.D. & SMITH C.B. 1986. *The kimberlites and lamproites of western Australia.* Geological Survey of Western Australia, Bulletin 132.

KELLEY, D. 2007. Indicator mineral methods in precious metal exploration. *In:* THORLEIFSON, L.H. & MCCLENAGHAN, M.B. (eds) *Exploration 07, Workshop 3: Indicator Mineral Methods in Mineral Exploration.* The Association of Applied Geochemists, post-publication insert.

KELLEY, K.D., EPPINGER, R.G., LANG, J., SMITH, S.M. & FEY, D.L. 2011. Porphyry Cu indicator minerals in till as an exploration tool: example from the giant Pebble porphyry Cu-Au-Mo deposit, Alaska, USA. *Geochemistry: Exploration, Environment, Analysis,* 11, 321–334.

KNIGHT, J.B., MORTENSEN, J.K. & MORISON, S.R. 1999. Lode and placer gold composition in the Klondike District, Yukon Territory, Canada: implication of the nature and genesis of Klondike placer and lode gold deposits. *Economic Geology,* 94, 649–664.

LOWELL, J.D. & GUILBERT, J.M. 1970. Lateral and vertical alteration-mineralization zoning in porphyry ore deposits. *Economic Geology,* 65, 373–408.

NOBLE, R.R.P, CAVALIERE, M, MORRIS, P.A., TENTEN PINCHAND, G. & HOUGH, R.M. 2013. Determination of micro and nanoparticulate fraction gold in regolith. *EXPLORE,* 159, 1–13.

OVIATT, N.M., MCCLENAGHAN, M.B., PAULEN, R.C., GLEESON, S.A., AVERILL, S.A. & PARADIS, S. 2013. *Indicator minerals in till and bedrock samples from the Pine Point Mississippi Valley-type (MVT) district, Northwest Territories.* Geological Survey of Canada, Open File 7423.

PLOUFFE, A., FERBEY, T., ANDERSON, B., HASHMI, S. & WARD, B. 2013. *New TGI-4 till geochemistry and mineralogy results near the Highland Valley, Gibraltar, and Mt. Polley mines, and Woodjam District: an aid to search for buried porphyry deposits.* Geological Survey of Canada, Open File in press.

RICHARDS, J.P., BOYCE, A.J. & PRINGLE, M.S. 2001. Geologic evolution of the Escondida area, northern Chile: a model of spatial and temporal localization of porphyry Cu mineralization. *Economic Geology,* 96, 271–306.

SILLITOE R.H. & BONHAM, H.F. 1990. Sediment-hosted gold deposits; distal products of magmatic-hydrothermal systems. *Geology,* 18, 157–161.

SIMPSON, R.G., WELHENER, H.E., BORNTRAEGER, B., LIPIEC, I. & REYES, R.M. 2012. *NI 43-101 technical report on preliminary economic assessment, Blackwater project, British Columbia*. Report prepared for New Gold Inc. Retrieved August 1, 2013, from www.sedar.com.

Application of iron-oxide chemistry in mineral exploration

Georges Beaudoin

Département de géologie et de génie géologique, Université Laval, Québec, Québec G1V 0A6
Author e-mail: Georges.Beaudoin@ggl.ulaval.ca

The iron oxides (magnetite and hematite) form major to accessory minerals in a range of mineral deposits and rocks. Iron oxides incorporate a large suite of minor to trace elements in their crystalline structure as a function of the thermodynamic conditions during crystallization. This variation in mineral composition is used to fingerprint a range of magmatic, hydrothermal and sedimentary mineral deposit types. Because iron oxides are resistive to mechanical abrasion and chemical alteration during transport and burial in sediments, and because they can be easily separated in magnetic fractions, they constitute a useful indicator mineral for exploration.

ANALYTICAL METHODS AND SAMPLE PREPARATION

The mineral grains were analyzed using the highly optimized analytical methods of the Electron Probe Micro-Analyzer (EPMA; Dupuis & Beaudoin 2011) and Laser Ablation Inductively Coupled Plasma Mass Spectrometry (LA-ICP-MS; Dare *et al.* 2012). EPMA analyses have detection limits to 10s ppm for small areas (beam diameter of 10 µm), which is sufficient to avoid small inclusions in a target mineral. LA-ICP-MS analyses have detection limits to ppb levels, but the required volume is larger; during analyses a linear trench is typically ablated with a 80 µm-diameter laser beam. This larger area required for analysis by LA-ICP-MS limits analyses to larger grains that are devoid of abundant inclusions. An advantage of the larger beam size of LA-ICP-MS is that small exsolutions formed by sub-solidus processes are incorporated in the mineral analysis, allowing measurement of the original composition of the grain before sub-solidus exsolution. Dare *et al.* (2012) indicated that both methods produce highly correlated analytical results down to the detection limit of the EPMA method.

For this study, bedrock samples were crushed to mimic the mechanical ablation produced by glaciers. The 0.5 to 2.0 mm heavy mineral ferromagnetic fractions of the till and disaggregated rock samples were prepared following the methods outlined by McClenaghan (2011). A representative subsample of grains from this ferromagnetic fraction was mounted in epoxy for EPMA analysis. These grains typically consisted of aggregates of one ferromagnetic mineral. Grains of less than 0.5 mm diameter do not have sufficient surface area for EPMA or LA-ICP-MS analyses and grains larger than 2.0 mm typically do not occur in sufficient numbers to be a representative subset. Statistical analysis indicates that in a subsample of ~100 grains, approximately 70% of these grains will have a polished surface large enough for analysis, which is a sufficient number to determine a chemical composition representative of the sample as a whole (Sappin *et al.* 2012).
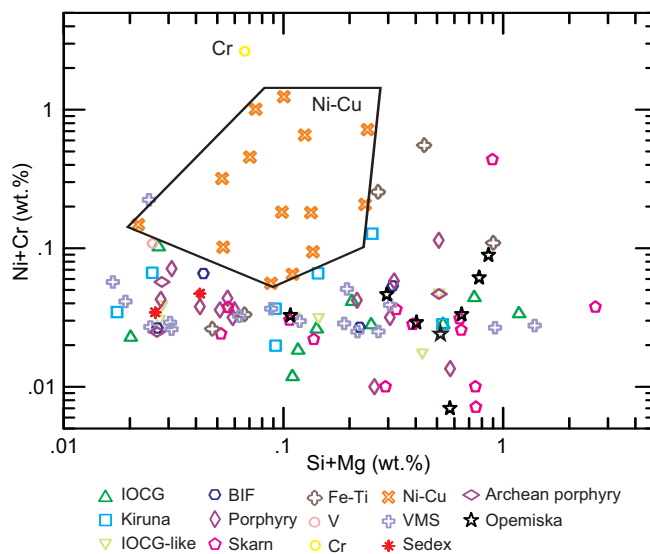

Fig. 1. The Ni+Cr versus Si+Mg discriminant diagram for Ni-Cu-PGE deposits (modified from Dupuis & Beaudoin 2011).

IRON OXIDES IN MINERAL DEPOSITS

Dupuis & Beaudoin (2011) constructed a series of discriminant diagrams using the average composition a deposit type to identify the distinct composition of iron oxides in a variety of deposit types. Dupuis & Beaudoin (2011) showed that Ni-Cu-PGE deposits can be distinguished from all other deposit types using the Ni+Cr versus Si+Mg diagram (Fig. 1). Further work on Ni-Cu deposits incorporating deposits with large ranges of age, magma types, and geological environments, including most major Ni-Cu deposits worldwide, has confirmed the efficiency of the Ni+Cr versus Si+Mg discriminant diagram (Boutroy *et al.* 2012.

A study of Ni-Cu deposits from the Sudbury district showed that the composition of magnetite evolves during the fractional crystallization of the sulphide liquid into the early Fe-rich monosulphide solid solution (MSS) cumulate and the residual Cu-rich intermediate solid solution (ISS; Dare *et al.* 2012). Lithophile elements are compatible in magnetite. Magnetite co-crystallization with MSS depletes the residual ISS in lithophile elements such that later forming magnetite, co-crystallized with ISS, is also depleted in lithophile elements (Fig. 2). This pattern is found in Ni-Cu deposits worldwide (Boutroy *et al.* 2012). The efficiency of the Ni+Cr versus Si+Mg diagram is in part a consequence of the contrasting behaviour of lithophile Cr and chalcophile Ni. Spider diagrams of lithophile elements (Fig. 3A) and chalcophile elements (Fig. 3B) show that most lithophile elements, such as Cr, that are enriched in MSS magnetite become depleted in the residual sul-
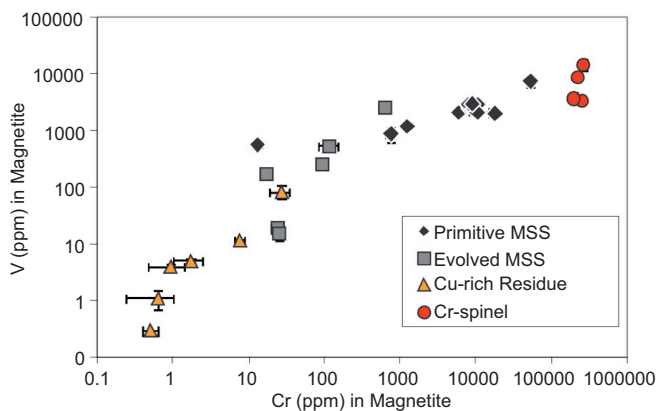
Fig 2. Covariation of lithophile elements in magnetite in the sulphide liquid during fractional crystallization from MSS to ISS and chrome spinel (Cr-spinel) crystallized from the mafic magma in Sudbury (modified from Dare *et al.* 2012).

phide melt forming ISS magnetite (Fig. 3A; Dare *et al.* 2012). In contrast, chalcophile elements, such as Ni, partition preferentially in the MSS depleting the coeval magnetite; whereas, the late-forming magnetite in the ISS preferentially incorporates Ni in the absence of competing Fe-sulphides (Fig. 3B; Dare *et al.* 2012). Boutroy *et al.* (2012) also showed that secondary magnetite in veins in massive sulphide bodies and disseminated in host rocks has a composition that is different from that of primary magmatic magnetite and, as Figure 1 shows, plots outside the field typical for Ni-Cu-PGE deposits.
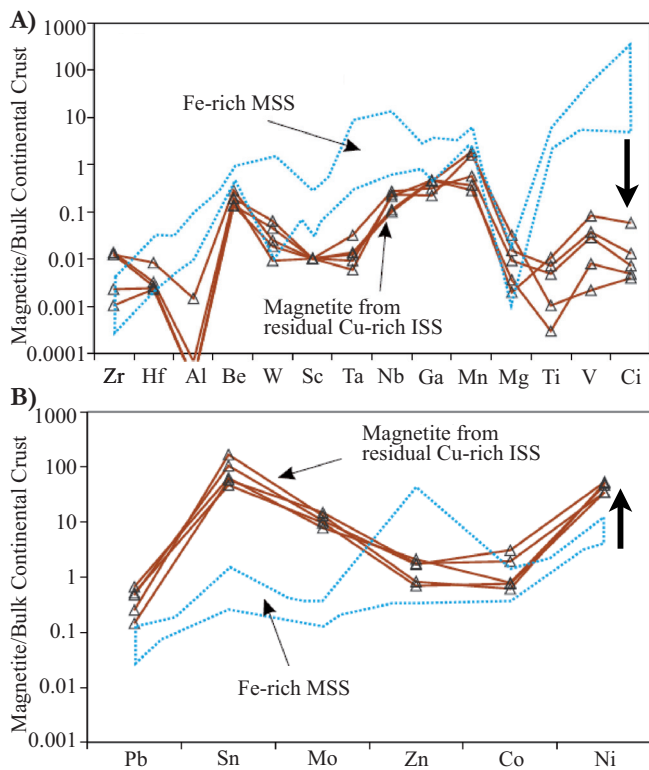
Fig 3. Spider diagrams of **(A)** lithophile and **(B)** chalcophile elements in MSS and ISS, normalized to bulk continental crust (Rudnick & Gao 2003). Arrows shows depletion of lithophile Cr (A), and enrichment of Ni (B), during fractional crystallization of the sulphide liquid from MSS to ISS (modified from Dare *et al.* 2012).
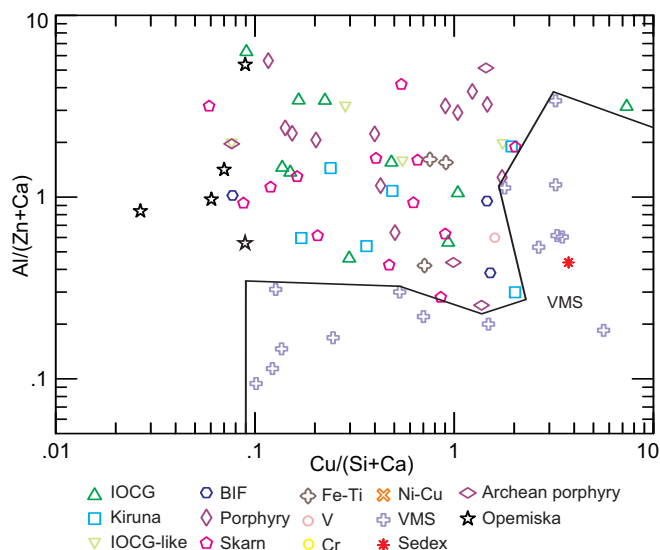
Fig 4. The Cu/(Si+Ca) versus Al/(Zn+Ca) discriminant diagram for Cu-Zn VMS and Zn-Pb SEDEX deposits (modified from Dupuis & Beaudoin 2011). Note that deposit average compositions that plot in the field for Ni-Cu deposits (Fig. 1) are not shown on this diagram.

The second step of data analysis is to test for iron oxides typical of Cu-Zn volcanogenic massive sulphide (VMS) and Zn-Pb SEDEX deposits using the Cu/(Si+Ca) versus Al/(Zn+Ca) diagram (Fig. 4; Dupuis & Beaudoin 2011). Magnetite in VMS and SEDEX deposits is typically a product of hydrothermal or metamorphic oxidation and replacement in the massive sulphide lens (Galley *et al.* 2000). In VMS deposits, magnetite is enriched in Si, Zn, and Ca, and depleted in Al, compared to other deposit types.

The final step of data analysis is to plot iron oxide compositions on the Ti+V versus Ni/(Cr+Mn) diagram (Fig. 5) to identify compositions typical of Fe-Ti-V, Kiruna Fe-P, Cu-Mo-

Fig 5. The Ti+V versus Ni/(Cr+Mn) discriminant diagram for Fe-Ti-V, Kiruna Fe-P, Cu-Mo-Au porphyry, iron-oxide-copper-gold (IOCG), Superior-type banded iron formation and skarn deposit types (modified from Dupuis & Beaudoin 2011). Note that deposit average compositions that plot in the field for Ni-Cu deposits (Fig. 1) and in the field for VMS and SEDEX deposits (Fig. 4) are not shown on this diagram.
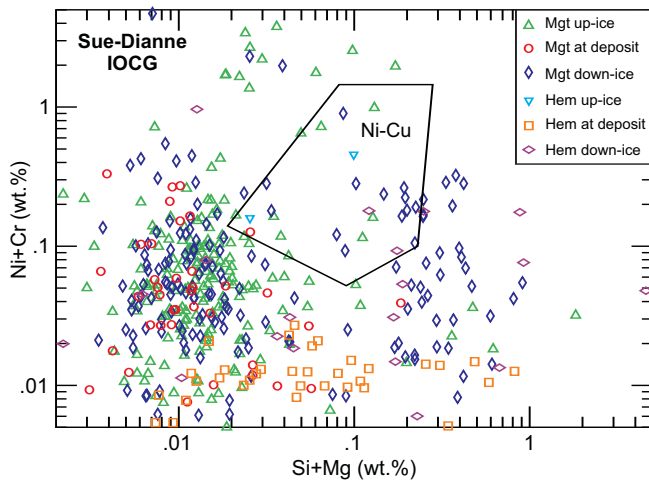
Fig 6. Magnetite and hematite composition from the ferromagnetic fraction of glacial tills up-ice, at the Sue-Dianne deposit (Great Bear Magmatic Zone, Northwest Territories, Canada) and down-ice, plotted in the Ni+Cr versus Si+Mg discriminant diagram for Ni-Cu-PGE deposits.

Fig 7. Magnetite and hematite composition from the ferromagnetic fraction of glacial tills up-ice, at the Pipe deposit (Thompson, Manitoba, Canada) deposit and down-ice, plotted in the Ni+Cr versus Si+Mg discriminant diagram for Ni-Cu-PGE deposits.

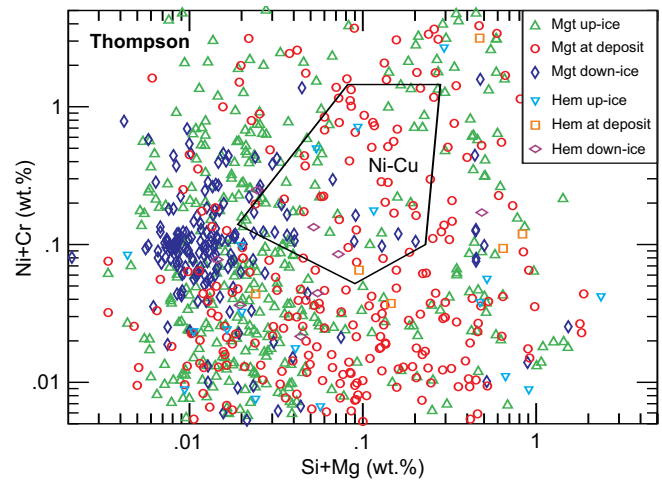Au porphyry, iron-oxide-copper-gold (IOCG), Superior-type banded iron formation (BIF), and skarn deposit types (Dupuis & Beaudoin 2011). In this diagram, magmatic Fe-Ti-V deposits plot at high Ti+V values, whereas magmatic-hydrothermal and sedimentary deposits are characterized by lower Ti+V values (Fig. 5). Another diagram using Ti+V versus Ca+Al+Mn yields similar results (Dupuis & Beaudoin 2011).

APPLICATION TO MINERAL EXPLORATION

Two case studies serve to illustrate the application of iron-oxide chemistry of the ferromagnetic fraction of till samples. The Sue-Dianne deposit is a hematite-dominant IOCG deposit located in the Great Bear Magmatic Zone (Northwest Territories, Canada). In this region, the potential for Ni-Cu deposits is low and there are no showings known of this deposit type. Figure 6 illustrates that hematite and magnetite from till samples collected up- and down-ice of the Sue-Dianne IOCG deposit, plot with few exceptions outside the field for Ni-Cu deposits on a Ni+Cr versus Si+Mg discriminant diagram. A similar survey along a profile up- and down-ice of the Thompson Nickel Belt (Manitoba, Canada), near the Pipe Ni-Cu deposit open pit, is shown in Figure 7. In contrast to the rare occurrence of oxide grains with the signature of Ni-Cu deposits near the Sue-Dianne IOCG deposit, the survey across the Pipe open pit shows a high proportion of iron oxide grains with this signature(Fig. 7).

CONCLUSIONS

Iron oxides have a chemical composition that is reflective of the environment at the time of their formation. Fractional crystallization of magma and sulphide liquid can be tracked by the change in composition of the iron oxides, which affords new tools to access the fertility of an intrusion for Ni-Cu deposits. Different deposit types have distinct iron oxide chemical signatures that can be used to identify the trace of an eroded deposit in a surficial sedimentary environment (fluvial, eolian, or glacial).

REFERENCES

BOUTROY, E., DARE, S.A.S., BEAUDOIN, G. & BARNES, S.-J. 2012. *Minor and trace element composition of magnetite from Ni-Cu deposits worldwide and its application to mineral exploration*. Geological Association of Canada-Mineralogical Association of Canada, Annual Meeting Program with Abstracts.

DARE, S.A.S., BARNES, S.-J. & BEAUDOIN, G. 2012. Variation in trace element content of magnetite crystallized from a fractionating sulfide liquid, Sudbury, Canada: Implications for provenance discrimination. *Geochimica et Cosmochimica Acta*, **88**, 27–50.

DUPUIS, C. & BEAUDOIN, G. 2011. Discriminant diagrams for iron oxide trace element fingerprinting of mineral deposit types. *Mineralium Deposita*, **46**, 319–335.

GALLEY, A.G., JONASSON, I.R. & WATKINSON, D.H. 2000. Magnetite-rich calc-silicate alteration in relation to synvolcanic intrusion at the Ansil volcanogenic massive sulfide deposit, Rouyn-Noranda, Quebec, Canada. *Mineralium Deposita*, **35**, 619–637.

MCCLENAGHAN, M.B. 2011. Overview of common processing methods for recovery of indicator minerals from sediment and bedrock in mineral exploration. *Geochemistry: Exploration, Environment, Analysis*, **11**, 265–278.

RUDNICK, R.L. & GAO, S. 2003. Composition of the continental crust. *In*: RUDNICK, R.L. (ed.) *The Crust. In*: HOLLAND, H.D. & TUREKIAN, K.K. (eds.) *Treatise on Geochemistry*. Elsevier, **3**, 1–64.

SAPPIN, A.-A., DUPUIS, C., BEAUDOIN, G. & MCMARTIN, I. 2012. *Grain size fraction and number of grains representative of iron oxide composition in till samples: the Sue-Dianne deposit area, Northwest Territories, Canada*. Geological Association of Canada-Mineralogical Association of Canada-Society of Economic Geology-Annual Meeting, Program with Abstracts.

The Ti-pa-haa-kaa-ning (TPK) gold grain glacial dispersal apron, northwestern Ontario, Canada

T.F. Morris

Northern Superior Resources Inc., 1351C Kelly Lake Road, Unit 7, Sudbury, Ontario, P3E 5P5
Author e-mail: tmorris@nsuperior.com

Superior Diamonds Inc. initiated an overburden sampling program in 2005 within the Stull-Wunnummin mining district of northwestern Ontario. The purpose of this initial sampling program was to assess the diamond potential for the area through recovering kimberlite indicator minerals (KIMs) from 10 kg (average) till samples. Although KIMs were recovered, of particular interest was the number of gold grains recovered from esker samples in what is now the southern-most part of the Ti-pa-haa-kaa-ning (TPK) gold property.

In 2007, Superior Diamonds was re-named Northern Superior Resources (NSR) and the company's focus shifted to gold exploration, specifically in the Stull-Wunnummin area. Subsequent exploration programs finally defined a large gold grain-in-till apron, the source of gold grains dispersed from splays off the main regional Stull-Wunnummin Fault. The system measures at least 24 km long though the length of glacial dispersal of gold grains from source is not fully understood, as the apron extends off the TPK property. At the head of the apron, gold grains are primarily pristine (≥70%), and as many as 1250 grains have been recovered from individual 10 kg (average) till samples. In addition to gold grains, the apron also includes mineralized boulders. This apron is one of the largest in North America, surpassed only by the gold grain-in-till apron associated with the Meliadine gold deposit, Nunavut, Canada (2.6 million ounces, proven and/or probable.

In 2011–2012, exploration programs completed by NSR to the west and north of the TPK apron defined a second gold grain-in-till dispersal train. As this train is at least 3 km wide, it is referred to as a corridor and was named after a local lake, the Keely Lake gold grain-in-till dispersal corridor. Associated gold grains were sourced from within the corridor and from a newly discovered greenstone belt at the head of the corridor. Mineralized boulders recovered from within the corridor indicate that the greenstone belt also has copper and silver potential.

The TPK property is located approximately 470 km northeast of Thunder Bay, Ontario, and 190 km northeast of Pickle Lake (Fig. 1). The size of this property has evolved since 2005, now stretching almost 30 km east to west and 20 km north to south. This contiguous claim block consists of 190 mining claims comprising 2506 units or 42,719 hectares (Fig. 2). The property now encompasses at least two regional mineral-bearing systems. The property is 100% owned and operated by Northern Superior Resources Inc. and is operated with the cooperation of the local First Nation, Neskantaga, under an "Early Economic Exploration Agreement".

PHYSIOGRAPHY

Topography is primarily controlled by the presence and distribution of glacial sediments, covering over 95% of the TPK

Fig. 1. Property location map.

property. The landscape is relatively low and flat, generally varying only 20 m over broad areas with occasional isolated ridges. The limited variation in relief results in poor drainage producing numerous swamps and lakes and few well developed rivers and streams. Northeast-oriented drumlins control the shape of lakes and the direction of drainage in the eastern part of the property (Parsons 2013).

BEDROCK GEOLOGY

The TPK property is associated with the Sachigo Superterrane, subdivided into the North Caribou Terrane consisting from south to north of the Uchi, North Caribou, Island Lake, and Oxford-Stull domains (Percival *et al.* 2006; Stott 2007) (Fig. 3). The Northern Superior Superterrane bounds the Sachigo Superterrane to the north, and both superterranes are continuous to the east under the Paleozoic cover of the James Bay Lowland.
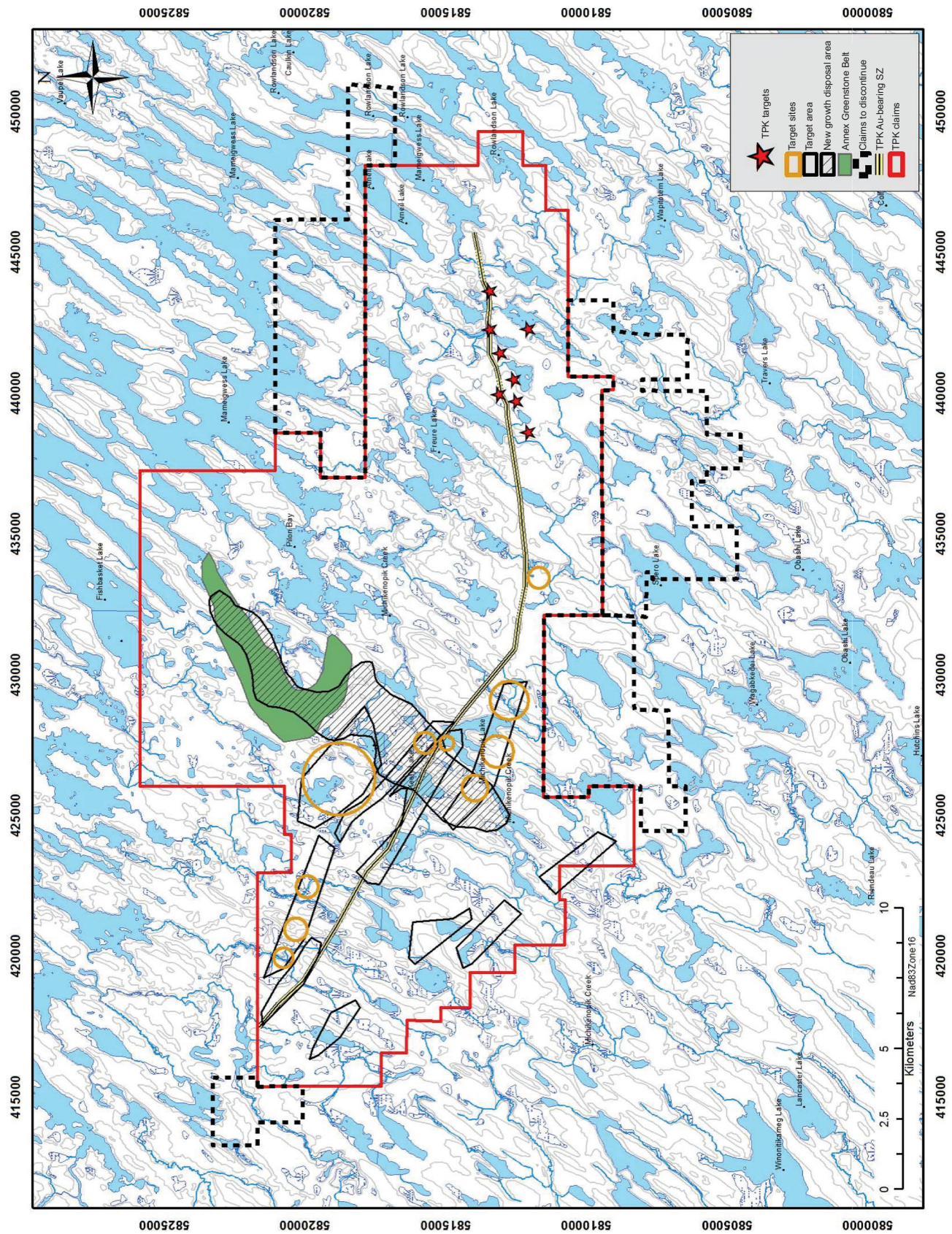
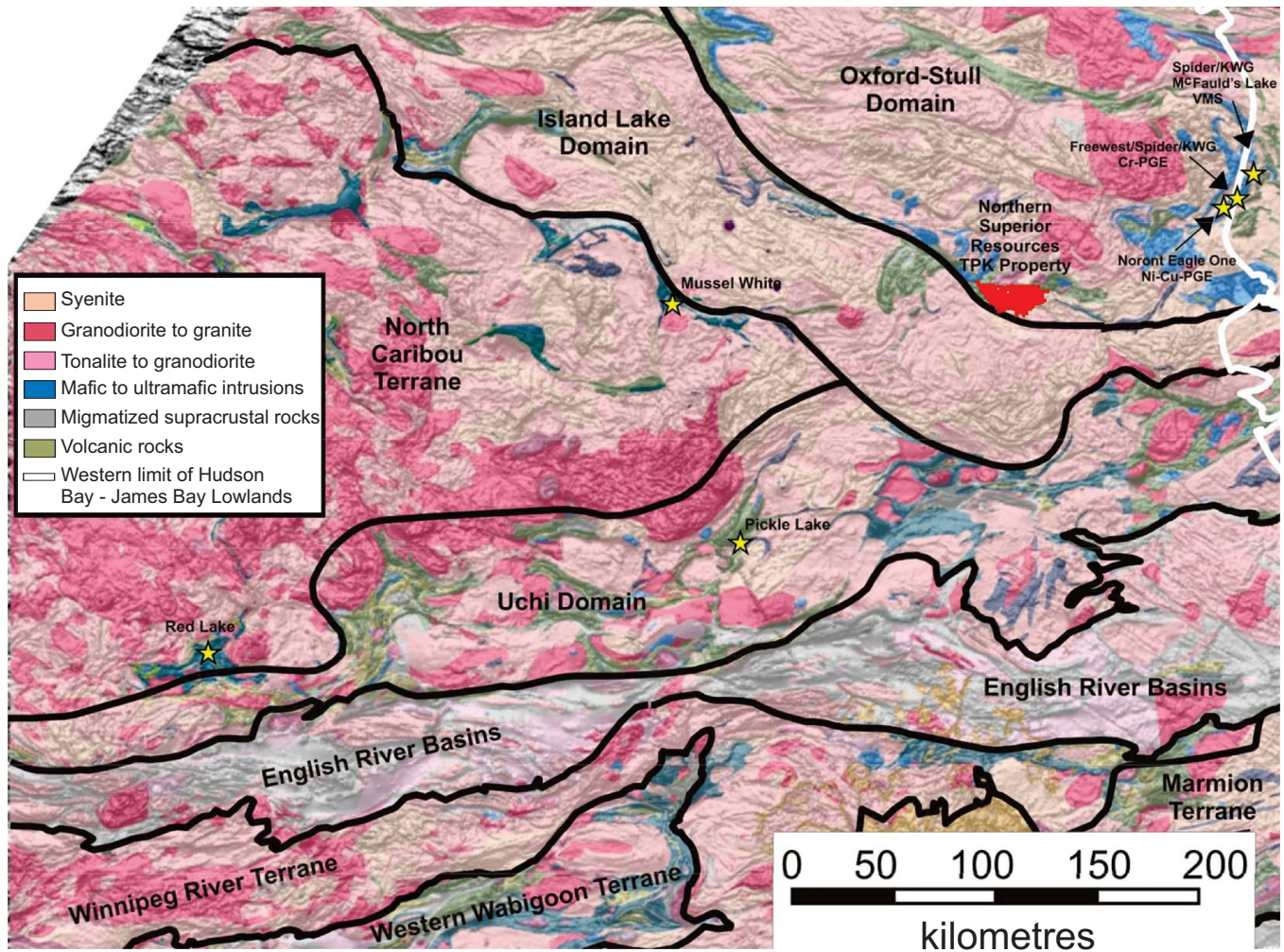**Fig 2.** Ti-pa-haa-kaa-ning gold property, northwestern Ontario, Canada.

Fig. 3. Regional geology of the eastern portion the Oxford-Stull Domain (Stott 2007).

The understanding of the local bedrock geology was primarily derived from regional compilations or reconnaissance-scale mapping (Bostock 1962; Prest 1963; Thurston & Carter 1970a,b; Mason & White 1995; Bradford 2001; Kaip and Childe 2002; Osmani & Samson 2002). The Bartman Lake greenstone belt is a generally northwest-trending supracrustal sequence that extends for approximately 75 km from the interpreted southeast limit near Barnhart Lake in the southeast to the Fishbasket intrusion to the northeast (Fig. 4). The eastern half of the belt is composed of metavolcanic rocks intruded by mafic to ultramafic units, and the western half consists of metavolcanic rocks and clastic metasedimentary rocks bounded by a mafic to ultramafic unit to the northwest. A northeast-trending arm of the belt composed of metavolcanic rocks is interpreted to extend for about 20 km along the northwest side of Fishbasket Lake. The belt measures up to 10 km in width, but is highly attenuated in the area west of Rowlandson Lake between a massive granitoid to the north and felsic gneisses to the south. Splays from the main trace of the Stull-Wunnummin fault trend to the southeast to east and are interpreted to form a 2–5 km wide duplex fault zone with apparent dextral displacement.

In 2010 and 2011, Overburden Drilling Management Limited (ODM) was contracted to complete two phases of reverse circulation drilling and a boulder prospecting program.

The program was focussed on the head of the gold grain-in-till dispersal apron in the eastern part of the TPK property. As part of this program, bedrock chips from the 192 reverse circulation holes were collected and analyzed. The observations made by ODM (Averill 2010; Averill *et al.* 2011)(Fig. 5) from these bedrock chips and mineralized boulders recovered from the boulder prospecting program, greatly enhanced the understanding of the bedrock geology and the relationship(s) between stratigraphy, plutonism, metamorphism, shear deformation, and gold mineralization for that area of the property. Key observations include (a) the Stull-Wunnummin fault follows the southern edge of the greenstone belt and is hosted by granodiorite of the Spero Lake Batholith; (b) west-northwest trending splay faults were identified in quartz monzonite of the 15 km long Freure Lake Batholith north of the belt and especially in leucogranite of the high-level Contact Stock between this synvolcanic batholith and the greenstones; (c) these splay faults are characterized by planar to anastomosing shear deformation and are locally mineralized with pyrite, arsenopyrite, and gold; and (d) the development of these splay faults appear to have been induced by deflection of the Stull-Wunnummin fault around the buttress formed by the lenticular Freure Lake Batholith. Averill *et al.* (2011) note that this metallogenic model is analogous to that of the Malartic- Val d'Or gold district in Québec.
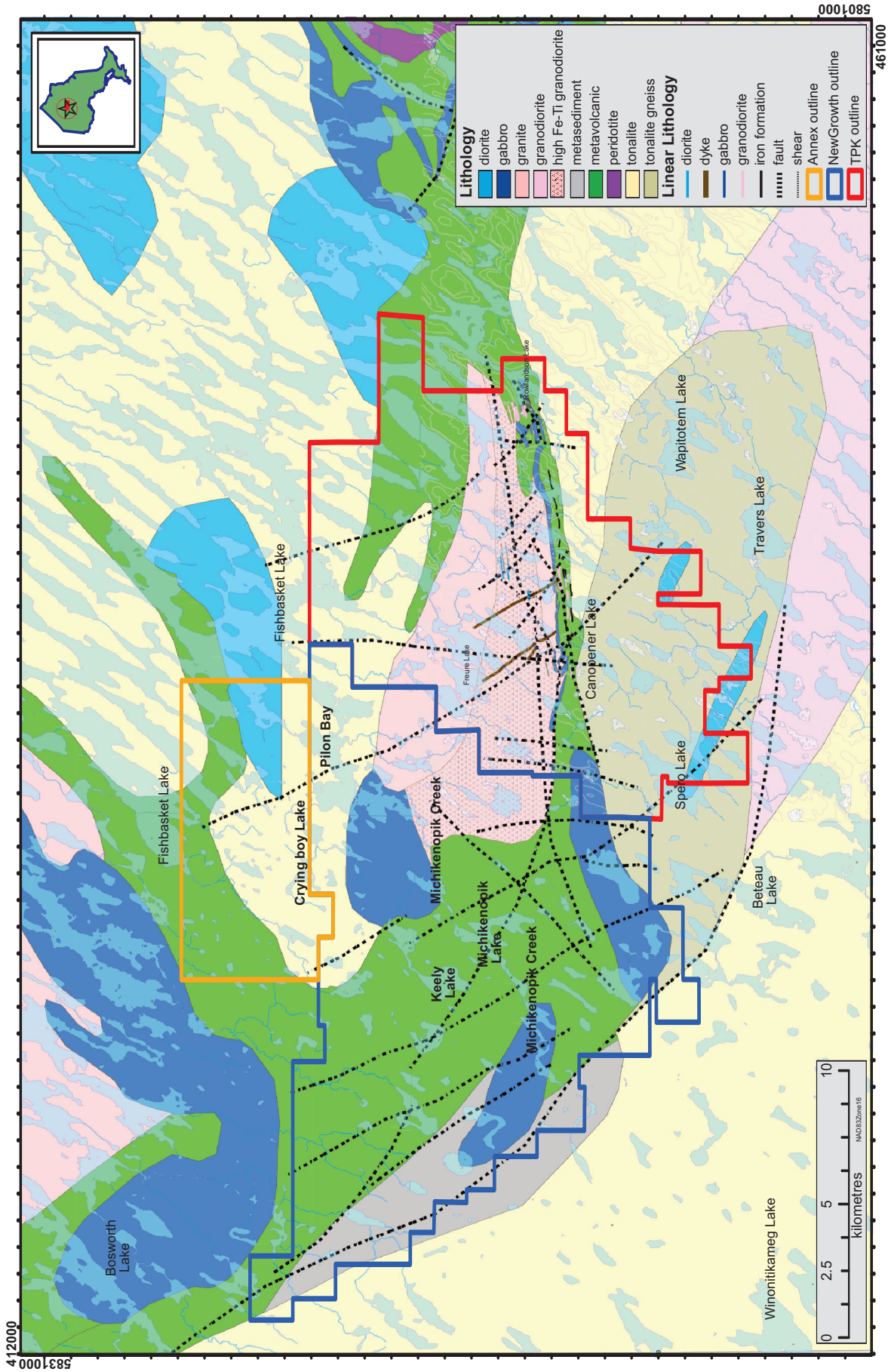
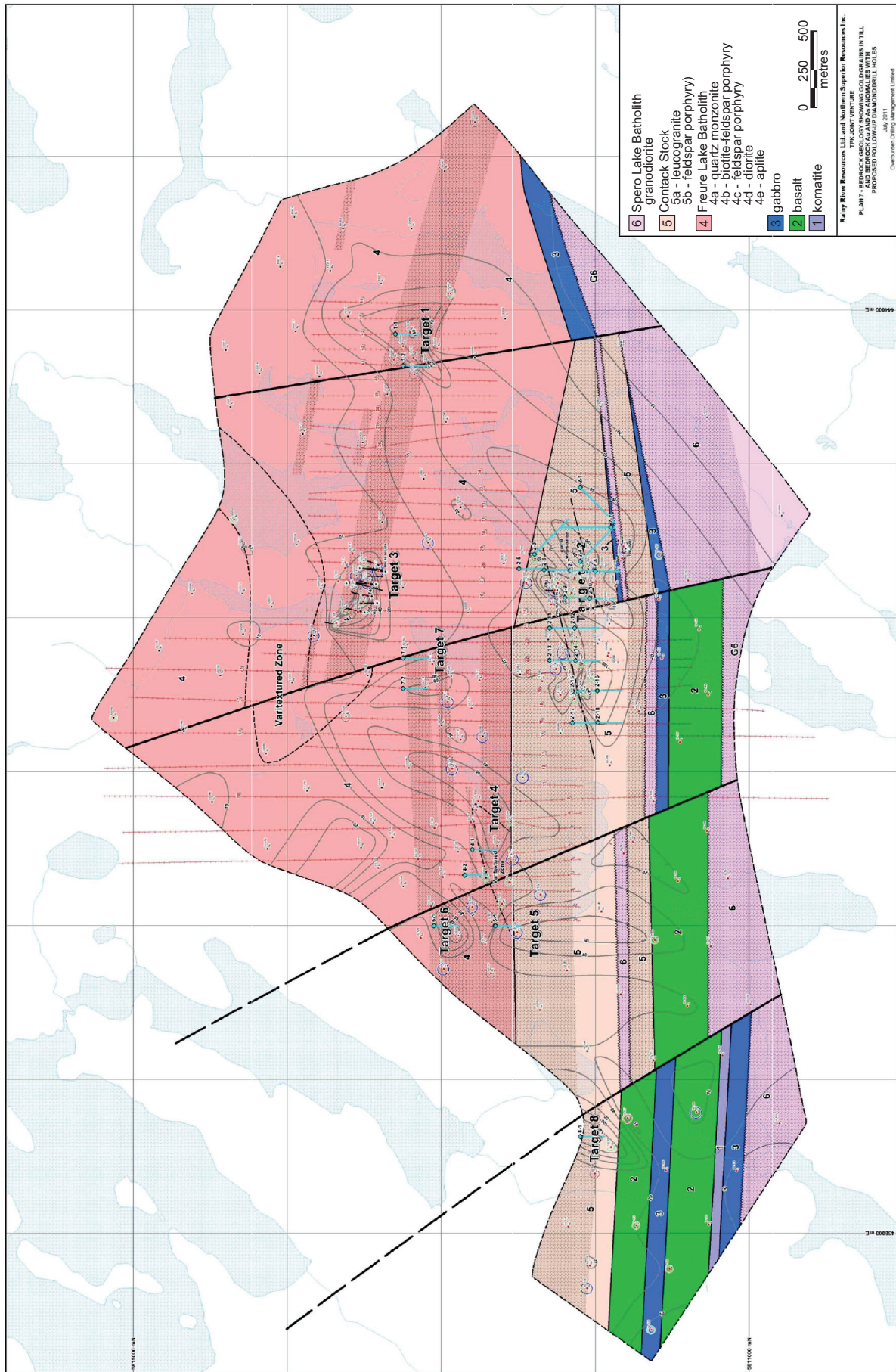**Fig 4.** Property-scale geology map (Hart & Boucher 2010).

Fig. 5. Bedrock geology from reverse circulation (RC) bedrock chips (Averill *et al.* 2011). The "Targets" refer to areas where gold grains are concentrated in till samples recovered from the RC program and represent excellent core drill targets.

OVERBURDEN GEOLOGY

Northern Ontario was likely covered with ice from the inception of the Wisconsinan approximately 115,000 years BP. The advance of glacial ice over the TPK property during this time was primarily southwest from an ice mass centred over Labrador, northeastern Canada. This flow is responsible for depositing much of the subglacial tills and moulding bedrock in north-central Ontario, and often representing a thin cover (usually <1 m) over bedrock. During the Late Wisconsinan, the ice margin began retreating towards the Hudson Bay Lowland with the direction of retreat recorded by the distribution and orientation of recessional moraine and glaciofluvial deposits. The recessional moraines are commonly composed of flow tills, coarse-grained glaciofluvial materials, and ice-contact stratified drift. Glaciofluvial deposits commonly consist of coarse-grained sand and gravel (Morris 2003).

Locally, five primary glacial deposit types were identified following the classification of Dreimanis (1989) and Dreimanis and Schluchter (1985). These include (a) thick, subglacial till blankets; (b) thin till veneers; (c) ice-contact stratified drift; (d) glaciofluvial sand and gravels; and (e) glaciolacustrine materials (Parsons 2008). From the reverse circulation drilling, it was observed that overburden thickness in the eastern part of the property varies between 3 and 10 m north of the greenstone belt, but south of this belt, till thickness locally exceeds 30 m. Through the central part of the property, a northeast-southwest belt of ice-contact stratified material exists, which is assumed to be thick due to a notable increase in elevation through this area. Overburden thickness in the western part of the property is assumed to be similar to that in the east.

THE TPK GOLD GRAIN-IN-TILL DISPERSAL APRON

The TPK gold grain-in-till dispersal apron is one of the largest, gold grain-in-till dispersal aprons in North America (Fig. 6). Gold grains associated with this apron are thought to have been dispersed from a series of gold-bearing shear zone(s) (see "Bedrock Geology" section above). These shear zones have a potential fertile strike length of 24 km. The extension of the gold-bearing shear-zones west from the eastern part of the property is defined by airborne geophysics, prospecting, and the distribution and concentration of anomalous arsenic geochemical values and gold grains recovered from surficial tills. The only "break" in the apron is due to a thick layer of ice-contact stratified drift (see "Overburden Geology" section above), presumably masking the underlying gold grain-bearing tills. The shear zone, however, can be easily traced along strike through this area as interpreted from high-resolution airborne geophysics.

Similar gold grain anomalies in other gold districts have consistently proven to represent an amalgamated response from a cluster of gold zones, indicating a large gold system or district rather than a single gold zone (Northern Superior Resources Inc., Rainy River Resources Ltd., press release, June 24, 2010). Examples of similar gold grain-in-till aprons include the Meladine (development stage) and Meadowbank (new mining operation) gold deposits in Nunavut, the Casa Berardi (mining operation) gold deposit in Québec, and the Rainy River (in development) gold deposit in Ontario.

Gold-bearing boulders (assaying up to 92 g/t gold) and mineralized boulder trains (Fig. 7) were discovered and defined within the eastern part of the gold grain-in-till dispersal apron (Averill *et al.* 2011).

The two phases of reverse circulation (RC) drilling defined eight core drill targets (Averill *et al.* 2011)(Fig. 5), from the distribution and concentration of gold grains within the lowermost basal till. Of the eight targets defined thus far, target two has generated the most interest. This target covers a broad area, defined by strong gold-in-till anomalies from RC drilling, a significant concentration of gold-bearing boulders, and several Induced Polarization (IP)/Resistivity geophysical anomalies. From target two, a strong gold grain-in-till dispersion train of at least 3 kms extends southwest down-ice of the target. The anomaly is also associated with anomalous concentrations of arsenic and zinc, and overlies a broad, shear-fractured leucogranite of the "contact stock". The leucogranite contains both spessartine garnet and fluorite alteration, important minerals commonly associated with gold mineralization in these environments. This target remains untested.

Core drilling completed so far has been focused on two of the lower priority targets (one and three) and an extension of the shear zone west of target two. It is very important to note that the two higher priority targets (two and four) have yet to be drilled. Nonetheless, several excellent intersections have been reported, including 28.75 g/t gold over 13.45 m (TPK-10-004) from target three.

KEELY LAKE GOLD GRAIN-IN-TILL DISPERSAL CORRIDOR

In the summer of 2011, Northern Superior completed a first-phase prospecting and overburden sampling program over the western part of the TPK property. Although the purpose of this program was to define the extension of the gold-bearing shear zone(s) west from the eastern side of the TPK property (and the program was successful in doing this), it soon became obvious that a strong gold grain-in-till dispersal corridor (named Keely Lake, up to 3.5 km width) existed north of the shear zone with a source for the associated gold grains to the northeast (Fig. 8). Prospecting also lead to the discovery of a large boulder that assayed 12.60 g/t gold, 111 g/t silver, and 4.05% copper (Northern Superior Resources press releases, September 14, October 25, December 6, 2011).

In the fall of 2011 a second overburden sampling and prospecting program was initiated to build on the discoveries made from the previous year. The head of the Keely Lake gold grain-in-till was defined north of the TPK property boundary, so additional staking was completed to capture the source of the gold grains. A second source of gold grains was identified within the dispersal corridor itself. From the prospecting program, 100 mineralized boulders (sampling terminated due to heavy snow fall) were recovered, 83 of which contained anomalous gold, silver, and copper values, one of which contained coarse visible gold (727 g/t gold).

Following this second phase of exploration on the western half of the property, a core drilling program consisting of 7 holes (2,241 m) was completed in the second quarter of 2012 (Northern Superior Resources press release, June 26, 2012). Highlights from this core drill program include an intersection of 4.62 g/t gold over 5.5 m.

GOING FORWARD

The opportunity for significant mineral discoveries on the
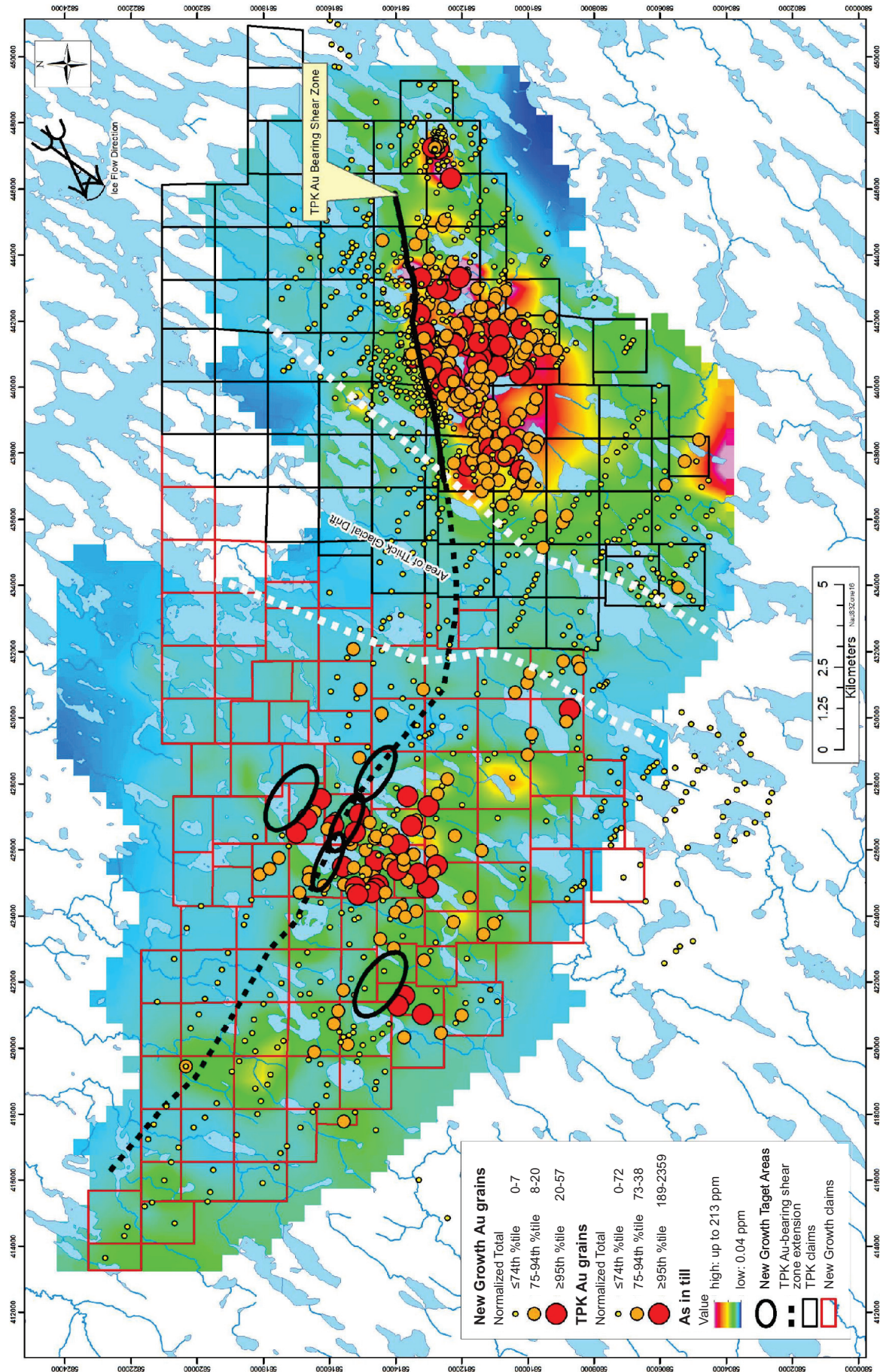
Fig. 6. The TPK gold grain-in-till dispersal apron. The location (solid line) and proposed location (dashed line) of the 24 km long gold-bearing shear zone(s) is also illustrated. Property outline is pre-2013

T.F. Morris
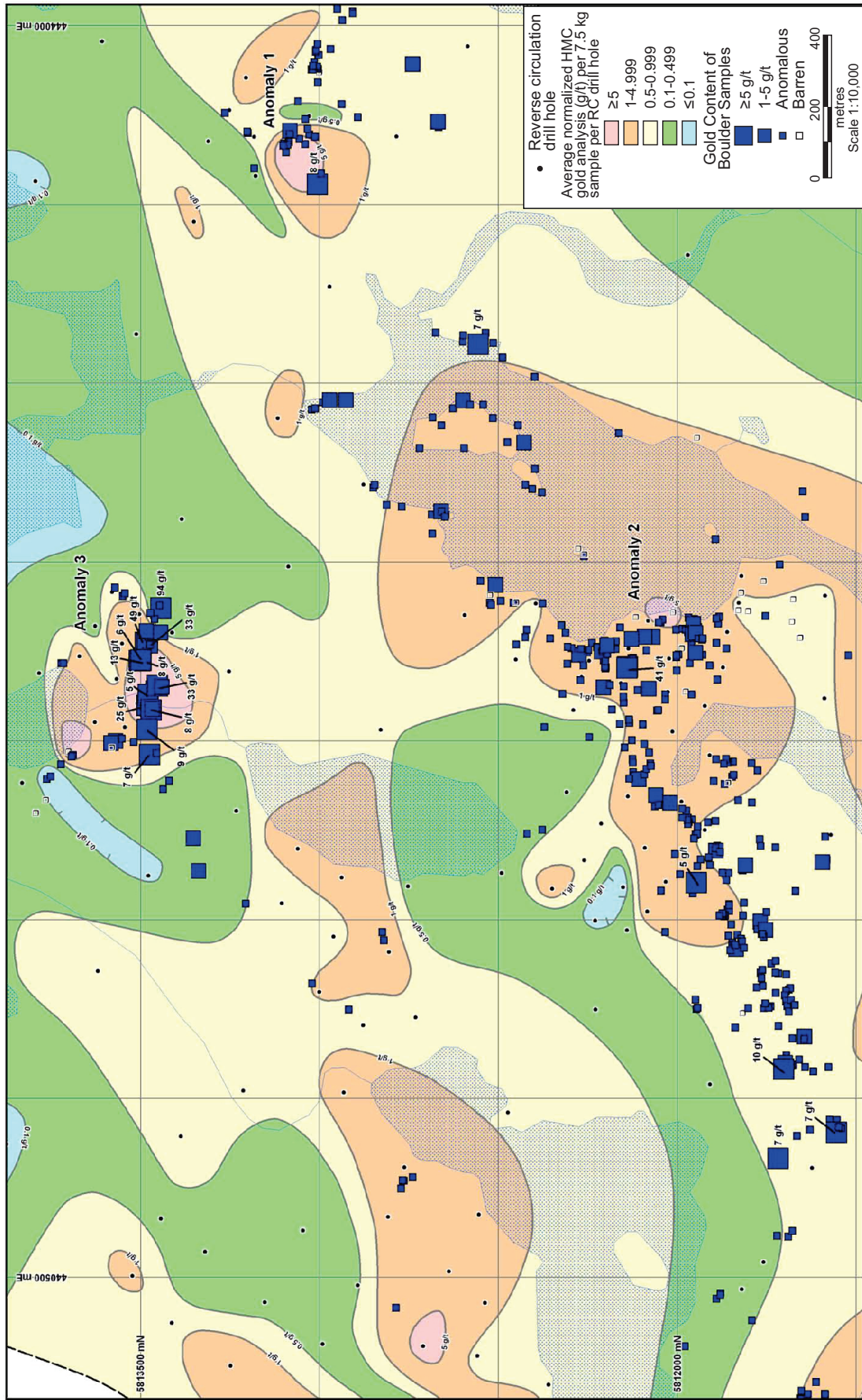
Fig. 7. Distribution of mineralized boulders and boulder dispersal train (Averill *et al.* 2011).
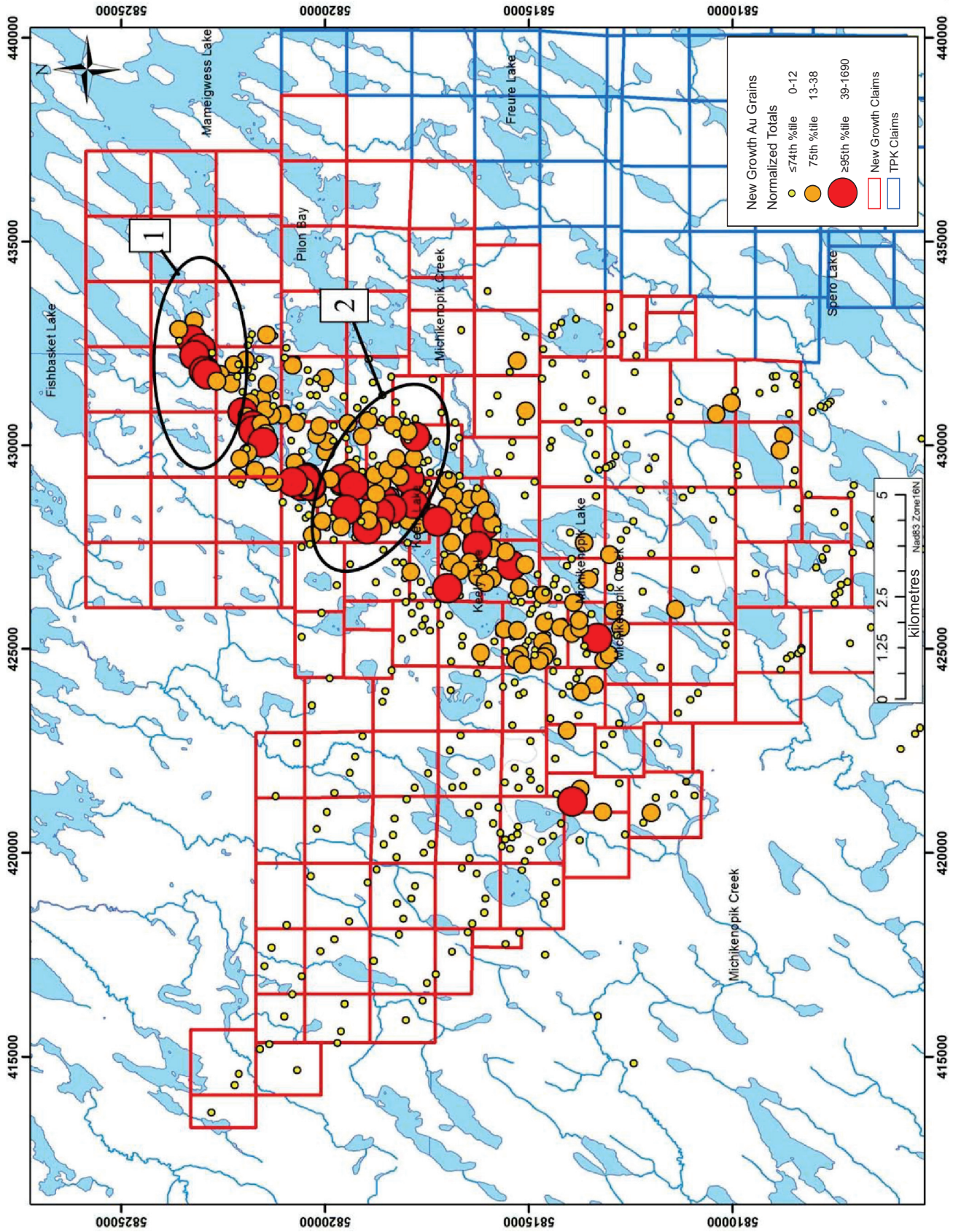
Fig. 8. Keely Lake dispersal corridor. Gold grain source at the head of the corridor (1) and within the corridor (2). See Figure 2 (dashed line) for the projected location of the gold-bearing shear zone.

TPK property is both unique and exceptional. Much of the "heavy-lifting" on this property has already been done with many untested, drill-ready targets defined. Infrastructure and access have been greatly improved with the addition of a year-round camp and access trails extending across the eastern part of the property from the camp. Relations with the local First Nation are excellent, with an extension of an Early Economic Benefits Agreement recently (July 2013) signed. The property is 100% Northern Superior Resources Inc. owned, is large, and captures two important mineral systems. Northern Superior Resources is currently looking for an option partner to participate and finance the next phase of exploration on the property.

ACKNOWLEDGEMENTS

REFERENCES

AVERILL, S.A. 2010. *Reverse circulation overburden drilling and heavy mineral geochemical sampling for gold, TPK project, Ontario.* Overburden Drilling Management Ltd. consulting report, October 22, 2010.

AVERILL, S.A., HOLMES, D.R.S. & HOZJAN, D.J. 2011. *Reverse circulation overburden drilling and heavy mineral geochemical sampling for gold, Phase II, TPK project, Ontario.* Overburden Drilling Management consulting report, July 29, 2011.

BOSTOCK, H.H. 1962. *Geology – Lansdowne House, Ontario.* Geological Survey of Canada Preliminary Series Map **4-1962**.

BRADFORD, J. 2001. *Aurora Platinum Corp. - INCO Ltd.: AEM Project, Geology and Exploration Potential of the Rowlandson Lake – Canopener Lake Area, Northwestern Ontario (NTS 43D/5).* Consultant report, August-September, 2001.

DREIMANIS, A. 1989. Tills: Their genetic terminology and classification. *In*: GOLDWAITE, R.P. & MATSCH, C.L. (eds) *Genetic Classification of Glaciogenic Deposits.* Balkema, Rotterdam, 17–83.

DREIMANIS, A. & SCHLUCHTER, C. 1985. Field criteria for the recognition of till or tillite. *Paleogeography, Paleoclimatology, Paleoecology*, **51**, 7-14.

HART, T.R. & BOUCHER, D.R. 2010. *Technical report on the Ti-pa-haa-kaa-ing Property, Lansdowne House, Northwest Ontario.* 43-101F Technical Report, January 28, 2010.

KAIP, A. & CHILDE, F. 2002. *AEM gold project, Northwestern Ontario & Northeastern Manitoba, Canada.* Consultant report, December 16, 2002.

MASON, J.K. & WHITE, G.D. 1995. *Mineral occurrences and prospects in the Fort Hope-Winisk area.* Ontario Geological Survey, Open File Report **5926**.

MORRIS, T.F. 2003. *Overburden sampling program, Property 1203076, Lansdowne Area, Northwestern Ontario.* Ministry of Northern Development and Mines, Assessment File AFRI# 43D14SE2001.

NORTHERN SUPERIOR RESOURCES INC. 2011a. *Northern Superior Resources Inc. reports sample from mineralized boulder returns 12.60 g/t gold, 111 g/t silver, 4.05% copper New Growth Gold Property, Northwestern Ontario.* Press Release, September 14, 2011.

NORTHERN SUPERIOR RESOURCES INC. 2011b. *Northern Superior Resources Inc. recovers gold-bearing boulder and further defines Keely Lake gold grain dispersal corridor, New Growth Gold Property, Northwestern Ontario.* Press Release, October 25, 2011.

NORTHERN SUPERIOR RESOURCES INC. 2011c. *Northern Superior Resources Inc. defines the extension of the Ti-pa-haa-kaa-ning (TPK) gold-bearing shear zone onto the New Growth Gold Property, Northwestern Ontario.* Press Release, December 6, 2011.

NORTHERN SUPERIOR RESOURCES INC. 2012. *Northern Superior drilling discovers gold mineralization, New Growth Annex with grades up to 4.62 g/t gold over 5.5m (Including 20.8 g/t gold over 1 m).* Press Release, June 26, 2012.

NORTHERN SUPERIOR RESOURCES INC. & RAINY RIVER RESOURCES INC. 2010. *Northern Superior Resources Inc. signs option/joint venture agreement with Rainy River Resources Ltd. respecting Ti-pa-haa-kaa-ning gold property.* Press release, June 24, 2010.

OSMANI, I.A. & SAMSON, J. 2002. *Aurora Platinum Corporation 2001 exploration program Lansdowne House property, Bartman Lake area, Northwestern Ontario.* Ministry of Northern Development and Mines, Assessment File AFRI# 43D11SW2001.

PARSONS, S.R.G. 2008. *Surficial geology of the Ti-pa-haa-kaa-ning property, Lansdowne House area, Northwestern Ontario, Canada.* Internal report, October 5, 2008.

PARSONS, S.R.G. 2013. T*echnical report on the Ti-pa-haa-kaa-ing property, Lansdowne House, Northwest Ontario.* 43-101F technical report, August, 2013.

PERCIVAL, J.A., SANBORN-BARRIE, M., SKULSKI, T., STOTT, G.M., HELMSTAEDT, H. & WHITE, D.J. 2006. Tectonic evolution of the western Superior Province from NATMAP and lithoprobe studies. *Canadian Journal of Earth Science*, **43**, 1085-1117.

PREST, V.K. 1963. *Surficial geology: Red Lake - Lansdowne House area. Ontario.* Geological Survey, Preliminary Series Map **5-1963**.

STOTT, G.M. 2007. *Precambrian geology of the Hudson Bay and James Bay lowlands region interpreted from aeromagnetic data – east sheet.* Ontario Geological Survey, Preliminary Map **P.3598**.

THURSTON, P.C. & CARTER, M.W. 1970a. *Operation Fort Hope.* Ontario Department of Mines Miscellaneous Paper **42**.

THURSTON, P.C. & CARTER, M.W., 1970b. *Operation Fort Hope, Lansdowne House – Fort Hope Sheet: Districts of Kenora (Patricia Portion) and Thunder Bay.* Ontario Department of Mines, Preliminary Map **P.562**.

Overview of tungsten indicator minerals scheelite and wolframite with examples from the Sisson W-Mo deposit, Canada

M.B. McClenaghan[1], M.A. Parkhill[2], A.A. Seaman[3], A.G. Pronk[3], M.W. McCurdy[1] & D.J. Kontak[4]

[1]*Geological Survey of Canada, 601 Booth Street, Ottawa, Ontario, Canada K1A 0E8 (e-mail: bmcclena@nrcan.gc.ca)*
[2]*New Brunswick Department of Energy and Mines, Geological Surveys Branch, P.O. Box 50, Bathurst, New Brunswick, Canada E2A 3Z1*
[3]*New Brunswick Department of Energy and Mines, Geological Surveys Branch, P.O. Box 6000, Fredericton, New Brunswick, Canada E3B 5H1*
[4]*Department of Earth Sciences, Laurentian University, Sudbury, Ontario, Canada P3E 2C6*

These short course notes provide an overview of published literature on the use of scheelite and wolframite as indicator minerals for W, Mo, and Au exploration. The use of scheelite and wolframite in stream sediments is well documented for mineral exploration but less so for using glacial sediments (Table 1). The Geological Survey of Canada has recently conducted a glacial till and stream sediment indicator mineral case study around the Sisson W-Mo deposit in eastern Canada. Preliminary indicator mineral results from this ongoing study are reported here.

SOURCES OF SCHEELITE AND WOLFRAMITE IN BEDROCK

Scheelite and wolframite are the main ore minerals of tungsten deposits, which form due to either magmatic-hydrothermal processes associated with felsic magmas (i.e. granite, pegmatite) or metamorphic processes (i.e. orogenic veins), with the former being by far the dominant in past and current production globally (see Kwak (1987) for review). Tungsten, more specifically scheelite, is also known to occur, albeit rarely, in stratiform/stratabound and commonly tourmaline-rich horizons associated with submarine basic volcanic rocks and clastic and chemical (i.e. carbonate) rocks. This mineralization model is, however, very controversial, one such example being the large Felertal scheelite deposit of Austria (Cheilletz 1988). In granite-related deposits, wolframite occurs in both greisen and veins, either within the intrusion or the surrounding country rock. The large Panasqueira, Portugal (Kelly & Rye 1979) and Pasto Buena, Peru (Landis & Rye 1974) deposits are good examples of granite-hosted, vein wolframite mineralization. The Mount Pleasant deposit in New Brunswick, Canada, is an example of a more complex system, both in terms of elements (W-Mo-Sn-Bi-Zn-In) and style, where greisen and stockwork mineralization occur (Kooiman *et al.* 1986).

Where the surrounding country rock is dominated by carbonate, scheelite is the main tungsten mineral and occurs as part of a hydrous assemblage (i.e. amphibole-biotite-sulphides) that overprints an earlier higher temperature garnet-pyroxene assemblage (Meinhert *et al.* 2005). The Cantung and Mac Tung deposits in northwestern Canada, which are among the western world's largest resources of W, are examples of such scheelite mineralization (Dick & Hodgson 1982). As noted above, in vein and greisen settings, other elemental associations

Table 1. List of regional surveys and case studies conducted around the world in which scheelite and/or wolframite in surficial sediments have been used as indicator minerals.

Mineral	Media	Location	Source of Information
scheelite	stream sediments	Pakistan	Asrarullah (1982)
wolframite	stream sediments	Burma	ESCAP Scretariat (1982)
scheelite, wolframite	stream sediments	USA	Theobald & Thompson (1960)
scheelite	stream sediments, soil	Thailand	Silakul (1986)
scheelite	stream sediments	Greenland	Hallenstein *et al.* (1981)
scheelite	stream sediments	Spain	Fernández-Turiel *et al.* (1992)
scheelite	stream sediments	India	de Smeth *et al.* (1985)
scheelite	stream sediments	Canada	Maurice (1986)
scheelite	till	Finland	Lindmark (1977)
scheelite	till	Sweden	Brundin & Bergström (1977)
scheelite	till	Finland	Johansson *et al.* (1986)
scheelite	till	Finland	Nikkarinen & Björklund (1976)
scheelite	stream sediments	Turkey	Özcan & Çağatay (1989)
scheelite	stream sediments	Norway	Petersen & Stendal (1987)
scheelite	till	Finland	Peuraneimi (1992)
scheelite	till	Finland	Salminen & Hartikainen (1986)
scheelite	till	Ireland	Steiger (1977)
scheelite	till	Sweden	Toverud (1984)
scheelite, wolframite	stream sediments	Malaysia	Rajah (1982)
scheelite	stream sediments	Norway	Stendal (1978)
scheelite, wolframite	eolian sediment	Saudia Arabia	Salpeteur (1985)
scheelite, wolframite	till, stream sediments	Canada	McClenaghan *et al.* (2013a, in press)

can occur; thus W-Mo endo- and exo-skarn deposits have been noted, the large Logtung deposit being one example (Noble *et al.* 1984). As is discussed below, the presence of other elements, in particular Mo, is an important feature of W deposits as the presence of Mo in scheelite can affects its properties (e.g. fluorescence). Tungsten deposits are often associated with Sn, in addition to Mo mineralization. Varying combinations of pyrrhotite, chalcopyrite, sphalerite, arsenopyrite, galena, native Bi, and bismuthinite (Horsnail 1979; Hosking 1982) may also be associated with tungsten deposits.

Scheelite

Scheelite ($CaWO_4$) can be used as an indicator mineral because it is chemically robust, hard (H=4-5), dense (SG 5.9–6.12), and has blue-white fluorescence under UV light, which means that it is relatively insoluble in the natural pH range of surface water, survives moderate distances of glacial or fluvial transport, and can be easily identified (Horsnail 1979; Hosking 1982; Ottensen & Theobald 1994). Scheelite, however, is brittle and thus it does not survive long distance transport as com-
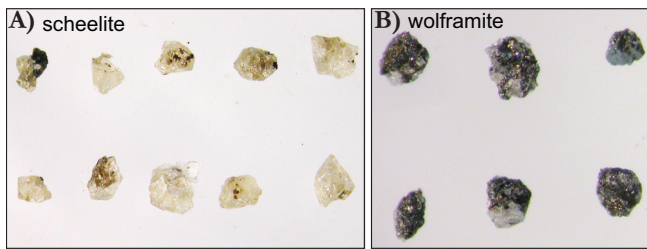
Fig. 1. Colour photographs of indicator minerals in bedrock heavy mineral concentrates from the Sisson W-Mo deposit: **A)** scheelite in sample 11-MPB-R07, 0.5–1.0 mm; **B)** wolframite in sample 11-MPB-R06, 0.25–0.5 mm (modified from McClenaghan *et al.* in press).

Fig. 2. Scheelite grains (0.25–0.5 mm) from till sample 11-MPB-504 mounted on a scanning electron microscope stub under **(A)** normal and **(B)** shortwave ultraviolet light (modified from McClenaghan *et al.* in press).

pared to other indicator minerals such as gold. Scheelite can be identified in heavy mineral concentrates (HMC) by its pale yellow colour (Fig. 1), cleavage, and its bright blue-white-yellow fluorescence under shortwave UV light (Fig. 2), which can vary due to Mo content (i.e. powellite substitution). Pure scheelite fluoresces strong blue, which with increasing Mo content changes from white at 0.5–1.0 wt% Mo, to yellow at >1 wt% Mo, to a deep orange-yellow at >4 wt% Mo (Hosking 1982). Zircon, another common fluorescent mineral in heavy mineral concentrates, can be distinguished from scheelite by its yellow-green-orange fluorescence under both short- and longwave ultraviolet light.

The angularity (and other features) of scheelite grains collected from streams can provide indications of relative distance of transport. For example, in southwest Poland, Mikulski &

Wierchowiec (2013) compared the shape of scheelite grains in bedrock versus those collected from fluvial sediments downstream(Fig. 3); they also compared scheelite, adamantine luster, and intergrowths of other minerals (e.g. quartz and titanite), and fluid inclusions. Scheelite in alluvial sediments ~1 km downstream of the bedrock source were subangular to subrounded, contained fluid inclusions that matched the bedrock source, but lacked intergrowths of other minerals. Scheelite grains transported >2.0 km from the source had a matte luster instead of glassy, and the surfaces of larger scheelite grains had coatings of clay minerals. In another study, Wildon & Hotz (1955) noted that the presence of quartz intergrown with scheelite in stream sediments could be indicative of transport distance as well as the type of bedrock source (i.e. quartz-vein hosted).

Several studies have noted that scheelite grain size decreases with increasing distance of transport, both in stream sediments
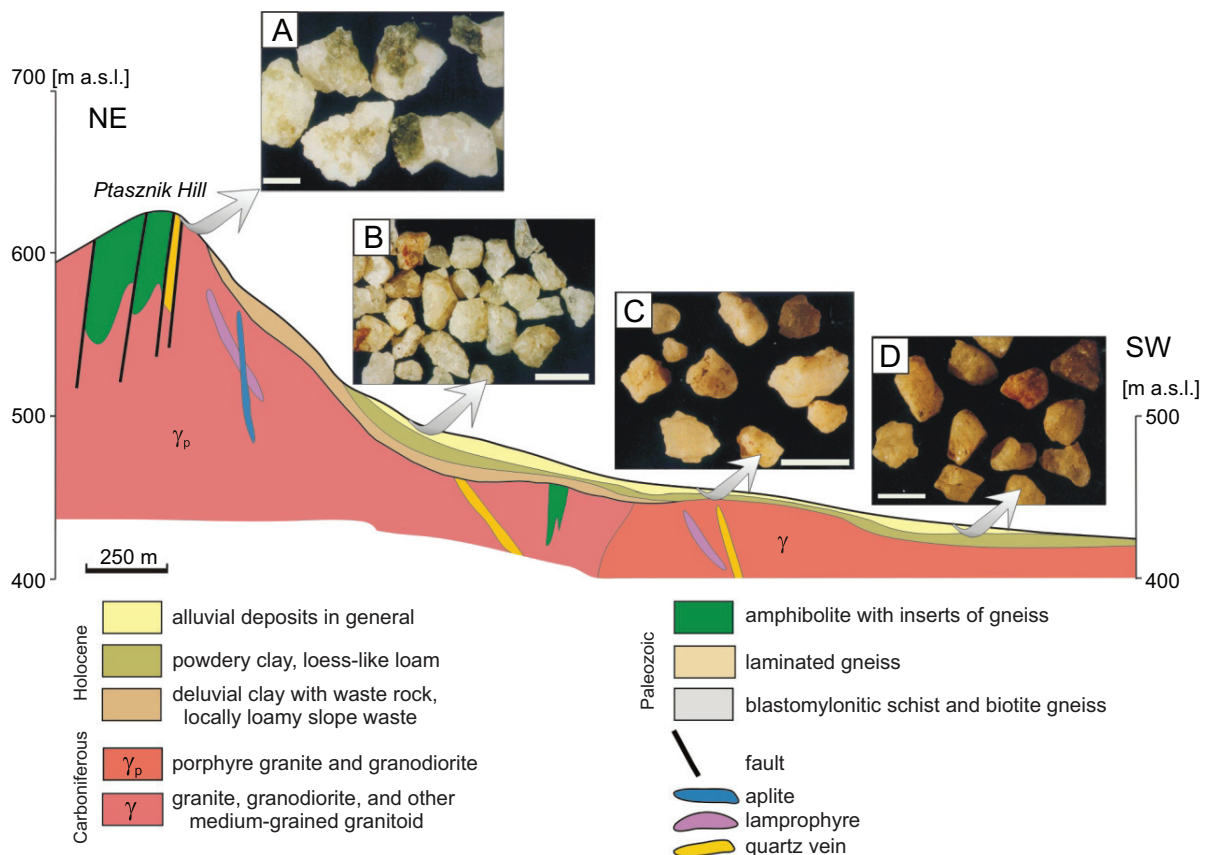
Fig. 3. Colour photographs of scheelite grains from bedrock **(A)** versus stream sediments **(B,C,D)** at increasing distances downstream from source in southwest Poland. Note the presence adamantine luster and intergrowths of other minerals on scheelite grains from bedrock sample A. Scheelite grains ~1 km downstream are subangular to subrounded with no intergrowths. Scheelite grains in alluvial sediments more than 1.5 km from source (C & D), have a matte luster and clay mineral coatings. Modified from Mikulski & Wierchowiec (2013).
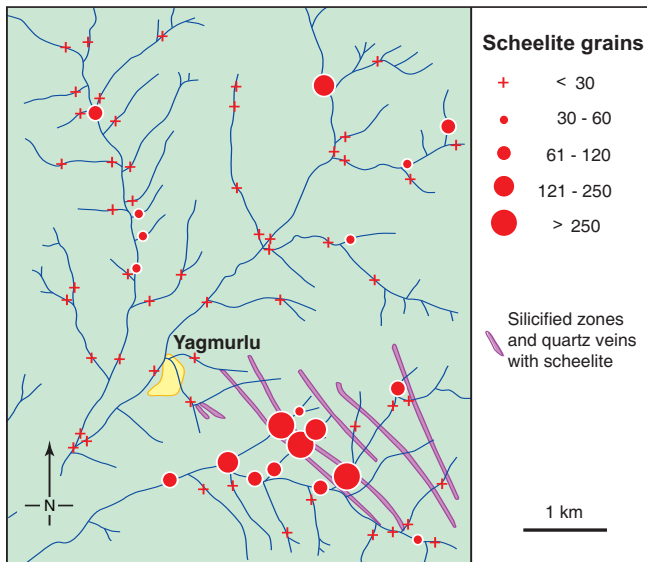
Fig. 4. Abundance of scheelite in <1.0 mm fraction of stream sediment concentrates from the Yagmurlu area of the Central Anatolian massif, Turkey (modified from Özcan & Çağatay 1989). Abundances are greatest overlying silicified zones and quartz veins with scheelite.

(e.g. Zeschke 1961; Stendal & Theoboald 1994) and till (e.g. McClenaghan *et al.* 2013b).

Mainly due its fluorescence, scheelite is easy to visually identify, and thus is globally one of the most commonly used indicator minerals in stream sediment surveys (Table 1) (e.g. Zeschke 1961) in support of W, Sn and Au exploration, including Turkey (Fig. 4) (e.g. Özcan & Çağatay 1989), Spain (e.g. Zantop & Nespereira 1979; Fernández-Turiel *et al.* 1992), Pakistan (e.g. Zeschke 1961; Asrarullah 1982), Malaysia (e.g. Rajah 1982), Somalia (Frizzo & Hassan 1983); USA (e.g. Theobald & Thompson 1960), and India (e.g. de Smeth *et al.* 1985). Scheelite has also been recovered from stream sediments in glaciated terrain, for example in Norway (e.g. Stendal 1978), Greenland (e.g. Hallenstein *et al.* 1981; Steenfelt 1987), and Canada (e.g. Maurice 1986; Allen *et al.* 1999). In some areas, scheelite content in stream sediments is sufficient for the sediments to be characterized as placer W deposits (e.g. Hess 1917; Wildon & Hotz 1955). Scheelite is used in soil surveys in some parts of the world in support of mineral exploration (e.g. Petersen & Stendal 1987; Özcan & Çağatay 1989; Surya Prakash Rao *et al.* 1989).

Recovery of scheelite from glacial sediments was first reported by Lindmark (1977) and Brundin & Bergström (1977) in the glaciated terrain of Fennoscandia. Lindmark (1977) described one of the first till sampling programs specifically designed to recover scheelite in till (Fig. 5), which was carried out as far back as the 1960s in Finland. Again, due to its fluorescent properties, it was easily identified in bulk till. In 1970, Brundin & Bergström (1977) were among the first to develop systematic methods for identifying indicator mineral in till in Sweden, including scheelite. They evaluated various sample weights (2.5 kg versus 25 kg), preconcentration methods (panning versus sluice box), and heavy liquid separation densities (SG 2.96 versus 3.3). In the 1970s and 1980s, several studies compared W contents of till to its scheelite abundance (e.g. Nikkarinen & Björklund 1976; Steiger 1977; Stea & O'Reilly 1982; Toverud, 1984; Johansson *et al.* 1986; Salminen & Hartikainen 1986; Petersen & Stendal 1987; Snow & Coker
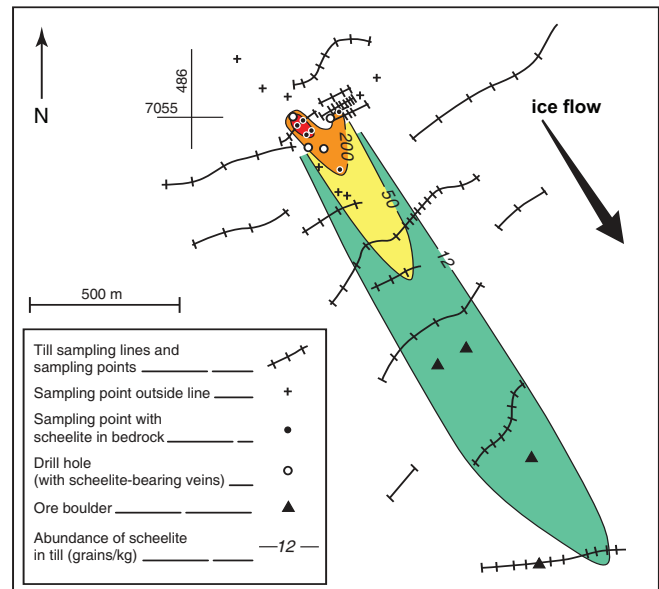

Fig. 5. Glacial dispersal train in west-central Finland defined by scheelite-bearing boulders (ore boulder in legend) and scheelite grains recovered from till samples by panning heavy minerals and examination under shortwave ultraviolet light (modified from Lindmark 1977).

1987; Peuraniemi 1992). It was often noted that scheelite in till formed larger anomalies than those outlined using W content. These early studies involved simply noting the presence scheelite and counting the number of scheelite grains in till heavy mineral concentrates under UV light.

Wolframite

The other common W-bearing indicator mineral is wolframite ((Fe,Mn)WO$_4$), which includes the solid solution series between hubnerite (MnWO$_4$) and ferberite (FeWO$_4$). Wolframite is by far the most commonly used indicator mineral of the series. It is a useful indicator mineral because it is relatively insoluble in the natural pH range of surface water (Horsnail 1979). Wolframite is identified in heavy mineral concentrates (HMC) by its black colour (Fig. 1B), prismatic crystal form, hardness (H=4.5, can be scratched with a needle), reddish brown streak, and lack of fluoresce under UV light. When rounded, it can be difficult to distinguish from other visually similar heavy minerals (e.g. hornblende, tourmaline, ilmenite) that can be abundant in stream sediments and till. Because of its brittle nature and perfect cleavage, wolframite breaks apart more readily than scheelite and thus tends to be rarer and, when present in stream sediments, is recovered in the finest fraction from within 2 to 3 km downstream of its bedrock source (ESCAP Secretariat 1982; Hosking 1982; Meizhong 1982).

Wolframite has been recovered in stream sediments surveys around the world (Table 1), including Spain (Zantop & Nespereira 1979; Fernández-Turiel *et al.* 1992), as well as from placer deposits (Hess 1917), such as those in Thailand (e.g. Pungrassami 1986), Burma (e.g. ESCAP Secretariat 1982), and the USA (e.g. Johnson 1910). The presence hubnerite in stream sediments in the southwest USA has been reported by Theobald & Thompson (1960). Recovery of wolframite from glacial sediments is occasionally noted when it occurs in association with scheelite (e.g. Brundin & Bergström 1977).

MINERAL CHEMISTRY

In addition to indicator mineral abundance, size, and shape, mineral chemistry can provide key information about the lithology or grade of a bedrock source. The best known example of this is the use of chemistry of kimberlite indicator grains in till for the preliminary evaluation of the diamond potential of an area or a kimberlite body (e.g. McClenaghan & Kjarsgaard 2007). Scheelite mineral chemistry has been reported by several authors (e.g. Hsu & Galli 1973; Sylvester & Ghaderi 1997; Ghaderi *et al.* 1999; Brugger *et al.* 2000a,b; Roberts *et al.* 2006; Dostal *et al.* 2009). Wolframite mineral chemistry has been reported by Nakashima *et al.* (1986) and Ferenc & Uher (2007).

Ongoing research into scheelite compositional criteria that can be used to characterize grains recovered from indicator mineral surveys includes the work of Poulin *et al.* (2013). Using scheelite grains recovered from a range of deposit types (W-bearing skarns, intrusion-related gold systems or orogenic, Au-bearing quartz-carbonate-sulphide veins), these authors are developing discrimination criteria based on scheelite composition and luminescence characteristics that are associated with a specific types of mineralization in bedrock. In turn these criteria may serve to identify potential bedrock sources of scheelite grains recovered from stream sediments or till.

SISSON W-Mo DEPOSIT CASE STUDY

The Sisson W-Mo deposit in west-central New Brunswick is a large, structurally controlled, intrusion-related W-Mo deposit consisting of four wide and steeply dipping zones of vein- and fracture-controlled W and Mo mineralization (Nast & William-Jones 1991; Marr 2009; Fyffe *et al.* 2010; Rennie 2012). Lang & Zahovskis (2013) reported resource estimates for the deposit of 383 Mt at 0.067% WO_3 and 0.021% Mo (measured and indicated) and 178 Mt 0.051 WO_3 and 0.021% Mo (inferred), making it one of the largest tungsten deposits in the world. In addition to W, the deposit has elevated concentrations of Cu, Zn, Pb, Bi, and As, which are directly related to late-stage quartz-scheelite and sulphide-rich veins and their sericite-sulphide envelopes. Scheelite ranges from <100 μm to 1 cm in size and overall wolframite is a minor mineral in the deposit. Bedrock outcrop on the Sisson property and surrounding area is rare due to the extensive till cover, which averages 8 m in thickness (Marr 2009). During the last glacial event, the subcropping surface was glacially eroded, mainly by southeast-flowing ice, resulting in metal-rich glacial debris (till) being deposited both overlying and down-ice (southeast) of the deposit (Seaman & McCoy 2008).

Methods

Methods and preliminary results presented here for the Sisson study are summarized from McClenaghan *et al.* (2013a,b, in press). Large (~15 kg) surface till samples up-ice, overlying, and up to 14 km down-ice (southeast) of the deposit along with mineralized bedrock samples were collected to document indicator mineral signatures of the deposit in till down-ice (southeast). Small bags of till were tested for their W and Mo content using a portable bench-top XRF to help guide sampling. Large (15 kg) stream sediment samples were collected up and down stream of the deposit to compare scheelite and wolframite abundance, size, and shape to those in till. Bedrock

samples were collected from mineralization and host rocks to determine which minerals were indicative of W-Mo mineralization in the Sisson deposit. All samples were processed using a combination of shaking table, panning, and heavy liquids (SG 3.2) to produce heavy mineral concentrates for picking. Pan concentrates, as well as the 0.25–0.5, 0.5–1.0, and 1.0–2.0 mm non-ferromagnetic fractions of samples were examined and potential indicator minerals of W-Mo mineralization counted/selected, which included scheelite, wolframite, molybdenite, and other sulphide minerals. All heavy mineral concentrates were systematically examined inside a black box using shortwave ultraviolet light to identify and count scheelite grains. Sample processing methods and indicator mineral abundance data for all samples are reported in McClenaghan *et al.* (2013a).

Indicator mineral species

The primary ore minerals recovered from till and stream sediments at the Sisson deposit include scheelite, wolframite (Fig. 1), and molybdenite. Secondary ore minerals associated with mineralization and from bedrock and sediment samples include chalcopyrite, Bi-rich minerals (joseite, native Bi, bismutite, bismuthinite), galena, sphalerite, arsenopyrite, pyrrhotite, and pyrite (Table 1). These secondary minerals though much less abundant are useful indicators of the polymetallic nature of the Sisson deposit.

Indicator mineral size

The size of W-Mo indicator minerals in till at Sisson is controlled primarily by the size of the grains in the source rock and the durability of the mineral during glacial and subsequent fluvial transport.

Scheelite recovered from bedrock, till, and stream sediments is most abundant in the pan concentrate (25–200 μm) and the 0.25–0.5 mm size fractions. Scheelite is also present in the 0.5–1.0 mm size fraction, and least abundant in the 1–2 mm size fraction (Table 2). Similar to scheelite, wolframite is present in the coarser fractions but most abundant in the 0.25–0.5 mm fraction of bedrock, till, and stream sediments (Table 2).

Indicator mineral abundance

Mineralized bedrock processed to recover indicator minerals was found to contain 10,000s grains/kg of scheelite. Till and stream sediment samples overlying and immediately down-ice of the deposit contained 1000s to 100s of scheelite grains/10 kg in the 0.25–0.5 mm fraction. Background scheelite content in till and stream sediments varies from 0 to 2, and 0 to 9 grains, respectively. Elevated contents of scheelite are present in till at least 10 km down-ice (southeast) of mineralization (Fig. 6), whereas only one till sample (overlying the deposit) contains wolframite. In stream sediments, elevated contents of both scheelite (Fig. 7A) and wolframite (Fig. 7B) are present at least 4 km directly downstream and at least 5.5 km southeast in streams that transect the deposit's glacial dispersal train.

Wolframite, which is rare in till, was recovered from only 1 of the 56 till samples. It is more common in stream sediment samples and was recovered from 4 of 16 samples. Its low abundance in both till and stream sediments (100s grains) reflects its low content in the deposit. Few till and stream sed-
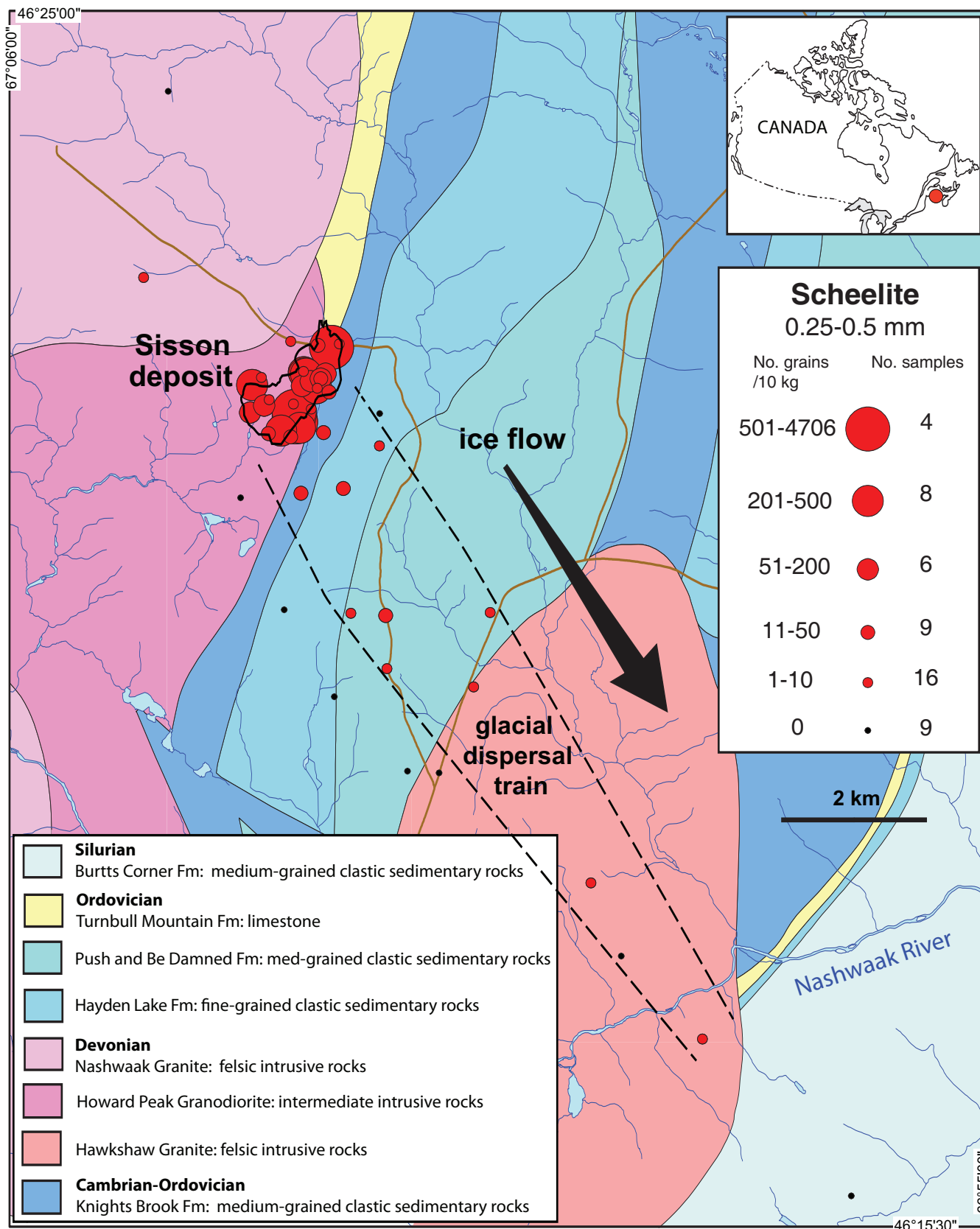
Table 2. Comparison of the abundance of indicator minerals in mineralized bedrock from the Sisson W-Mo deposit (normalized to 1 kg) to till and stream sediments (normalized to 10 kg) at varying distances, up-ice or upstream, overlying, and down-ice or downstream of the deposit. Data are reported for four size fractions. Pan concentrate counts are not normalized.

Sample Media	Sample	Interpretation	Distance from Deposit (m)	Scheelite				Wolframite				Molybdenite	Chalcopyrite	Arsenopyrite	Sphalerite	Bi minerals	Pyrite
				pan conc	0.25-0.5 mm	0.5-1.0 mm	1.0-2.0 mm	pan conc	0.25-0.5 mm	0.5-1.0 mm	1.0-2.0 mm	0.25-0.5 mm	0.25-0.5 mm	0.25-0.5 mm	0.25-0.5 mm	0.25-0.5 mm	0.25-0.5 mm
bedrock	11-MPB-R05	mineralized quartz vein	0	10000	22026	3671	140	0	11013	587	95	0	13216	0	2203	0	367
till	11-MPB-520	background up ice	-4000	0	0	0	0	0	0	0	0	0	0	0	0	0	0
	11-MPB-521	background up ice	-2250	0	2	0	0	0	0	0	0	0	0	0	0	0	0
	11-MPB-507	overlying mineralization	0	150,000	4706	0	0	0	0	0	0	0	0	0	0	0	0
	11-MPB-568	overlying mineralization	0	50	450	0	6	0	0	0	0	4	7	1	1	1	18
	11-MPB-567	overlying mineralization	0	50	261	0	7	0	0	0	0	87	8	0	0	2	217
	11-MPB-573	overlying mineralization	0	5,000	1852	0	0	0	0	0	0	4	0	0	0	4	2
	12-MPB-1026	overlying mineralization	0	200	280	105	2	0	112	38	0	0	2	1	0	0	1
	11-MPB-574	proximal down ice	20	50	5	0	1	0	0	0	0	0	1	7	0	0	29
	11-MPB-502	proximal down ice	50	0	40	2	0	0	0	0	0	0	6	0	0	2	1200
	11-MPB-562	proximal down ice	100	200	404	0	1	0	0	0	0	0	1	0	0	1	10
	11-MPB-511	proximal down ice	400	0	36	0	2	0	0	0	0	0	2	0	0	0	0
	11-MPB-544	proximal down ice	1100	0	49	0	1	0	0	0	0	0	1	0	0	0	0
	11-MPB-519	proximal down ice	1100	0	6	0	0	0	0	0	0	0	0	0	0	0	0
	11-MPB-546	distal down ice	2500	0	2	0	1	0	0	0	0	0	2	0	0	1	0
	11-MPB-526	distal down ice	3600	0	2	0	0	0	0	0	0	0	0	0	0	0	0
	11-MPB-531	distal down ice	4000	0	3	0	0	0	0	0	0	0	0	0	0	4	0
	11-MPB-525	distal down ice	4300	0	8	0	0	0	0	0	0	0	0	0	0	0	0
	11-MPB-539	distal down ice	10000	0	7	0	0	0	0	0	0	0	0	0	0	0	0
	11-MPB-540	background down ice	13000	0	0	0	0	0	0	0	0	0	0	0	0	0	0
stream sediments	21J06-2012-2006	background up stream	-4000	0	9	1	0	0	0	0	0	0	0	0	0	0	0
	21J06-2012-2004	background up stream	-4500	0	3	0	0	0	0	0	0	0	0	0	0	0	0
	21J06-2012-2005	background up stream	-4500	0	2	3	0	0	0	0	0	0	0	0	0	0	2
	21J06-2012-2011	background up stream	-1500	0	2	0	0	0	0	0	0	0	1	1	1	0	2475
	21J06-2012-2018	overlying	0	200	150	50	1	0	1	0	0	0	0	0	0	0	0
	21J06-2012-2007	overlying	0	500	2000	250	40	2	153	82	22	2	2	2	0	0	0
	21J06-2012-2019	overlying	0	50	300	57	3	0	5	0	0	0	0	0	0	0	0
	21J06-2012-2016	proximal downstream	100	0	0	0	0	0	0	0	0	0	0	0	0	0	5
	21J06-2012-2017	downstream	4000	0	80	17	1	0	13	4	2	0	4	0	0	0	8
	21J06-2012-2015	background	4000	0	5	3	0	0	0	0	0	0	0	0	0	0	1
	21J06-2012-2010	downstream of glacial dispersal train	4500	0	15	0	0	0	0	0	0	0	0	0	0	0	0
	21J06-2012-2012	downstream of glacial dispersal train	5500	0	80	7	0	0	0	0	0	0	3	0	0	0	1
	21J06-2012-2002	background	6500	0	0	0	0	0	0	0	0	0	0	0	0	0	1
	21J06-2012-2013	background	8000	0	7	1	0	0	0	0	0	0	2	0	0	0	19
	21J06-2012-2003	background	9500	0	0	0	0	0	0	0	0	0	0	0	0	0	0

Fig. 6. Location of the Sisson area in eastern Canada (inset map), and the distribution of scheelite grains in the 0.25–0.5 mm fraction of till normalized to 10/kg plotted on the local bedrock geology of the Sisson W-Mo deposit area. The outline of the glacial dispersal train down-ice (southeast) of the deposit was first identified by Seaman and McCoy (2008). Bedrock geology modified from Smith and Fyffe (2006a-d). Deposit subcrop outline in black from Rennie (2012). Modified from McClenaghan *et al.* (in press).
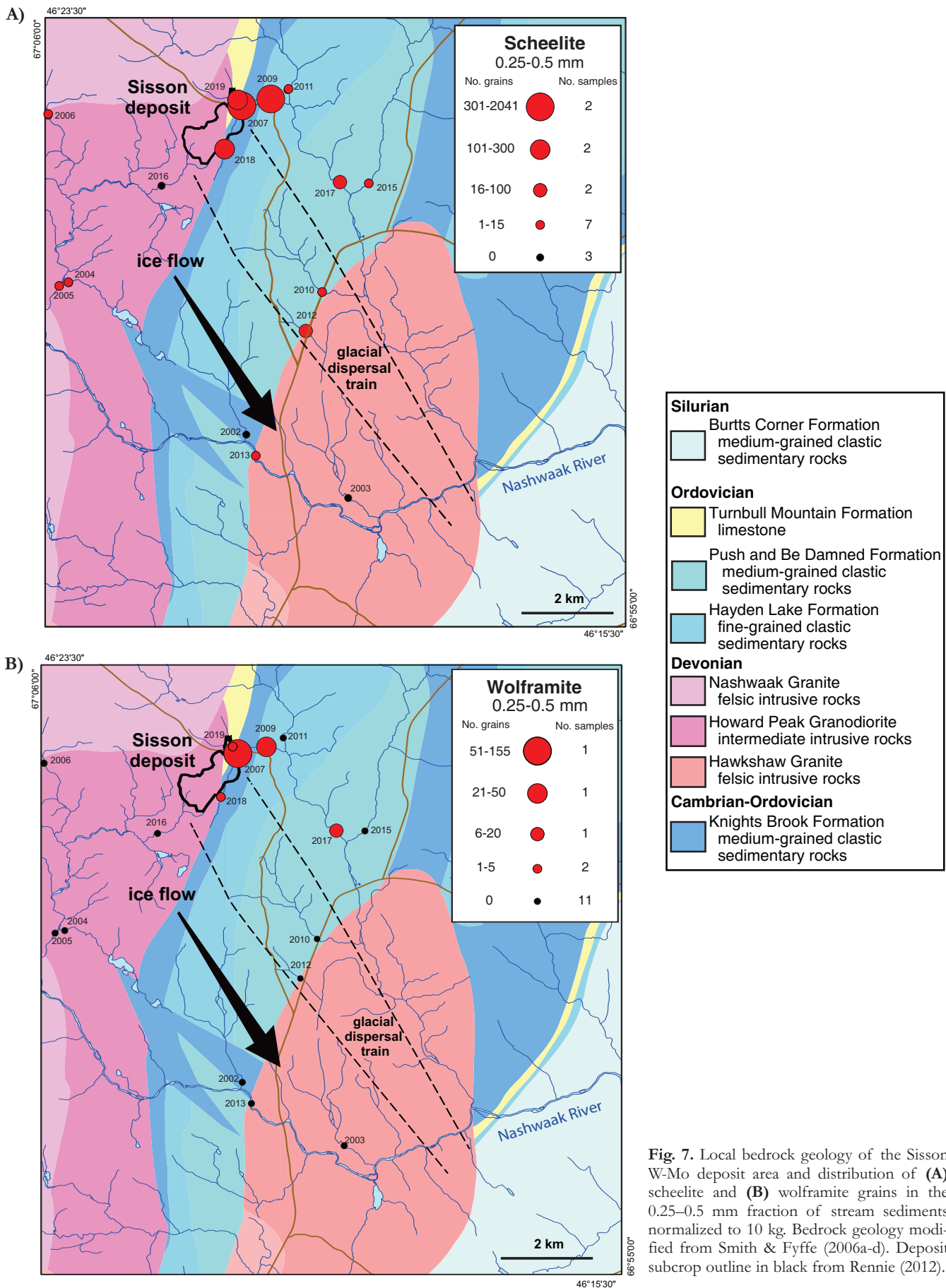
Fig. 7. Local bedrock geology of the Sisson W-Mo deposit area and distribution of **(A)** scheelite and **(B)** wolframite grains in the 0.25–0.5 mm fraction of stream sediments normalized to 10 kg. Bedrock geology modified from Smith & Fyffe (2006a-d). Deposit subcrop outline in black from Rennie (2012).

iment samples contain molybdenite (Table 1), reflecting its extreme softness and thus its inability to survive glacial or fluvial transport. The other indicator minerals present also occur in very low (trace) amounts (1 to 10 grains/10 kg).

ACKNOWLEDGMENTS

The Sisson case study was conducted as part of the Geological Survey of Canada's Targeted Geoscience Initiative 4 (TGI-4) and is a collaborative research effort between the Geological Survey of Canada the New Brunswick Department of Energy and Mines, Laurentian University, Northcliff Resources Ltd., and Hunter Dickinson Inc. A. Plouffe (GSC) is thanked for his manuscript review.

REFERENCES

Allen, T.L., Hart, C.J.R. & Marsh, E.E. 1999. Placer gold and associated heavy minerals of the Clear Creek drainage, central Yukon: past to present. *In:* Roots, C.F & Emonds, D.S. (eds) *Yukon Exploration and Geology 1998.* Exploration and Geological Services Division, Yukon Indian and Northern Affairs, 197–214.

Asrarullah. 1982. Investigations for tungsten in Pakistan. *In:* Hepworth, J.V. (ed) *Tungsten Geology Symposium, Jangxi, China.* ESCAP/RMRDC Bandung, Indonesia, 9–13.

Brugger, J., Beittol, A.A., Costa, S., Lahaye, Y., Bateman, R., Lambert, D.D. & Jamieson, D.N. 2000a. Mapping REE distribution in scheelite using luminescence. *Mineralogical Magazine,* **64**, 891–903.

Brugger, J., Lahaye, Y., Costa, S., Lambert, D.D. & Bateman, R. 2000b. Inhomogeneous distribution of REE in scheelite and dynamics of Archean hydrothermal systems (Mt. Charlotte and Drysdale gold deposits, Western Australia). *Contributions to Mineralogy and Petrology,* **139**, 251–264.

Brundin, N.H. & Bergström, J. 1977. Regional prospecting for ores based on heavy minerals in glacial till. *Journal of Geochemical Exploration.* **7**, 1–19.

de Smeth, J.B., Rao, K.S. & Schuling, R.D. 1985. Gold-scheelite mineralization in the Veligallu schist belt, Andhra Pradesh, India. *Economic Geology,* **80**, 1996–2000.

Cheilletz, A. 1988. Stratiform tungsten deposits: a review. *Geologie en Mijnbouw,* **67**, 293–311.

Dick, L.A. & Hodgson, C.J. 1982.The Mac Tung W-Cu (Zn) contact metasomatic and related deposits of the northeastern Canadian Cordillera. *Economic Geology,* **77**, 845-867.

Dostal, J., Kontak, D.J. & Chatterjee, A.K. 2009. Trace element geochemistry of scheelite and rutile from metaturbidite-hosted quartz vein gold deposits, Meguma Terrane, Nova Scotia, Canada: genetic implications. *Mineralogy and Petrology,* **97**, 95-109.

ESCAP Secretariat 1982. Note on tungsten occurrences in Burma. *In:* Hepworth, J.V. (ed) *Tungsten Geology Symposium, Jangxi, China.* ESCAP/RMRDC Bandung, Indonesia, 45-48.

Fernández-Turiel, J.L., Durán, M.E., Querol, X. & López-Soler, A. 1992. Comparison between analytical and mineralometric methods in regional scheelite exploration. *Journal of Geochemical Exploration,* **43**, 205–211.

Ferenc, S. & Uher, P. 2007. Magnesina wolframite from hydrothermal quartz veins in the Rochovce granite exocontact, Ochtiná, Western Carpathains, Slovakia. *Journal of Mineralogy and Geochemistry,* **183**, 165–172.

Frizzo, P. & Hassan, A.H. 1983. Scheelite in stream sediments in the crystalline basement of northern Somalia (area NNE of Hargheisa). *Bollettino della Societa Geologica Italiana,* **102**, 385–390.

Fyffe, L.R., Seaman, A., Thorne, K. & Martin, D.A. 2010. Part 1: Sisson Brook W–Mo–Cu deposit. *In:* Fyffe, L.R and Thorne, K (compilers) *Polymetallic deposits of Sisson Brook and Mount Pleasant, New Brunswick, Canada.* New Brunswick Department Natural Resources, Field Guide No. 3, 7–33.

Ghaderi, M., Palin, J.M., Campbell, I.H., and Sylvester, P.J. 1999. Rare earth element systematics in scheelite from hydrothermal gold deposits in the Kalgoorlie-Norseman region, Western Australia. *Economic Geology,* **94**, 423–437.

Hallenstein, C.P., Pedersen, J.L. & Stendal, H. 1981. Exploration for scheelite in East Greenland- a case study. *Journal of Geochemical Exploration,* **15**, 381–392.

Hess, F.L. 1917. *Tungsten minerals and deposits.* United States Geological Survey, Bulletin 652.

Horsnail, R.F. 1979. The geology of tungsten. *In: Proceedings of the First Tungsten Symposium.* Stockholm, September 5-7, 1979, Mining Journal Books Limited, 18–31.

Hosking, K.F.G. 1982. A general review of the occurrence of tungsten in the world. *In:* Hepworth, J.V. (ed) *Symposium on Tungsten Geology, Jiangxi, China.* ESCAP/RMRDC Bandung, Indonesia and Geological Publishing House, Beijing, China, 59–86.

Hsu, L.C. & Galli, P.E. 1973. Origin of scheelite-powellite series of minerals. *Economic Geology,* **68**, 681–696.

Johansson, K., Keinänen, V. & Lehmuspelto, P. 1986. Geochemical exploration of tungsten in glaciogenic deposits in Soretiapulju, Western Finnish Lapland. *In: Prospecting in Areas of Glaciated Terrain.* Institute of Mining and Metallurgy 61–68.

Johnson, B.L. 1910. *Occurrence of wolframite and cassiterite in the gold placers of Deadwood Creek, Birch Creek district (Alaska).* United States Geological Survey, Bulletin 442, 246–250.

Kelly, W.C. & Rye, R.O. 1979. Geologic, fluid inclusion and stable isotope studies of the tin-tungsten deposits of Panasqueira, Portugal. *Economic Geology,* **74**, 1721–1822.

Kooiman, G.J.A., McLeod, M.J. & Sinclair, W.D. 1986. Porphyry tungsten-molybdenum orebodies, polymetallic veins and replacement bodies and tin-bearing greisen zones in the Fire Tower Zone, Mount Pleasant, New Brunswick. *Economic Geology,* **81**, 1356–1373.

Kwak, T.A. P. 1987. *W-Sn skarn deposits and related metamorphic skarns and granitoids.* Developments in Economic Geology, 24, Elsevier.

Landis, G.P. & Rye, R.O. 1974. Geologic, fluid inclusion and stable isotope studies of the Pasto Buena tungsten-base metal ore deposit, northern Peru. *Economic Geology,* **69**, 1025–1059.

Lang, J. & Zahovskis, C. 2013. Geology and hydrothermal characteristics of the Sisson W-Mo deposit, New Brunswick, with a status update on advanced economic feasibility and environmental studies. *In: Abstracts.* Mineral Exploration Roundup 2013, 44–45.

Lindmark, B. 1977. Till-sampling methods used in exploration for scheelite in Kaustinen, Finland. *In: Prospecting in Areas of Glaciated Terrain 1977.* Institute of Mining and Metallurgy, 46–48.

Marr, J. M., 2009. *Sisson Brook tungsten molybdenum deposit, New Brunswick, preliminary economic assessment.* 2009 Technical and Economic Update, September 16th, 2009, National Instrument 43-101 technical report by Geodex Minerals Ltd.

Maurice, Y.T. 1986. Interpretation of a reconnaissance geochemical heavy mineral survey in the Eastern Townships of Quebec. *In: Current Research, Part A.* Geological Survey of Canada, Paper 86-1A, 307–317.

McClenaghan, M.B. & Kjarsgaard, B.A. 2007. Indicator mineral and surficial geochemical exploration methods for kimberlite in glaciated terrain, examples from Canada. *In:* Goodfellow, W.D. (ed.) *Mineral Resources of Canada: A Synthesis of Major Deposit Types, District Metallogeny, the Evolution of Geological Provinces and Exploration Methods.* Geological Association of Canada, Special Paper 5, 983–1006.

McClenaghan, M.B., Parkhill, M.A., Averill, S.A., Pronk, A.G., Seaman, A.A., Boldon, R., McCurdy, M.W. & Rice, J.M. 2013a. *Indicator mineral abundance data for bedrock, till, and stream sediment samples from the Sisson W-Mo deposit, New Brunswick.* Geological Survey of Canada, Open File 7387.

McClenaghan, M.B., Parkhill, M.A., Averill, S.A. & Kjarsgaard, I.M. 2013b. *Indicator mineral signatures of the Sisson W-Mo deposit, New Brunswick: part 1 bedrock samples.* Geological Survey of Canada, Open File 7431.

McClenaghan, M.B., Parkhill, M.A., Seaman, A.A., Pronk, A.G., Averill, S.A., Rice, J.M. & Pyne M. in press. *Indicator mineral signatures of the Sisson W-Mo deposit, New Brunswick: part 2 till samples.* Geological Survey of Canada, Open File 7467.

Meinert, L.D., Dipple, G.M. & Nicolescu, S. 2005, World skarn deposits. *In:* Hedenquist, J.W., Thompson, J.F.H., Goldfarb, R.J. & Richards, J.P. (ed.) *Economic Geology 100th Anniversary Volume.* Society of Economic Geologists, Littleton, Colorado, USA.

Meizhong, Y. 1982. Basic theory and chief methods applied in tungsten prospecting in Jiangxi Province. *In:* Hepworth, J.V. (ed.) *Tungsten Geology Symposium, Jangxi, China.* ESCAP/RMRDC, Bandung, Indonesia, 489–502.

Mikulski, S.Z. & Wierchowiec, J. 2013. Placer scheelite and gold from alluvial sediments as indicators of primary mineralization — examples from SW Poland. *Geological Quarterly,* **57**.. doi:10.7306/gQ.1107

Nakashima, K., Watanabe, M. & Soeda, A. 1986. Regional and local variations in the composition of the wolframite series from SW Japan and possible factors controlling compositional variations. *Mineralium Deposita,* **21**, 200–206.

Nast, H.J. & Williams-Jones, A.E. 1991. The role of water-rock interaction and fluid evolution in the forming of the porphyry-related Sisson Brook W-Cu-Mo deposit, New Brunswick. *Economic Geology,* **86**, 302–317.

Nikkarinen, M. & Björklund, A. 1976. Kaustinen: the use of till in tungsten prospecting. *Journal of Geochemical Exploration,* **21**, 247–248.

Noble, S.R., Spooner, E.T.C., & Harris, F.R.1984. The Logtung large tonnage, low-grade W (scheelite)-Mo porphyry deposit, south-central Yukon Territory. *Economic Geology,* **79**, 848–868.

Ottensen, R.T. & Theobald, P.K. 1994. Chapter 5, Stream sediments in mineral exploration. *In:* Hale, M. & Plant, J.A. (eds) *Handbook of Exploration Geochemistry*. Elsevier, 6, 147–185

Özcan, A. & Çağatay, M.N., 1989. Tungsten exploration in semiarid environment: Central Anatolian massif, Turkey. *Journal of Geochemical Exploration*, **31**, 185–199.

Petersen, L.R. & Stendal, H. 1987. Tungsten exploration in the Valnesfjord region, Nordland, northern Norway. *Journal of Geochemical Exploration*, **29**, 151–163

Peuraniemi, V. 1992. Hieronmaki: W, Sn, Cu and Zn concentrations of till near a scheelite mineralization in hilly region. *In:* Kauranne,K., Salminen, R. & Salonen, V-P. (eds) *Handbook of Exploration Geochemistry: Regolith Exploration Geochemistry in Arctic and Temperate Terrains, Espoo, Finland*. Elsevier, 277–282.

Poulin, R.S., McDonald, A.M., Kontak, D.J. & McClenaghan, M.B. 2013. Discrimination of scheelite from differing geological settings: Application of cathodoluminescence. *In: Program with Abstracts*. Geological Association of Canada-Mineralogical Association of Canada, Annual Meeting 2013, 165.

Pungrassami, T. 1986. Cassiterite and wolframite deposits in and around the Hat Yai Basin, Songkhla Province, Thailand. *In:* Thiramongkol, N. (ed.) *Proceedings of the Workshop on Economic Geology, Tectonics, Sedimentary Processes and Environment of the Quaternary in Southeast Asia*. 3-7 February, 1986, Haad Yai, Thailand, 135–155.

Rajah, S.S. 1982. Tungsten mineralization in Peninsular Malaysia. *In:* Hepworth, J.V. (ed.) *Tungsten Geology Symposium, Jangxi, China*. ESCAP/RMRDC Bandung, Indonesia, 179–195.

Rennie, D.W. 2012. *Technical report on the Sisson Project, New Brunswick, Canada*. June 29, 2012, National Instrument 43-101 technical report by Northcliff Resources Ltd.

Roberts, S., Palmer, M.R. & Waller, L. 2006. Sm-Nd and REE characteristics of tourmaline and scheelite from the Björkdal gold deposit, northern Sweden: evidence of an intrusion-related gold deposit? *Economic Geology*, **101**, 1415–1425.

Salminen, R. & Hartikainen, A. 1986. Tracing gold, molybdenum and tungsten mineralization by use of a step by step geochemical study in Ilomantsi, eastern Finland. *In: Prospecting In Areas of Glaciated Terrain 1986*. Institution of Mining and Metallurgy, London, 201–209.

Salpeteur, I. 1985. Geochemical dispersion from the Bir Tawilah wolfram-quartz veins in the pediplain of Saudia Arabia. *In: Prospecting in Areas of Desert Terrain*. Institution of Mining and Metallurgy, London, 141–154.

Seaman, A.A. & McCoy, S.M. 2008. Multiple Wisconsinan tills in the Sisson Brook exploration trench of Geodex Minerals Ltd., York County, west-central New Brunswick. *In:* Martin, G.L. (ed.) *Geological Investigations in New Brunswick for 2007*. New Brunswick Department of Natural Resources, Minerals, Policy and Planning Division, Mineral Resource Report 2008-1, 1–34.

Silakul, T. 1986. The use of stream sediment and soil media for tungsten exploration geochemistry around Doi Mok, northern Thailand. *Bulletin of the Geological Institutions of the University of Uppsala*, **12**, 49–102.

Smith, E.A. & Fyffe, L.R. (compilers) 2006a. *Bedrock geology of the Burtts Corner area (NTS 21 J/02), York County, New Brunswick*. New Brunswick Department of Natural Resources, Map Plate 2006-3.

Smith, E.A. & Fyffe, L.R. (compilers) 2006b. *Bedrock geology of the Millville area (NTS 21 J/03), York and Carleton counties, New Brunswick*. New Brunswick Department of Natural Resources, Map Plate 2006-4.

Smith, E.A. & Fyffe, L.R. (compilers) 2006c. *Bedrock geology of the Coldstream area (NTS 21 J/06), York and Carleton counties, New Brunswick*. New Brunswick Department of Natural Resources, Map Plate 2006-7.

Smith, E.A. & Fyffe, L.R. (compilers) 2006d. *Bedrock geology of the Napadogan area (NTS 21 J/07), York and Carleton counties, New Brunswick*. New Brunswick Department of Natural Resources, Map Plate 2006-8.

Snow, R.J. & Coker, W.B. 1987. Overburden geochemistry related to W-Cu-Mo mineralization at Sisson Brook, New Brunswick, Canada: an example of short- and long-distance glacial dispersal. *In:* Garrett, R.G. (ed.) *Geochemical Exploration 1985*. Journal of Geochemical Exploration, **28**, 353–368.

Stea, R.R. & O'Reilly, G.A. 1982. Till geochemistry of the Meguma Terrane in Nova Scotia and its metallogenic implications. *In: Prospecting in Areas of Glaciated Terrain 1982*. Institute of Mining and Metallurgy, 82–104.

Steiger, R. 1977. Prospecting for lithium and tungsten in Ireland. *In: Prospecting in Areas of Glaciated Terrain 1977*. Institute of Mining and Metallurgy, 14–24.

Stendal, H. 1978. Heavy minerals in stream sediments, southwest Norway. *Journal of Geochemical Exploration*, **10**, 91–102.

Stendal, H. & Theobald, P.K. 1994. Heavy-mineral concentrates in geochemical exploration. *In:* Hale, M. & Plant, J.A. (ed.) *Drainage Geochemistry*. Elsevier, Handbook of Exploration Geochemistry, **6**, 185–225.

Steenfelt, A. 1987. Geochemical mapping and prospecting in Greenland- a review of results and experience. *Journal of Geochemical Exploration*, **29**, 183–205.

Surya Prakash Rao, K., Sastry, R.S.N. & Raju, S.V. 1989. Scheelite as a prospecting tool in the Ramagiri greenstone belt, Andhra Pradesh, India. *Journal of Geochemical Exploration*, **31**, 307–317.

Sylvester, P.J. & Ghaderi, M. 1997. Trace element analysis of scheelite by excimer laser ablation-inductively coupled plasma-mass spectrometry (ELA-ICP-MS) using a synthetic silicate glass standard. *Chemical Geology*, **14**, 49–65.

Theobald, P.K & Thompson, C.E. 1960. *Geochemical prospecting with heavy-mineral concentrates used to locate a tungsten deposit*. United States Geological Survey, Circular 411.

Toverud, O. 1984. Dispersal of tungsten in glacial drift and humus in Bergslagen, south central Sweden. *Journal of Geochemical Exploration*, **21**, 261–272.

Wildon, R. & Hotz, P.E. 1955. A gold-scheelite-cinnabar placer in Humboldt County, Nevada. *Economic Geology*, **50**, 661–668.

Zantop, H. & Nespereira, J. 1979. Heavy-mineral panning techniques in the exploration for tin and tungsten in NW Spain. *In:* Watterson, J.R. & Theobald, P.K. (eds) *Geochemical Exploration 1978*. Association of Exploration Geochemists, 329–336.

Zeschke, G. 1961. Prospecting for ore deposits by panning heavy minerals from river sands. *Economic Geology*, **56**, 1250–1257.